
Non-Relativistic Dynamics of a Neutral Particle in Various Magnetic Fields



SUBMITTED BY
Junwoo Shin

Nicht relativistische Dynamik eines neutralen Teilchen in unterschiedlichen magnetischen Feldern

Bachelorarbeit

FAKULTÄT FÜR PHYSIK
AN DER LUDWIG-MAXIMILIANS-UNIVERSITÄT
MÜNCHEN

VORGELEGT VON

Junwoo Shin

MÜNCHEN, 29.1.2025

Non-Relativistic Dynamics of a Neutral Particle in Various Magnetic Fields

Bachelor Thesis

FACULTY OF PHYSICS
AT THE LUDWIG-MAXIMILIANS-UNIVERSITÄT
MUNICH

SUBMITTED BY

Junwoo Shin

MUNICH, 29.1.2025

Supervised by

Priv.-Doz. Dr. Dirk André Deckert

Prof. Dr. Hartmut Ruhl

Siddhant Das

1	Introduction	1
1.1	Motivation	1
1.2	Overview about the Chapters	2
1.2.1	Dynamics with the Switching-Off ConstantMagnetic field	2
1.2.2	Dynamics with the Magnetic Barrier	2
1.3	Notation	3
1.4	Mathematical Background	3
1.4.1	Fourier Transform	3
1.4.2	Laplace Transformation	4
1.4.3	Propagator	4
1.4.4	Weak Solution with Distribution	7
2	Chapter 02	11
2.1	Free Particle	11
2.1.1	Hamiltonian and Schrödinger Equation	11
2.1.2	Time-Independent Solution	11
2.1.3	Time-Dependent Solution	13
2.2	Particle in Constant Magnetic Field	14
2.2.1	Hamiltonian and Pauli Equation	14
2.2.2	Solutions	14
2.3	Particle in Uniform Magnetic Field Abruptly Turned Off at Time T	16
2.3.1	Hamiltonian	16
2.3.2	Solutions	16
2.4	Probability Density ρ^Ψ and Probability Current Density \mathcal{J}^Ψ	17
2.4.1	Non-Dimensionalization Convention	18
2.4.2	Probability Density	19
2.4.3	Probability Current Density	20
2.4.4	Relative Magnitudes of Convective and Spin Fluxes	23
3	Chapter 03	27
3.1	Hamiltonian and Pauli Equation	27
3.2	Time-Dependent Solution to the Pauli Equation	27
3.3	Probability Density ρ^ψ and Probability Current Density \mathcal{J}^ψ	31
3.3.1	Non-Dimensionalization Convention	31
3.3.2	Probability Density	32
3.3.3	Probability Current Density	36
3.3.4	Backflow and Stability	39
4	Conclusion	47
4.1	Results of the Analysis	47
4.2	Outlook	47

A Derivation for Chapter 2	49
A.1 Propagator for Free Particle	49
A.2 Time-Dependent Wavefunction for a Free Particle	52
A.3 Wavefunction as a Solution to the Schrödinger Equation	53
B Derivation for Chapter 3	55
B.1 Propagator for a Delta-Potential	55
B.1.1 Solution to the Laplace-transformed Schrödinger Equation	55
B.1.2 Inverse Laplace Transform of the Solution	58
B.2 Wave function as a Weak Solution	59
C Derivation of Formula	61
C.1 Laplace Transformation with Complementary Error Function	61
C.2 Extension of Cauchy-Schlömilch Transformation	62
C.3 Infinite Integral with Complementary Error Function	65
Bibliography	67

1.1 Motivation

In quantum physics, the Schrödinger equation for a spinless particle is introduced as a fundamental differential equation to express the dynamics of the wave function $\Psi : \mathbb{R} \times \mathbb{R}^3 \rightarrow \mathbb{C}$, $(t, \vec{r}) \mapsto \Psi_t(\vec{r})$:

$$i\hbar \frac{\partial}{\partial t} \Psi_t(\vec{r}) = \left[-\frac{\hbar^2}{2m} \nabla^2 + V(\vec{r}) \right] \Psi_t(\vec{r}) \quad (1.1)$$

From this equation the probability density $\rho : \mathbb{R} \times \mathbb{R}^3 \rightarrow \mathbb{R}$, $(t, \vec{r}) \mapsto \rho^{\Psi_t}(\vec{r}) := \Psi_t^*(\vec{r})\Psi_t(\vec{r})$ is derived. The physical interpretation of the probability density was given by Born's rule: $\rho^{\Psi_t}(\vec{r})d^3x$ gives the probability of finding a particle in the volume element d^3x in (t, \vec{r}) , which is also experimentally tested [Jin+17; Söl+11]. This consistency of the probability interpretation requires fulfilling:

$$\frac{\partial}{\partial t} \rho^{\Psi_t}(\vec{r}) + \nabla \cdot \mathcal{J}^{\Psi_t}(\vec{r}) = 0 \quad (1.2)$$

$$\text{where } \mathcal{J} : \mathbb{R} \times \mathbb{R}^3 \rightarrow \mathbb{R}^3, (t, \vec{r}) \mapsto \mathcal{J}^{\Psi_t}(\vec{r}) = \frac{\hbar}{m} \text{Im}[\Psi_t^*(\vec{r})\nabla\Psi_t(\vec{r})] \quad (1.3)$$

This equation is called the continuity equation and \mathcal{J} is the probability current density, which is expressed in the standard form. There are other forms that satisfy the continuity equation, especially when the spin of a particle is considered. (see below, equation (1.6))

In contrast to the probability density, the statistical interpretation for the probability current density, which is also called quantum flux, is not commonly discussed. Despite this, it appears in the literature discussing scattering experiments as a crossing probability $\mathcal{J}^{\Psi_t}(\vec{r}) \cdot d\vec{s}dt$, which is supposed to express the probability that a particle crosses a surface element $d\vec{s}$ in time dt . This interpretation requires $\mathcal{J}^{\Psi_t}(\vec{r}) \cdot d\vec{s}$ not to be negative. Nevertheless, in some situations this current positivity condition can be violated. This phenomenon is called quantum backflow effect. Such situations are interesting because they challenge the given interpretation given that backflow can occur and be detected. Therefore, it is of interest and meaningful to study such situations to see how the quantum backflow is provoked and enhanced for detection, with the anticipation of worthy consequences for scattering theory.

To date, a lot of literature and research papers discussed the quantum backflow effect [Gou21; Von14]. To provoke the quantum backflow effect, usually settings that induce interference of wave functions are employed. Still, not much backflow is found. Also, a particle with spin is not much discussed.

If a particle with spin- $\frac{1}{2}$ is considered, the dynamics of its wave function is described by the Pauli equation [Gre00, p.125, converted to SI units]:

$$i\hbar \frac{\partial}{\partial t} \Psi_t(\vec{r}) = \frac{1}{2m} \left[(-i\hbar\nabla - q\vec{A})^2 + q\hbar\vec{\sigma} \cdot \vec{B} + qA_0 \right] \Psi_t(\vec{r}) \quad (1.4)$$

$\vec{\sigma}$ is the Pauli vector, which is defined as follows:

$$\vec{\sigma} = \sigma_x \vec{e}_x + \sigma_y \vec{e}_y + \sigma_z \vec{e}_z \quad (1.5)$$

$$\text{where } \sigma_x = \begin{bmatrix} 0 & 1 \\ 1 & 0 \end{bmatrix}, \sigma_y = \begin{bmatrix} 0 & -i \\ i & 0 \end{bmatrix}, \sigma_z = \begin{bmatrix} 1 & 0 \\ 0 & -1 \end{bmatrix}$$

From the Pauli equation follows also the continuity equation, leading to the Pauli current $\mathcal{J}_{Pauli} : \mathbb{R} \times \mathbb{R}^3 \rightarrow \mathbb{R}^3, (t, \vec{r}) \mapsto \mathcal{J}_{Pauli}^{\Psi_t}(\vec{r})$ [Wil20, eq.20]:

$$\mathcal{J}_{Pauli}^{\Psi_t}(\vec{r}) = \frac{\hbar}{m} \text{Im} [\Psi_t^*(\vec{r}) \nabla \Psi_t(\vec{r})] + \frac{\hbar}{2m} \nabla \times [\Psi_t^*(\vec{r}) \vec{\sigma} \Psi_t(\vec{r})] \quad (1.6)$$

The first term is called **Convective Flux** or **Convective Probability Current Density** and the second term is called **Spin Flux** or **Spin Probability Current Density**. Since the probability current includes now an additional term compared to equation (1.3), which depends on spin, the spin actually matters. The spin flux may help to amplify backflow through interaction with an external field. Therefore, a neutral particle with spin $\frac{1}{2}$ in a magnetic field will be studied in two different situations to provoke and enhance backflow for detection. The particle is chosen to be neutral to simplify calculations, and to avoid unnecessary interactions with electric fields, which are difficult to screen in experimental setup. In the first situation, a particle is projected in the spatially homogeneous magnetic field that will be switched off at some moment in time. In the second situation, a particle is projected towards a delta-shaped magnetic field, which will be called delta-magnetic field or magnetic barrier.

1.2 Overview about the Chapters

1.2.1 Dynamics with the Switching-Off Constant Magnetic field

In Chapter 2, a spin- $\frac{1}{2}$ neutral particle is projected in the spatially constant magnetic field. Thanks to the interaction of spin with the magnetic field through magnetic dipole moment, the spin state of the particle changes. At some moment, the magnetic field is switched off and the dynamics of the spin state disappears.

In the analysis, two features are found. First, its probability current density exhibits rotative motion due to the spin flux. Even though the probability density is not affected by the magnetic field because the time evolution of the spin state is unitary and independent of position, backflow can be provoked given that the magnetic field is strong enough.

Second, the spin flux decays faster than convective flux. It is found that the probability current density converges to convective flux as time passes. The rotative motion disappears independent of the intensity of the magnetic field. This feature leads to the suppression of backflow, which makes practical detection challenging.

1.2.2 Dynamics with the Magnetic Barrier

In Chapter 3, a particle is projected toward a delta-magnetic field, which is a magnetic barrier. The wave function in this situation propagates at first like a free particle until it reaches the magnetic barrier. After this moment, a part of the wave function is reflected at the barrier, which starts to intensely interfere with the incident wave function, because of which the probability density also shows interference pattern. Also, its probability current density exhibits

complicated dynamics.

In the analysis, the interference after strong interaction with the magnetic barrier provokes backflow enormously. However, it turns out in the further analysis that the backflow produced is not much stable for detection.

As a conclusion, backflow is provoked and enhanced as intended. However, its instability in time and position poses significant challenges detection in this experimental setup. It suggests another setup, which may stabilize it, to be studied.

1.3 Notation

In this thesis, the following notations are used:

\mathcal{F}	Fourier transform
\mathcal{L}	Laplace transform
K_0	Propagator for a free particle
K_δ	One dimensional Propagator for delta potential
K_Δ	Three dimensional Propagator for delta potential
L^2	Space of square integrable functions
$H^p(1 \leq p \leq \infty)$	Hardy spaces
$C_{compact}^\infty$	Space of compactly supported infinitely differentiable functions

1.4 Mathematical Background

In this section, important mathematical objects such as Laplace transform, Fourier transform and propagator, and the notions of weak solutions are introduced, which are employed in the following chapters and appendix. Readers who are already familiar with these notions can skip this part.

1.4.1 Fourier Transform

Fourier transform is one of the integral transform, which, in physics, maps a function in the position or time space to the momentum or frequency space respectively. Mathematically it is defined as follows [RS75, p.1, p.10]:

Definition 1.4.1. *Let $f : \mathbb{R}^n \rightarrow \mathbb{C}, \vec{x} \mapsto f(\vec{x})$ be a absolute integrable function. Then, the **Fourier Transform** of f is defined as follows:*

$$\mathcal{F} : L^2(\mathbb{R}^n) \rightarrow L^2(\mathbb{R}^n),$$

$$f \mapsto \mathcal{F}[f] = \left(\vec{k} \in \mathbb{R}^n \mapsto \frac{1}{(2\pi)^{\frac{n}{2}}} \int_{\mathbb{R}^n} e^{-i\vec{k}\cdot\vec{x}} \psi(\vec{x}) d^n x \in \mathbb{C} \right) =: \tilde{f} \quad (1.7)$$

Inverse Fourier transform is

$$\mathcal{F}^{-1} : L^2(\mathbb{R}^n) \rightarrow L^2(\mathbb{R}^n),$$

$$\tilde{f} \mapsto \mathcal{F}^{-1}[\tilde{f}] = \left(\vec{x} \in \mathbb{R}^n \mapsto \frac{1}{(2\pi)^{\frac{n}{2}}} \int_{\mathbb{R}^n} e^{-i\vec{k}\cdot\vec{x}} \psi(\vec{x}) d^n k \in \mathbb{C} \right) = f \quad (1.8)$$

Fourier transform is often employed to simplify a differential equation by changing the basis.

1.4.2 Laplace Transformation

Similar to the Fourier transform, the Laplace transform is used to simplify differential equations. It is defined as follows [Sch99, p.1; Hof07, p.104]:

Definition 1.4.2. Let $f : (0, \infty) \rightarrow \mathbb{C}, t \mapsto f(t)$ be a complex valued function and $s \in \mathbb{C}$. Also, a set $L_{\mathcal{L}}$ is defined as follows:

$$L_{\mathcal{L}} = \left\{ g : (0, \infty) \rightarrow \mathbb{C}, t \mapsto g(t) \mid e^{-st}g(t) \in L^2(0, \infty), s \in \mathbb{C} \right\} \quad (1.9)$$

Then, the **Laplace Transform** of f is defined as

$$\mathcal{L} : L_{\mathcal{L}} \rightarrow H^2 \quad (1.10)$$

$$f \mapsto \mathcal{L}[f] = \left(s \mapsto \int_0^{\infty} e^{-st} f(t) dt \right) =: \tilde{f}, \quad (1.11)$$

if $\tilde{f} : s \mapsto \tilde{f}(s)$ exists.

The Laplace transform converts $f(t)$ from the time domain to the frequency domain. When applied to a differential equation, it converts the equation into an algebraic problem.

The inverse Laplace Transform is uniquely defined if the function f in this definition is continuous, and it can be found usually in tables of transforms, if it exists [Sch99, p.24]:

$$\mathcal{L}^{-1} : H^2 \rightarrow L_{\mathcal{L}} \quad (1.12)$$

$$\tilde{f} \mapsto \mathcal{L}^{-1}[\tilde{f}] = f \quad (1.13)$$

1.4.3 Propagator

In quantum mechanics, the wave function solving the time-dependent Schrödinger equation is naturally time-dependent. Mathematically, solving the Schrödinger equation is done in terms of an initial value problem. To simplify this procedure, the propagator is introduced:

Definition 1.4.3. Let $\Psi_t \in L^2(\mathbb{R}^3)$ be a wave function at time t , and $U(t, t_0) : L^2(\mathbb{R}^3) \rightarrow L^2(\mathbb{R}^3), \Psi_{t_0} \mapsto \Psi_t$ be a time evolution operator that is unitary, which satisfies the following equation:

$$\Psi_t = U(t, t_0)\Psi_{t_0} \quad (1.14)$$

$$\text{where } \Psi_{t_0} \text{ is an initial value.} \quad (1.15)$$

This can be expressed in the position basis as follows, using completeness relation of the eigenfunctions of position operator:

$$\Psi_t(\vec{r}) = \int_{\mathbb{R}^3} K(\vec{r}, t, \vec{r}', t_0) \Psi_{t_0}(\vec{r}') d\vec{r}' \quad (1.16)$$

$K(\vec{r}, t, \vec{r}', t_0)$, the kernel of the integral operator, is called **Propagator** [SN20].

The propagator has the advantage of being dependent only on the form of the Hamiltonian \hat{H} , not on the initial wave function. When applied to the initial wave function $\Psi_{t_0}(\vec{r}')$, the propagator specifies the wave function $\Psi_t(\vec{r})$ at time t as a function of position. In other words, it describes how a particle in the initial state transitions to another state after a given time period.

The explicit form of Propagator $K(x, t, x', t_0)$ can be derived by applying the Laplace transform to the Schrödinger equation. For simplicity, the derivation is performed in one dimension:

$$\begin{aligned} \mathcal{L} \left[i\hbar \frac{\partial}{\partial t} \Psi_t(x) \right] &= \mathcal{L} \left[-\frac{\hbar^2}{2m} \partial_x^2 \Psi_t(x) + V(x) \Psi_t(x) \right] \\ i\hbar \mathcal{L} \left[\frac{\partial}{\partial t} \Psi_t(x) \right] &= -\frac{\hbar^2}{2m} \partial_x^2 \mathcal{L} [\Psi_t(x)] + V(x) \mathcal{L} [\Psi_t(x)] \\ i\hbar \int_0^\infty dt e^{-st} \frac{\partial}{\partial t} \Psi_t(x) &= -\frac{\hbar^2}{2m} \partial_x^2 \Phi_s(x) + V(x) \Phi_s(x) \\ i\hbar \left[e^{-st} \Psi_t(x) \right]_{t=0}^{t=\infty} - i\hbar \int_0^\infty dt (-s) e^{-st} \Psi_t(x) &= -\frac{\hbar^2}{2m} \partial_x^2 \Phi_s(x) + V(x) \Phi_s(x) \\ i\hbar s \Phi_s(x) - i\hbar \Psi_0(x) &= -\frac{\hbar^2}{2m} \partial_x^2 \Phi_s(x) + V(x) \Phi_s(x) \end{aligned} \quad (1.17)$$

In the third line it was integrated by parts and $\mathcal{L}[\Psi_t(x)]$ is denoted as $\Phi_s(x)$. It is a non-homogeneous ordinary differential equation of second order. This differential equation can be solved, if the homogeneous solutions are known. Let $u_s^1(x)$, $u_s^2(x)$ be homogeneous solutions, then the general solution is:

$$\Phi_s(x) = \Phi_s^p(x) + \alpha_s u_s^1(x) + \beta_s u_s^2(x), \quad (1.18)$$

where α_s, β_s are coefficients of the homogeneous solutions. These coefficients can be determined under the boundary conditions. $\Phi_s^p(x)$ is the particular solution that can be obtained with $W[u_s^1, u_s^2]$, which is called the Wronskian of the two homogeneous solutions [Ros07, p.155]:

$$\Phi_s^p(x) = -\frac{2mi}{\hbar} \left[u_s^1(x) \int^x \frac{u_s^2(x')}{W[u_s^1, u_s^2]} \Psi_0(x') dx' - u_s^2(x) \int^x \frac{u_s^1(x')}{W[u_s^1, u_s^2]} \Psi_0(x') dx' \right] \quad (1.19)$$

$$W[u_s^1, u_s^2] = \det \begin{bmatrix} u_s^1(x) & u_s^2(x) \\ \partial_x u_s^1(x) & \partial_x u_s^2(x) \end{bmatrix} = u_s^1(x) \partial_x u_s^2(x) - u_s^2(x) \partial_x u_s^1(x) \quad (1.20)$$

This particular solution (1.19) can be derived by using the ansatz $\Phi_s^p(x) = v_1(x) u_s^1(x) + v_2(x) u_s^2(x)$. The first and second derivative of $\Phi_s^p(x)$ can be calculated by imposing a freely chosen second condition $[\partial_x v_1(x)] u_s^1(x) + [\partial_x v_2(x)] u_s^2(x) = 0$, which simplifies the first derivative

of $\Phi_s^p(x)$:

$$\begin{aligned}\partial_x \Phi_s^p(x) &= [\partial_x v_1(x)] u_s^1(x) + [\partial_x v_2(x)] u_s^2(x) + v_1(x) \partial_x u_s^1(x) + v_2(x) \partial_x u_s^2(x) \\ &= v_1(x) \partial_x u_s^1(x) + v_2(x) \partial_x u_s^2(x)\end{aligned}$$

$$\partial_x^2 \Phi_s^p(x) = \partial_x v_1(x) \partial_x u_s^1(x) + \partial_x v_2(x) \partial_x u_s^2(x) + v_1(x) \partial_x^2 u_s^1(x) + v_2(x) \partial_x^2 u_s^2(x)$$

By substituting the second derivative in equation (1.17):

$$\begin{aligned}-i\hbar\Psi_0(x) &= -\frac{\hbar^2}{2m} \left[\partial_x v_1(x) \partial_x u_s^1(x) + \partial_x v_2(x) \partial_x u_s^2(x) + v_1(x) \partial_x^2 u_s^1(x) + v_2(x) \partial_x^2 u_s^2(x) \right] \\ &\quad + [V(x) - i\hbar s] \left[v_1(x) u_s^1(x) + v_2(x) u_s^2(x) \right] \\ &= v_1(x) \left[-\frac{\hbar^2}{2m} \partial_x^2 u_s^1(x) + [V(x) - i\hbar s] u_s^1(x) \right] \\ &\quad + v_2(x) \left[-\frac{\hbar^2}{2m} \partial_x^2 u_s^2(x) + [V(x) - i\hbar s] u_s^2(x) \right] \\ &\quad + -\frac{\hbar^2}{2m} \left[\partial_x v_1(x) \partial_x u_s^1(x) + \partial_x v_2(x) \partial_x u_s^2(x) \right] \\ &= -\frac{\hbar^2}{2m} \left[\partial_x v_1(x) \partial_x u_s^1(x) + \partial_x v_2(x) \partial_x u_s^2(x) \right]\end{aligned}$$

In the last step, the first two terms are zero, since the $u_s^1(x)$, $u_s^2(x)$ are homogeneous solutions. Then, two equations are obtained:

$$\begin{cases} [\partial_x v_1(x)] u_s^1(x) + [\partial_x v_2(x)] u_s^2(x) = 0 \\ \partial_x v_1(x) \partial_x u_s^1(x) + \partial_x v_2(x) \partial_x u_s^2(x) = \frac{2mi}{\hbar} \Psi_0(x) \end{cases} \quad (1.21)$$

This equations can be solved using matrix representation:

$$\begin{bmatrix} u_s^1(x) & u_s^2(x) \\ \partial_x u_s^1(x) & \partial_x u_s^2(x) \end{bmatrix} \begin{bmatrix} \partial_x v_1(x) \\ \partial_x v_2(x) \end{bmatrix} = \begin{bmatrix} 0 \\ \frac{2mi}{\hbar} \Psi_0(x) \end{bmatrix} \quad (1.22)$$

Since $u_s^1(x)$, $u_s^2(x)$ are linearly independent homogeneous solutions, $W[u_s^1, u_s^2] \neq 0$. Then, the solutions v_1, v_2 can be derived as follows:

$$\begin{bmatrix} \partial_x v_1(x) \\ \partial_x v_2(x) \end{bmatrix} = \frac{1}{W[u_s^1, u_s^2]} \begin{bmatrix} \partial_x u_s^2(x) & -u_s^2(x) \\ -\partial_x u_s^1(x) & u_s^1(x) \end{bmatrix} \begin{bmatrix} 0 \\ \frac{2mi}{\hbar} \Psi_0(x) \end{bmatrix} \quad (1.23)$$

$$= \frac{2mi}{\hbar W[u_s^1, u_s^2]} \begin{bmatrix} -u_s^2(x) \Psi_0(x) \\ u_s^1(x) \Psi_0(x) \end{bmatrix} \quad (1.24)$$

$$\implies \begin{bmatrix} v_1(x) \\ v_2(x) \end{bmatrix} = \frac{2mi}{\hbar} \begin{bmatrix} \int^x \frac{-u_s^2(x') \Psi_0(x')}{W[u_s^1(x'), u_s^2(x')] } dx' \\ \int^x \frac{u_s^1(x') \Psi_0(x')}{W[u_s^1(x'), u_s^2(x')] } dx' \end{bmatrix} \quad (1.25)$$

Subsequently, the particular solution $\Phi_s^p(x)$ is:

$$\begin{aligned}\Phi_s^p(x) &= v_1(x) u_s^1(x) + v_2(x) u_s^2(x) \\ &= -\frac{2mi}{\hbar} \left[u_s^1(x) \int^x \frac{u_s^2(x')}{W[u_s^1, u_s^2]} \Psi_0(x') dx' - u_s^2(x) \int^x \frac{u_s^1(x')}{W[u_s^1, u_s^2]} \Psi_0(x') dx' \right]\end{aligned} \quad (1.26)$$

Alongside the complementary solution $\Phi_s^c(x) = \alpha_s u_s^1(x) + \beta_s u_s^2(x)$, the general solution to the non-homogeneous differential equation (1.17) is as given in equation (1.18):

$$\Phi_s(x) = \Phi_s^p(x) + \alpha_s u_s^1(x) + \beta_s u_s^2(x) \quad (1.27)$$

$$= -\frac{2mi}{\hbar} \left[\int^x \frac{u_s^1(x)u_s^2(x') - u_s^2(x)u_s^1(x')}{W[u_s^1, u_s^2]} \Psi_0(x') dx' \right] + \alpha_s u_s^1(x) + \beta_s u_s^2(x) \quad (1.28)$$

The coefficients α_s, β_s are decided with boundary conditions, which cannot be given in this step, because the potential is unknown. In Appendix A.1 and B.1, it will be shown that the general solution will be brought into the following form with given boundary conditions in a concrete situation:

$$\Phi_s(x) = \int_{-\infty}^{\infty} \tilde{K}(x, s, x', s_0 = 0) \Psi_{t_0}(x') dx' \quad (1.29)$$

As a last step, the inverse-Laplace transform is applied to $\Phi_s(x)$, leading to $\Psi_t(x)$:

$$\mathcal{L}^{-1}[\Phi_s](x) = \Psi_t(x) = \int_{-\infty}^{\infty} \mathcal{L}^{-1}[\tilde{K}](x, t, x', t_0) \Psi_{t_0}(x') dx' \quad (1.30)$$

As mentioned in the definition, the Kernel of the integral operator is the propagator.

$$K(x, t, x', t_0) = \mathcal{L}^{-1}[\tilde{K}](x, t, x', t_0) \quad (1.31)$$

1.4.4 Weak Solution with Distribution

The goal of an ordinary differential equation (ODE) and a partial differential equation (PDE) is to find a solution that satisfies the given differential equation. The Schrödinger equation is also a differential equation, and hence it is expected to have a solution. However, the Schrödinger equation and Hamiltonian in Chapter 2 and 3 are not continuous, and the solution is also not a smooth function. In such cases, the derivative of the solution may not exist. Nevertheless, this kind of solution can satisfy the Schrödinger equation as a weak solution. These types of solutions are called **Weak Solutions** [Eva98, p.8].

The Schrödinger equation is multiplied by a smooth, compactly supported function $\phi \in \mathcal{C}_{compact}^{\infty}(\mathbb{R} \times \mathbb{R}^3, \mathbb{R})$, and then integrated by parts [Eva98, p.137].

Definition 1.4.4. Let \hat{H} be the Hamiltonian, and $\Psi_t \in L^2(\mathbb{R}^3)$ be a solution to the Schrödinger equation:

$$i\hbar \frac{\partial}{\partial t} \Psi_t(\vec{r}) = \hat{H} \Psi_t(\vec{r}) = \left(-\frac{\hbar^2}{2m} \nabla^2 + V \right) \Psi_t(\vec{r}). \quad (1.32)$$

Assume that $\phi \in \mathcal{C}_{compact}^{\infty}(\mathbb{R} \times \mathbb{R}^3, \mathbb{R})$ is a test function. Then, $\Psi_t(\vec{r})$ is an integral solution of the Schrödinger equation if the following equation holds for arbitrary test function ϕ :

$$-i\hbar \int_{\mathbb{R}^4} \Psi_t(\vec{r}) \frac{\partial}{\partial t} \phi(t, \vec{r}) d\vec{r} dt + \int_{\mathbb{R}^4} \left(\frac{\hbar^2}{2m} \Psi_t(\vec{r}) \nabla^2 \phi(t, \vec{r}) - V \Psi_t(\vec{r}) \phi(t, \vec{r}) \right) d\vec{r} dt = 0 \quad (1.33)$$

This demonstrates that the differential equation can have solutions that are not differentiable. This weak solution will be employed in Chapter 2 and 3 to ensure that the derived solution satisfies the discontinuous Schrödinger equation. In Chapter 2, the Schrödinger equation is discontinuous only at $t = T$. In this case, the spatial integration in equation (1.33) does not contribute as a condition for the weak solution. Thus, the condition simplifies to a simpler form.

Theorem 1.4.5. *Let $\Psi_t \in L^2(\mathbb{R}^3)$ be a solution to the Schrödinger equation that is discontinuous in $t = T$ due to time-dependent potential $V = V(t)$, and let $\phi(t, \vec{r}) \in \mathcal{C}_{compact}^\infty(\mathbb{R} \times \mathbb{R}^3, \mathbb{R})$ be a test function. Then the condition for the weak solution is*

$$-i\hbar \int_{\mathbb{R}} \Psi_t(\vec{r}) \frac{\partial}{\partial t} \phi(t, \vec{r}) dt = \int_{\mathbb{R}} \hat{H} \Psi_t(\vec{r}) \phi(t, \vec{r}) dt \quad (1.34)$$

Proof. Since the wave function $\Psi_t \in L^2(\mathbb{R}^3)$ is smooth in $\vec{r} = (x, y, z)$, the second-order spatial derivative term in equation (1.33) can be integrated by parts twice, and the integration order can be changed using Fubini's theorem:

$$\int_{\mathbb{R}^3} \left[\int_{\mathbb{R}} \left(-i\hbar \Psi_t(\vec{r}) \frac{\partial}{\partial t} \phi(t, \vec{r}) + \frac{\hbar^2}{2m} \phi(t, \vec{r}) \nabla^2 \Psi_t(\vec{r}) - V(t) \Psi_t(\vec{r}) \phi(t, \vec{r}) \right) dt \right] d\vec{r} = 0 \quad (1.35)$$

This implies

$$\int_{\mathbb{R}} \left(-i\hbar \Psi_t(\vec{r}) \frac{\partial}{\partial t} \phi(t, \vec{r}) - \hat{H} \Psi_t(\vec{r}) \phi(t, \vec{r}) \right) dt = 0 \quad (1.36)$$

Thus, equation 1.35 is true when the time integral equals zero. \square

Similarly, in Chapter 3, the integration over t, y, z will not be considered because the Schrödinger equation is not continuous at $x = 0$.

Theorem 1.4.6. *Let $\xi_t, \eta_t, \zeta_t \in L^2(\mathbb{R})$, and $\Psi_t \in L^2(\mathbb{R}^3)$ be a separable solution to the Schrödinger equation as follows*

$$\Psi_t(\vec{r}) = \xi_t(x) \eta_t(y) \zeta_t(z), \quad (1.37)$$

which is discontinuous in $x = X$ due to the potential $V = V(x)$. Define $\phi(t, \vec{r}) \in \mathcal{C}_{compact}^\infty(\mathbb{R} \times \mathbb{R}^3, \mathbb{R})$ as a test function. Then the condition for the weak solution is:

$$\int_{\mathbb{R}} \left(-\frac{\hbar^2}{2m} \xi_t(x) \frac{\partial^2 \phi(t, \vec{r})}{\partial x^2} + V(x) \xi_t(x) \phi(t, \vec{r}) \right) dx = \int_{\mathbb{R}} \hat{H}_\xi \xi_t(x) \phi(t, \vec{r}) dx \quad (1.38)$$

$$\text{where } \hat{H}_\xi \xi_t(x) = i\hbar \frac{\partial}{\partial t} \xi_t(x) = \left(-\frac{\hbar^2}{2m} \frac{\partial^2}{\partial x^2} + V(x) \right) \xi_t(x) \quad (1.39)$$

Proof. Similar to the proof to theorem 1.4.5, the partial integration is applied with regards to t, y, z coordinates because the wave function is smooth in these parameters:

$$\begin{aligned} & \int_{\mathbb{R}^3} \int_{\mathbb{R}} \left(i\hbar \phi(t, \vec{r}) \frac{\partial}{\partial t} \xi_t(x) + \frac{\hbar^2}{2m} \xi_t(x) \frac{\partial^2}{\partial x^2} \phi(t, \vec{r}) - V(x) \xi_t(x) \phi(t, \vec{r}) \right) dx \eta_t(y) \zeta_t(z) dy dz dt \\ & + \int_{\mathbb{R}^3} \int_{\mathbb{R}} \left(i\hbar \phi(t, \vec{r}) \frac{\partial}{\partial t} \eta_t(y) + \frac{\hbar^2}{2m} \phi(t, \vec{r}) \frac{\partial^2}{\partial y^2} \eta_t(y) \right) dy \xi_t(x) \zeta_t(z) dx dz dt \\ & + \int_{\mathbb{R}^3} \int_{\mathbb{R}} \left(i\hbar \phi(t, \vec{r}) \frac{\partial}{\partial t} \zeta_t(z) + \frac{\hbar^2}{2m} \phi(t, \vec{r}) \frac{\partial^2}{\partial z^2} \zeta_t(z) \right) dz \xi_t(x) \eta_t(y) dx dy dt = 0 \end{aligned} \quad (1.40)$$

Note that the second and third term on the left-hand side of this equation vanishes thanks to:

$$i\hbar \frac{\partial}{\partial t} \eta_t(y) + \frac{\hbar^2}{2m} \frac{\partial^2}{\partial y^2} \eta_t(y) = 0 \quad (1.41)$$

$$i\hbar \frac{\partial}{\partial t} \zeta_t(z) + \frac{\hbar^2}{2m} \frac{\partial^2}{\partial z^2} \zeta_t(z) = 0. \quad (1.42)$$

These equations can be obtained from the Schrödinger equation. Now, only the first term in equation (1.40) have to satisfy the following condition:

$$\int_{\mathbb{R}} \left(i\hbar \phi(t, \vec{r}) \frac{\partial}{\partial t} \xi_t(x) + \frac{\hbar^2}{2m} \xi_t(x) \frac{\partial^2}{\partial x^2} \phi(t, \vec{r}) - V(x) \xi_t(x) \phi(t, \vec{r}) \right) dx = 0 \quad (1.43)$$

□

In this chapter, the behavior of a neutral particle will be demonstrated in a scenario where a constant magnetic field is turned off at a specific moment. To achieve this, the solutions to the Schrödinger equation will first be derived for the cases of a free particle and a particle in the constant magnetic field, respectively. Thereafter, the solution to the Schrödinger equation for the constant magnetic field that is turned off at a specific moment, will be derived by combining those two solutions found previously. Finally, the dynamics of the neutral particle will be analyzed qualitatively and quantitatively.

The time-dependent Schrödinger equation

$$i\hbar \frac{\partial \Psi_t(\vec{r})}{\partial t} = \hat{H} \Psi_t(\vec{r}), \quad (2.1)$$

where \hat{H} is the Hamiltonian, and $\Psi_t(\vec{r})$ is the wave function of the particle, will be studied for different Hamiltonians \hat{H} , which are introduced below.

2.1 Free Particle

2.1.1 Hamiltonian and Schrödinger Equation

To begin, we consider the Schrödinger equation for a freely moving particle, where the potential $V = 0$. For this, the Hamiltonian is given by (see equation (1.1)):

$$\hat{H} = \frac{\hat{P}^2}{2m} = -\frac{\hbar^2}{2m} \nabla^2 \quad (2.2)$$

2.1.2 Time-Independent Solution

Now the solution to Schrödinger equation for a free particle will be derived. At first, a time-independent solution will be found, and then the time-dependent solution will be derived using propagator. To find the time-independent solution for a free particle, the time-dependent solution is assumed to be separable as $\Psi_t(\vec{r}) = \psi(\vec{r})\kappa(t)$, and the time-independent Schrödinger equation with respect to $\psi(\vec{r})$,

$$\hat{H}\psi(\vec{r}) = -\frac{\hbar^2}{2m} \nabla^2 \psi(\vec{r}) = E\psi(\vec{r}), \quad (2.3)$$

has to be solved. In eigenvalue problem, $\psi(\vec{r})$ is a eigenfunction of the time-independent Schrödinger equation and E is the corresponding eigenvalue, which represents the energy of a particle in this eigenstate. Thanks to many books on quantum mechanics, the solution is well known [GS18]:

$$\psi(\vec{r}) = A_{\vec{k}} \exp(i\vec{k} \cdot \vec{r}) \quad \text{with} \quad |\vec{k}| = \frac{\sqrt{2mE}}{\hbar}. \quad (2.4)$$

$A_{\vec{k}}$ is a coefficient with respect to \vec{k} . This eigenvector, however, cannot be a physical solution because it is not a square-integrable function, which is not an element of the Hilbert space. In this case, general solutions that are square-integrable can be constructed by means of a linear combination of the eigenfunctions. One of the appropriate general solutions is a Gaussian wave packet. The Gaussian wave packet with a average momentum $\vec{p}_0 = \hbar\vec{k}_0$ can be derived by applying the Fourier transformation to the Gaussian wave packet $\phi(\vec{k})$, which is centered at $\vec{k} = \vec{k}_0$ in momentum space:

$$\psi(\vec{r}) = \mathcal{F}[\phi(\vec{k})] \quad (2.5)$$

where

$$\phi(\vec{k}) = \left(\frac{2b}{\pi}\right)^{\frac{3}{4}} \exp\left(-b(\vec{k} - \vec{k}_0)^2\right) \quad (2.6)$$

Applying the inverse Fourier transformation results in (see equation (1.8)):

$$\begin{aligned} \psi(\vec{r}) &= \frac{1}{(2\pi)^{\frac{3}{2}}} \int_{\mathbb{R}^3} d^3k \exp(i\vec{k} \cdot \vec{r}) \phi(\vec{k}) \\ &= \frac{1}{(2\pi)^{\frac{3}{2}}} \left(\frac{2b}{\pi}\right)^{\frac{3}{4}} \int_{\mathbb{R}^3} d^3k \exp(i\vec{k} \cdot \vec{r}) \exp\left(-b(\vec{k} - \vec{k}_0)^2\right) \\ &= \frac{1}{(2\pi)^{\frac{3}{2}}} \left(\frac{2b}{\pi}\right)^{\frac{3}{4}} \int_{\mathbb{R}^3} d^3k \exp(ik_x x + ik_y y + ik_z z) \exp\left(-b(\vec{k}^2 - 2\vec{k} \cdot \vec{k}_0 + \vec{k}_0^2)\right) \\ &= \frac{1}{(2\pi)^{\frac{3}{2}}} \left(\frac{2b}{\pi}\right)^{\frac{3}{4}} \exp(-b\vec{k}_0^2) \int_{\mathbb{R}} dk_x \exp(ik_x x - bk_x^2 + 2bk_x k_{0x}) \\ &\quad \cdot \int_{\mathbb{R}} dk_y \exp(ik_y y - bk_y^2 + 2bk_y k_{0y}) \int_{\mathbb{R}} dk_z \exp(ik_z z - bk_z^2 + 2bk_z k_{0z}) \end{aligned}$$

This integral can be calculated using completing the square and Gaussian integral,

$$mx^2 + nx + l = m\left(x + \frac{n}{2m}\right)^2 + l - \frac{n^2}{4m} \quad (2.7)$$

$$\int_{\mathbb{R}} dx \exp\left(-m\left(x + \frac{n}{2m}\right)^2\right) = \sqrt{\frac{\pi}{m}}, \quad (2.8)$$

resulting in the wave function in position space:

$$\begin{aligned} \psi(\vec{r}) &= \left(\frac{1}{2\pi b}\right)^{\frac{3}{4}} \exp\left(-\frac{\vec{r}^2}{4b} + i\vec{k}_0 \cdot \vec{r}\right) \\ &= \left(\frac{2a}{\pi}\right)^{\frac{3}{4}} \exp\left(-a\vec{r}^2 + i\vec{k}_0 \cdot \vec{r}\right) \quad \text{with } a = \frac{1}{4b}. \end{aligned} \quad (2.9)$$

Considering the center of the Gaussian wave packet \vec{r}_c , the wave functions is shifted:

$$\psi(\vec{r}) = \left(\frac{2a}{\pi}\right)^{\frac{3}{4}} \exp\left[-a(\vec{r} - \vec{r}_c)^2 + i\vec{k}_0 \cdot \vec{r}\right]. \quad (2.10)$$

This is the initial wave function $\psi(\vec{r})$.

2.1.3 Time-Dependent Solution

The time-dependent wave function can be obtained by integrating the initial wave function $\psi_0(\vec{r})$ with respect to x' with the propagator $K(x, t, x', 0)$. The one-dimensional propagator $K_0(x, t, x', 0)$ for a free particle is (for the derivation, see Appendix A.1)

$$K_0(x, t, x', 0) = \sqrt{\frac{m}{2\pi i\hbar t}} \exp\left[\frac{im(x-x')^2}{2\hbar t}\right]. \quad (2.11)$$

In Subsection 2.1.2 the initial wave function with Gaussian wave packet $\psi_0(\vec{r})$ was found (equation (2.10)), which is separable in x, y, z coordinates:

$$\begin{aligned} \psi_0(\vec{r}) &= \xi_0(x)\eta_0(y)\zeta_0(z) \\ &= \left(\frac{2a}{\pi}\right)^{\frac{1}{4}} \exp\left(-a(x-x_c)^2 + ik_{0x}x\right) \\ &\quad \cdot \left(\frac{2a}{\pi}\right)^{\frac{1}{4}} \exp\left(-a(y-y_c)^2 + ik_{0y}y\right) \left(\frac{2a}{\pi}\right)^{\frac{1}{4}} \exp\left(-a(z-z_c)^2 + ik_{0z}z\right), \end{aligned} \quad (2.12)$$

$$\text{where } \vec{r} = (x, y, z)^T \quad \text{and} \quad \vec{k}_0 = (k_{0x}, k_{0y}, k_{0z})^T$$

Thanks to this separation of the initial wave function, the propagator K_0 can be applied separately in x, y, z coordinates as well, namely:

$$\begin{aligned} \psi_t(\vec{r}) &= \xi_t(x)\eta_t(y)\zeta_t(z) \\ &= \int_{-\infty}^{\infty} K_0(x, t, x', 0)\xi_0(x')dx' \int_{-\infty}^{\infty} K_0(y, t, y', 0)\eta_0(y')dy' \int_{-\infty}^{\infty} K_0(z, t, z', 0)\zeta_0(z')dz' \end{aligned}$$

Each integral in this equation is symmetrical, thus it suffices to calculate only one of the integrals, and the first integral results in $\xi_t(x)$:

$$\begin{aligned} \xi_t(x) &= \int_{-\infty}^{\infty} K_0(x, t, x', 0)\xi_0(x')dx' \\ &= \left(\frac{2a}{\pi}\right)^{\frac{1}{4}} \sqrt{\frac{m}{m+2i\hbar at}} \exp\left[\frac{-ma}{m+2i\hbar at} \left(x-x_c - \frac{\hbar k_{0x}t}{m}\right)^2 + i\left(k_{0x}x - \frac{\hbar^2 k_{0x}^2 t}{2m\hbar}\right)\right] \end{aligned} \quad (2.13)$$

By substituting γ_t with $\frac{m}{m+2i\hbar at}$, the time-dependent wave function $\xi_t(x)$ is simplified:

$$\xi_t(x) = \left(\frac{2a}{\pi}\right)^{\frac{1}{4}} \sqrt{\gamma_t} \exp\left[-a\gamma_t \left(x-x_c - \frac{\hbar k_{0x}t}{m}\right)^2 + i\left(k_{0x}x - \frac{\hbar^2 k_{0x}^2 t}{2m\hbar}\right)\right] \quad (2.14)$$

As mentioned above, the other separated wave functions $\eta_t(y)$, $\zeta_t(z)$ have the same form:

$$\eta_t(y) = \left(\frac{2a}{\pi}\right)^{\frac{1}{4}} \sqrt{\gamma_t} \exp\left[-a\gamma_t \left(y-y_c - \frac{\hbar k_{0y}t}{m}\right)^2 + i\left(k_{0y}y - \frac{\hbar^2 k_{0y}^2 t}{2m\hbar}\right)\right] \quad (2.15)$$

$$\zeta_t(z) = \left(\frac{2a}{\pi}\right)^{\frac{1}{4}} \sqrt{\gamma_t} \exp\left[-a\gamma_t \left(z-z_c - \frac{\hbar k_{0z}t}{m}\right)^2 + i\left(k_{0z}z - \frac{\hbar^2 k_{0z}^2 t}{2m\hbar}\right)\right] \quad (2.16)$$

As a result, the time-dependent wave function $\psi_t(\vec{r})$ is:

$$\begin{aligned}\psi_t(\vec{r}) &= \xi_t(x)\eta_t(y)\zeta_t(z) \\ &= \left(\frac{2a}{\pi}\right)^{\frac{3}{4}} \gamma_t^{\frac{3}{2}} \exp \left[-a\gamma_t \left(\vec{r} - \vec{r}_c - \frac{\hbar\vec{k}_0 t}{m} \right)^2 + i \left(\vec{k}_0 \cdot \vec{r} - \frac{\hbar^2 \vec{k}_0^2}{2m\hbar} t \right) \right]\end{aligned}\quad (2.17)$$

Now, it must be ensured that this time-dependent wave function $\psi_t(\vec{r})$ is a solution to the Schrödinger equation for a free particle. It is shown in Appendix A.3.

2.2 Particle in Constant Magnetic Field

In this Section, the solution to the Schrödinger equation for a neutral spin- $\frac{1}{2}$ particle with a magnetic moment in a constant magnetic field will be derived. For simplicity we will consider space-spin separated wave packets that are easier to handle using the results from the previous section.

2.2.1 Hamiltonian and Pauli Equation

When a neutral particle moves in a magnetic field, it interacts with the field. Usually the principle of electromagnetic minimal coupling is applied to the Hamiltonian to describe it. However, it does not aid in finding the Hamiltonian for a neutral particle in a magnetic field as it has no charge. Nevertheless, the interaction of a neutral particle with a magnetic field can be described by Pauli equation with the experimentally measured magnetic dipole moment. The Hamiltonian \hat{H} of Pauli equation is given by [AS23, eq.1]:

$$\hat{H} = \frac{\hat{P}^2}{2m} - \mu \vec{\sigma} \cdot \vec{B}\quad (2.18)$$

Here, \vec{B} is the magnetic field, μ is magnetic dipole moment, and $\vec{\sigma}$ is Pauli vector (see equation (1.5)). The substitution of momentum operator $\hat{P} = -i\hbar\nabla$ is applied to this Hamiltonian, resulting in:

$$\hat{H} = -\frac{\hbar^2}{2m}\nabla^2 - \mu \vec{\sigma} \cdot \vec{B}(t, \vec{r})\quad (2.19)$$

2.2.2 Solutions

In this subsection, the solutions to the Pauli equation in a constant magnetic field will be derived. To begin, we will consider a uniform magnetic field whose direction defines the z -axis of our coordinate system without loss of generality. This choice simplifies our calculations because the σ_z matrix is diagonal. With this setup, Pauli equation for a constant magnetic field is

$$i\hbar \frac{\partial}{\partial t} \Psi_t(\vec{r}) = -\frac{\hbar^2}{2m} \nabla^2 \Psi_t(\vec{r}) - \mu \sigma_z B_z \Psi_t(\vec{r}).\quad (2.20)$$

For simplicity, let us consider space-spin separated wave functions: Those of the form $\Psi_t(\vec{r}) = \psi_t(\vec{r})\chi_t$, where ψ_t is a spin-0 or scalar wave function introduced earlier and χ_t is a two-spinor

dependent only on time. ψ_t is called spatial wave function and χ is called spin wave function, for which equation (2.20) implies:

$$\begin{aligned} i\hbar[\partial_t\psi_t(\vec{r})]\chi_t + i\hbar\psi_t(\vec{r})\partial_t\chi_t &= -\frac{\hbar^2}{2m}[\nabla^2\psi_t(\vec{r})]\chi_t - \mu\sigma_z B_z\psi_t(\vec{r})\chi_t \\ &= -\frac{\hbar^2}{2m}[\nabla^2\psi_t(\vec{r})]\chi_t - \psi_t(\vec{r})\mu\sigma_z B_z\chi_t \end{aligned} \quad (2.21)$$

Rearranging the terms gives:

$$\left[i\hbar\partial_t\psi_t(\vec{r}) + \frac{\hbar^2}{2m}\nabla^2\psi_t(\vec{r}) \right] \chi_t + \psi_t(\vec{r}) [i\hbar\partial_t\chi_t + \mu\sigma_z B_z\chi_t] = 0. \quad (2.22)$$

Since the terms enclosed in each square bracket must independently equal zero in order for the equation to be satisfied at each \vec{r} and t , Pauli equation decouples into two differential equations:

$$\begin{cases} i\hbar\partial_t\psi_t(\vec{r}) + \frac{\hbar^2}{2m}\nabla^2\psi_t(\vec{r}) = 0 \\ i\hbar\partial_t\chi_t + \mu\sigma_z B_z\chi_t = 0 \end{cases} \quad (2.23)$$

Assuming ψ_t is a Gaussian at $t = 0$, the solution to the first differential equation was already found (see Subsection (2.1.3)). The solution to the second equation is straightforward:

$$\chi_t = \exp\left(\frac{i\mu\sigma_z B_z t}{\hbar}\right) \chi_0, \quad (2.24)$$

where χ_0 is the initial spin state of the particle, which is expressed in the form of a Bloch vector:

$$\chi_0 = \begin{bmatrix} \sin\left(\frac{\theta}{2}\right) \\ \cos\left(\frac{\theta}{2}\right) \exp(i\phi) \end{bmatrix} \quad (2.25)$$

Combining this with the spatial wave function, the total time-dependent wave function $\Psi_t(\vec{r})$ is

$$\begin{aligned} \Psi_t(\vec{r}) &= \psi_t(\vec{r})\chi_t \\ &= \left(\frac{2a}{\pi}\right)^{\frac{3}{4}} \gamma_t^{\frac{3}{2}} \exp\left[-a\gamma_t\left(\vec{r} - \vec{r}_c - \frac{\hbar\vec{k}_0}{m}t\right)^2 + i\left(\vec{k}_0 \cdot \vec{r} - \frac{\hbar k_0^2}{2m}t\right)\right] \exp\left(\frac{i\mu\sigma_z B_z t}{\hbar}\right) \chi_0 \end{aligned} \quad (2.26)$$

The spatial wave function was already shown to be a solution to the first term on the left-hand side of equation (2.22), which is a Schrödinger equation for a free particle. The spin wave function was directly obtained by solving the differential equation in the second term in equation (2.22). Thus, this time-dependent wave function $\Psi_t(\vec{r})$ is a solution to the Pauli equation (2.20).

In the following section, this solution together with the solution for a free particle (see equation (2.17)) will be employed to prove that the time-dependent wave function in the switching-off magnetic field is also a solution to the discontinuous Pauli equation.

2.3 Particle in Uniform Magnetic Field Abruptly Turned Off at Time T

As mentioned at the beginning of this chapter, the goal is to find a solution to the Pauli equation in a scenario where the magnetic field is abruptly turned off. To achieve this, solutions to the Pauli equation for a free particle and a constant magnetic field were derived in the previous sections. These solutions will now be combined to model the situation of switching off the magnetic field. To this end, we assume the same setups as previous subsections: Uniform magnetic field defines its direction as z -axis, and the wave function Ψ_t is space-spin separated as $\Psi_t(\vec{r}) = \psi_t(\vec{r})\chi_t$ with the spatial wave function ψ_t , which is an Gaussian at $t = 0$, multiplied by a spin wave function χ_t .

2.3.1 Hamiltonian

This scenario is mathematically represented by assuming the magnetic field is turned off at time $t = T$. This can be mathematically modeled using the Heaviside step function $\Theta(t)$, which is defined as follows:

$$\Theta(t) = \begin{cases} 1 & \text{for } t \geq 0 \\ 0 & \text{for } t < 0 \end{cases} \quad (2.27)$$

Using the Heaviside step function, the magnetic field is expressed as follows:

$$\vec{B} = \begin{bmatrix} 0 \\ 0 \\ B_z\Theta(T-t) \end{bmatrix}. \quad (2.28)$$

The Hamiltonian for this system is then given as follows:

$$\hat{H} = -\frac{\hbar^2}{2m}\nabla^2 - \mu\sigma_z B_z\Theta(T-t) \quad (2.29)$$

2.3.2 Solutions

The solution Ψ_t to the Pauli equation

$$i\hbar\frac{\partial}{\partial t}\Psi_t(\vec{r}) = \left[-\frac{\hbar^2}{2m}\nabla^2 - \mu\sigma_z B_z\Theta(T-t)\right]\Psi_t(\vec{r}) \quad (2.30)$$

can be constructed by combining the solution for a free particle (2.17) and the solution for a constant magnetic field (2.26) as follows, with the substitution $\vec{r}_t = \vec{r} - \vec{r}_c - \frac{\hbar\vec{k}_0}{m}t$:

$$\Psi_t(\vec{r}) = \begin{cases} \left(\frac{2a}{\pi}\right)^{\frac{3}{4}}\gamma_t^{\frac{3}{2}}\exp\left[-a\gamma_t\vec{r}_t^2 + i\left(\vec{k}_0 \cdot \vec{r} - \frac{\hbar^2\vec{k}_0^2}{2m\hbar}t\right)\right]\exp\left(\frac{i\mu\sigma_z B_z t}{\hbar}\right)\chi_0, & t \leq T \\ \left(\frac{2a}{\pi}\right)^{\frac{3}{4}}\gamma_t^{\frac{3}{2}}\exp\left[-a\gamma_t\vec{r}_t^2 + i\left(\vec{k}_0 \cdot \vec{r} - \frac{\hbar^2\vec{k}_0^2}{2m\hbar}t\right)\right]\exp\left(\frac{i\mu\sigma_z B_z T}{\hbar}\right)\chi_0, & t > T \end{cases} \quad (2.31)$$

This solution was not directly obtained by solving the given Pauli equation. Therefore, it must be shown that this solution satisfies the Pauli equation. However, This solution is not smooth at $t = T$ because the Hamiltonian (2.29) is discontinuous at $t = T$. Consequently, the solution is

not differentiable at $t = T$. However, it is still possible to demonstrate that this solution is valid in the weak sense using a test function $\phi(t)$. In other words, it must be shown that this solution is a weak solution. Let $\phi(t) \in \mathcal{C}_c^\infty(\mathbb{R}, \mathbb{R})$ be a smooth, compactly supported function, and the solution $\Psi_t(\vec{r})$ be a weak solution. Then, this solution must satisfy the following equation (see Theorem 1.4.5):

$$\int_{-\infty}^{\infty} \hat{H}\Psi_t(\vec{r})\phi(t)dt = -i\hbar \int_{-\infty}^{\infty} \Psi_t(\vec{r})\frac{\partial}{\partial t}\phi(t)dt \quad (2.32)$$

The right-hand side of this equation is integrated by parts:

$$\int_{-\infty}^{\infty} \hat{H}\Psi_t(\vec{r})\phi(t)dt = -i\hbar \left[\Psi_t(\vec{r})\phi(t) \Big|_{-\infty}^{\infty} - \int_{-\infty}^{\infty} \phi(t)\frac{\partial}{\partial t}\Psi_t(\vec{r})dt \right] \quad (2.33)$$

Since $\phi(t)$ is compactly supported, the boundary term vanishes, leaving:

$$\int_{-\infty}^{\infty} \hat{H}\Psi_t(\vec{r})\phi(t)dt = i\hbar \int_{-\infty}^{\infty} \phi(t)\frac{\partial}{\partial t}\Psi_t(\vec{r})dt \quad (2.34)$$

Breaking the integral into two regions near $t = T$:

$$i\hbar \int_{-\infty}^{\infty} \phi(t)\frac{\partial}{\partial t}\Psi_t(\vec{r})dt = i\hbar \lim_{\epsilon \rightarrow 0} \int_{-\infty}^{T-\epsilon} \phi(t)\frac{\partial}{\partial t}\Psi_t(\vec{r})dt + i\hbar \lim_{\epsilon \rightarrow 0} \int_{T+\epsilon}^{\infty} \phi(t)\frac{\partial}{\partial t}\Psi_t(\vec{r})dt \quad (2.35)$$

The wave function $\Psi_t(\vec{r})$ in the first term of this equation satisfies the Pauli equation for a constant magnetic field. Hence, this can be expressed using Hamiltonian $\hat{H}_{const} = -\frac{\hbar^2}{2m}\nabla^2 - \mu\sigma_z B_z$. For the second term in equation (2.35) the wave function $\Psi_t(\vec{r})$ is the solution to the Pauli equation for a free particle. Accordingly, the time derivative can be replaced by $\hat{H}_{free} = -\frac{\hbar^2}{2m}\nabla^2$.

$$i\hbar \lim_{\epsilon \rightarrow 0} \int_{-\infty}^{T-\epsilon} \phi(t)\frac{\partial}{\partial t}\Psi_t(\vec{r})dt + i\hbar \lim_{\epsilon \rightarrow 0} \int_{T+\epsilon}^{\infty} \phi(t)\frac{\partial}{\partial t}\Psi_t(\vec{r})dt \quad (2.36)$$

$$= \lim_{\epsilon \rightarrow 0} \int_{-\infty}^{T-\epsilon} \phi(t) \left(-\frac{\hbar^2}{2m}\nabla^2 - \mu\sigma_z B_z \right) \Psi_t(\vec{r}) + \lim_{\epsilon \rightarrow 0} \int_{T+\epsilon}^{\infty} \phi(t) \left(-\frac{\hbar^2}{2m}\nabla^2 \right) \Psi_t(\vec{r})dt \quad (2.37)$$

$$= \int_{-\infty}^{\infty} \phi(t) \left(-\frac{\hbar^2}{2m}\nabla^2 - \mu\sigma_z B_z \Theta(T-t) \right) \Psi_t(\vec{r})dt = \int_{-\infty}^{\infty} \phi(t)\hat{H}\Psi_t(\vec{r})dt \quad (2.38)$$

This confirms that the given wave function (2.31) is a weak solution to the Pauli equation (2.30).

2.4 Probability Density ρ^Ψ and Probability Current Density \mathcal{J}^Ψ

To analyze the dynamics of a neutral particle in a uniform magnetic field that is switched off at time T , let us investigate the probability density and the probability current density for the

given situation. The probability density $\rho^{\Psi_t}(\vec{r})$ and the probability current density $\mathcal{J}^{\Psi_t}(\vec{r})$ can be calculated (see equation (1.3) for Pauli current). The probability density is

$$\begin{aligned}\rho^{\Psi_t}(\vec{r}) &= \Psi_t^*(\vec{r})\Psi_t(\vec{r}) \\ &= \left(\frac{2a}{\pi}\right)^{\frac{3}{2}} |\gamma_t|^3 \exp\left[-a(\gamma_t^* + \gamma_t)\tilde{r}_t^2\right] \\ &= \left(\frac{2a}{\pi}\right)^{\frac{3}{2}} |\gamma_t|^3 \exp\left[-2a|\gamma_t|^2\tilde{r}_t^2\right]\end{aligned}\quad (2.39)$$

The probability current density is

$$\mathcal{J}^{\Psi_t}(\vec{r}) = \frac{\hbar}{m} \text{Im}[\Psi_t^*(\vec{r})\nabla\Psi_t(\vec{r})] + \frac{\hbar}{2m} \nabla \times [\Psi_t^*(\vec{r})\vec{\sigma}\Psi_t(\vec{r})] \quad (2.40)$$

The second term can be greatly simplified for wave functions that are space-spin separated: The curl of $\Psi_t^*(\vec{r})\vec{\sigma}\Psi_t(\vec{r})$ can be expressed as $\nabla[\Psi_t^*(\vec{r})\Psi_t(\vec{r})] \times [\chi_t^*\vec{\sigma}\chi_t]$, since χ_t does not depend on the coordinate \vec{r} :

$$\begin{aligned}&\frac{\hbar}{m} \text{Im}[\Psi_t^*(\vec{r})\nabla\Psi_t(\vec{r})] + \frac{\hbar}{2m} \nabla \times [\Psi_t^*(\vec{r})\vec{\sigma}\Psi_t(\vec{r})] \\ &= \frac{\hbar}{m} \left(\frac{2a}{\pi}\right)^{\frac{3}{2}} |\gamma_t|^3 \exp\left[-a(\gamma_t^* + \gamma_t)\tilde{r}_t^2\right] \text{Im}\left[-2a\gamma_t\vec{r}_t + i\vec{k}_0\right] + \frac{\hbar}{2m} \nabla[\psi_t^*(\vec{r})\psi_t(\vec{r})] \times [\chi_t^*\vec{\sigma}\chi_t] \\ &= \frac{\hbar}{m} \left(\frac{2a}{\pi}\right)^{\frac{3}{2}} |\gamma_t|^3 \exp\left[-2a|\gamma_t|^2\tilde{r}_t^2\right] \text{Im}\left[-2a\gamma_t\vec{r}_t + i\vec{k}_0\right] \\ &\quad + \frac{\hbar}{2m} \left(\frac{2a}{\pi}\right)^{\frac{3}{2}} |\gamma_t|^3 \exp\left[-2a|\gamma_t|^2\tilde{r}_t^2\right] \left[-4a|\gamma_t|^2\vec{r}_t\right] \times [\chi_t^*\vec{\sigma}\chi_t] \\ &= -\frac{a\hbar}{m} \left(\frac{2a}{\pi}\right)^{\frac{3}{2}} |\gamma_t|^3 \exp\left[-2a|\gamma_t|^2\tilde{r}_t^2\right] \left(\text{Im}\left[2\gamma_t\vec{r}_t - i\vec{k}_0\right] + 2|\gamma_t|^2\vec{r}_t \times \chi_t^*\vec{\sigma}\chi_t\right),\end{aligned}\quad (2.41)$$

Where the time-dependent spin wave function χ_t is

$$\chi_t = \begin{cases} \exp\left[i\frac{\mu\sigma_z B_z t}{\hbar}\right]\chi_0 = \begin{bmatrix} \sin\left(\frac{\theta}{2}\right) \exp\left(i\frac{\mu B_z t}{\hbar}\right) \\ \cos\left(\frac{\theta}{2}\right) \exp\left(i\phi - i\frac{\mu B_z t}{\hbar}\right) \end{bmatrix}, & t \leq T \\ \exp\left[i\frac{\mu\sigma_z B_z T}{\hbar}\right]\chi_0 = \begin{bmatrix} \sin\left(\frac{\theta}{2}\right) \exp\left(i\frac{\mu B_z T}{\hbar}\right) \\ \cos\left(\frac{\theta}{2}\right) \exp\left(i\phi - i\frac{\mu B_z T}{\hbar}\right) \end{bmatrix}, & t > T \end{cases} \quad (2.42)$$

Notably, the probability density (2.40) is independent of the spin polarization angles θ and ϕ as well as the strength of the magnetic field, viz., B_z . In contrast, the probability current density is dependent on both spin polarization angles and B_z . Interestingly, this shows that the probability current densities for different spin polarization and B_z are not the same, while probability density is the same.

2.4.1 Non-Dimensionalization Convention

Before analyzing the dynamics of a neutral particle in the given magnetic field, it is useful to adopt a non-dimensionalization convention. Without this step, the coefficients involved may be so small or so large that numerical analysis becomes inefficient. The variables are substituted as follows:

$$\sqrt{a}\vec{r} = \vec{\bar{r}}, \quad \frac{\vec{k}}{\sqrt{a}} = \vec{\bar{k}}, \quad \frac{\mu m B}{\hbar^2 a} = \bar{B}, \quad \frac{\hbar a t}{m} = \bar{t}, \quad \frac{\Psi_t(\vec{r})}{a^{\frac{3}{4}}} = \bar{\Psi}_t(\vec{\bar{r}}) \quad (2.43)$$

After substitution, the overline notation is omitted for simplicity. With this non-dimensionalization convention, the wave function $\Psi_t(\vec{r})$ and the function γ_t are given by:

$$\Psi_t(\vec{r}) = \begin{cases} \left(\frac{2}{\pi}\right)^{\frac{3}{4}} \gamma_t^{\frac{3}{2}} \exp\left[-\gamma_t \vec{r}_t^2 + i\left(\vec{k}_0 \cdot \vec{r} - \frac{k_0^2}{2}t\right)\right] \exp(i\sigma_z B_z t) \chi_0, & t \leq T \\ \left(\frac{2}{\pi}\right)^{\frac{3}{4}} \gamma_t^{\frac{3}{2}} \exp\left[-\gamma_t \vec{r}_t^2 + i\left(\vec{k}_0 \cdot \vec{r} - \frac{k_0^2}{2}t\right)\right] \exp(i\sigma_z B_z T) \chi_0, & t > T \end{cases} \quad (2.44)$$

$$\gamma_t = \frac{1}{1 + 2it} \quad (2.45)$$

The probability density $\rho^{\Psi_t}(\vec{r})$ and the probability current density $\mathcal{J}^{\Psi_t}(\vec{r})$ are then given by:

$$\rho^{\Psi_t}(\vec{r}) = \left(\frac{2}{\pi}\right)^{\frac{3}{2}} |\gamma_t|^3 \exp\left[-2|\gamma_t|^2 \vec{r}_t^2\right] \quad (2.46)$$

$$\mathcal{J}^{\Psi_t}(\vec{r}) = -\left(\frac{2}{\pi}\right)^{\frac{3}{2}} |\gamma_t|^3 \exp\left[-2|\gamma_t|^2 \vec{r}_t^2\right] \left(-\frac{4t}{1 - 4t^2} \vec{r}_t - \vec{k}_0 + 2|\gamma_t|^2 \vec{r}_t \times \chi_t^* \vec{\sigma} \chi_t\right), \quad (2.47)$$

where

$$\vec{r}_t = \vec{r} - \vec{r}_c - \vec{k}_0 t \quad (2.48)$$

$$\chi_t = \begin{cases} \exp[i\sigma_z B_z t] \chi_0 = \begin{bmatrix} \sin\left(\frac{\theta}{2}\right) \exp(iB_z t) \\ \cos\left(\frac{\theta}{2}\right) \exp(i\phi - iB_z t) \end{bmatrix}, & t \leq T \\ \exp[i\sigma_z B_z T] \chi_0 = \begin{bmatrix} \sin\left(\frac{\theta}{2}\right) \exp(iB_z T) \\ \cos\left(\frac{\theta}{2}\right) \exp(i\phi - iB_z T) \end{bmatrix}, & t > T \end{cases} \quad (2.49)$$

In this non-dimensionalization, it is immediately evident how large or small the variables are. To recover the units, the width of the Gaussian wave packet for a neutron is set to 50nm, i.e. $a = \frac{1}{2\sigma^2} = 2 \cdot 10^{14} \text{m}^{-2}$, which leads to the following corresponding relations from equation (2.43):

- $x = 1$ corresponds to $7.0710678119 \cdot 10^{-8} \text{m}$
- $k = 1$ corresponds to $1.414213562 \cdot 10^7 \text{m}^{-1}$
- $t = 1$ corresponds to $7.941273265 \cdot 10^{-8} \text{s}$
- $B = 1$ corresponds to -0.137436653 T

In the following subsections, it will be assumed that the center of the initial wave function is placed at the origin, $\vec{r}_c = 0$, and the wave function propagates along x -axis with $\vec{k}_0 = (5, 0, 0)^T$. Also, the spin polarization is chosen to $\theta = \frac{\pi}{2}$ and $\phi = 0$.

2.4.2 Probability Density

The probability density given by equation (2.46) has a Gaussian profile with a time-dependent magnitude and width. The behavior of the magnitude and width can be analyzed with the following equation:

$$|\gamma_t| = \sqrt{\frac{2}{1 + 4t^2}} \quad (2.50)$$

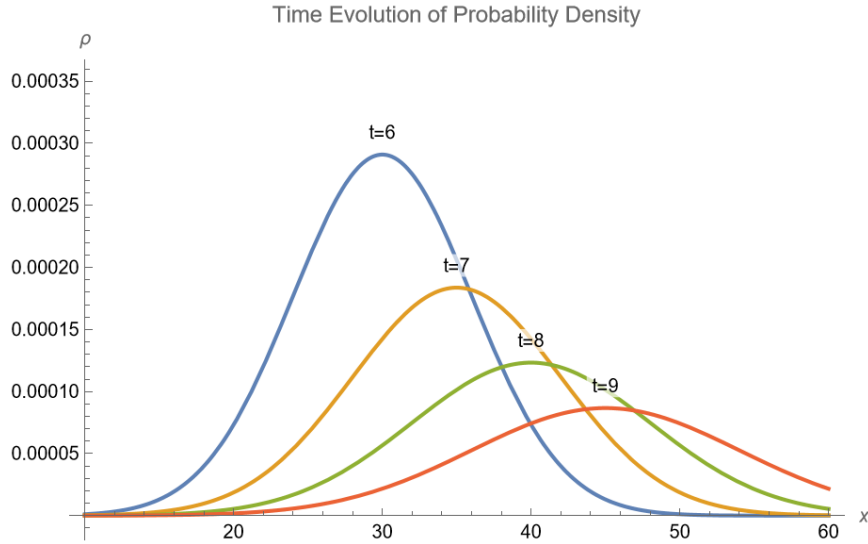


Figure 2.1: The Probability density is illustrated for x and $t=4, 5, 6, 7$, while variables y, z are fixed to zero. This figure demonstrates how the magnitude, width, and center position of the probability density evolve over time.

Figure 2.1 illustrates the evolution of $\rho^{\Psi_t}(x)$. The width of the wave packet increases as time progresses, which can be confirmed as follows:

$$\frac{1}{\sqrt{2}|\gamma_t|} = \sqrt{\frac{1+4t^2}{4}} \quad (2.51)$$

Simultaneously, the center of the probability density moves along the direction of the wave vector \vec{k}_0 . Additionally, the magnitude decreases with time, which is verified by:

$$\left(\frac{2}{\pi}|\gamma_t|\right)^{\frac{3}{2}} = \left(\frac{4}{\pi(1+4t^2)}\right)^{\frac{3}{2}} \quad (2.52)$$

2.4.3 Probability Current Density

Unlike the probability density $\rho^{\Psi_t}(x)$, the probability current density $\mathcal{J}^{\Psi_t}(\vec{r})$ depends on both the magnetic field and the spin of the particle. This dependency is evident in the spin probability current density $\mathcal{J}_{spin}^{\Psi_t}$, which is expressed as:

$$\mathcal{J}_{spin}^{\Psi_t}(\vec{r}) = -\frac{4\sqrt{2}}{\sqrt{\pi^3}}|\gamma_t|^5 \exp[-2|\gamma_t|^2\vec{r}_t^2] \vec{r}_t \times \chi_t^* \vec{\sigma} \chi_t \quad (2.53)$$

For a single Gaussian wave packet, the convective probability current density $\mathcal{J}_{conv}^{\Psi_t}$

$$\mathcal{J}_{conv}^{\Psi_t}(\vec{r}) = \left(\frac{2}{\pi}\right)^{\frac{3}{2}} |\gamma_t|^3 \exp[-|\gamma_t|^2\vec{r}_t^2] \left(\frac{4t}{1-4t^2}\vec{r}_t + \vec{k}_0\right) \quad (2.54)$$

alone cannot stimulate backflow in the absence of interaction [MM20]. This is evident from the term in the last parentheses, where \vec{k}_0 is constant, and each component of \vec{r}_t does not influence the other components. In other words, the first component of $\mathcal{J}_{conv}^{\Psi_t}$ depends on x , the second on y , and the third on z . Therefore, variation of one component of \vec{r} cannot change the sign of

the components of $\mathcal{J}_{conv}^{\Psi_t}$ that depends on the other components of \vec{r} .

However, when considering the spin probability current density $\mathcal{J}_{spin}^{\Psi_t}$, each component of $\mathcal{J}_{spin}^{\Psi_t}$ can depend on multiple spatial variable due to the cross-product term. This implies, for example, that the quantum flux on a flat surface perpendicular to x -axis can be negative because of variation of y and z .

Initially, the convective probability current density $\mathcal{J}_{conv}^{\Psi_t}$ is oriented along x -axis, determined by the wave vector \vec{k}_0 . The spin term modifies this direction as shown in Figure 2.2.

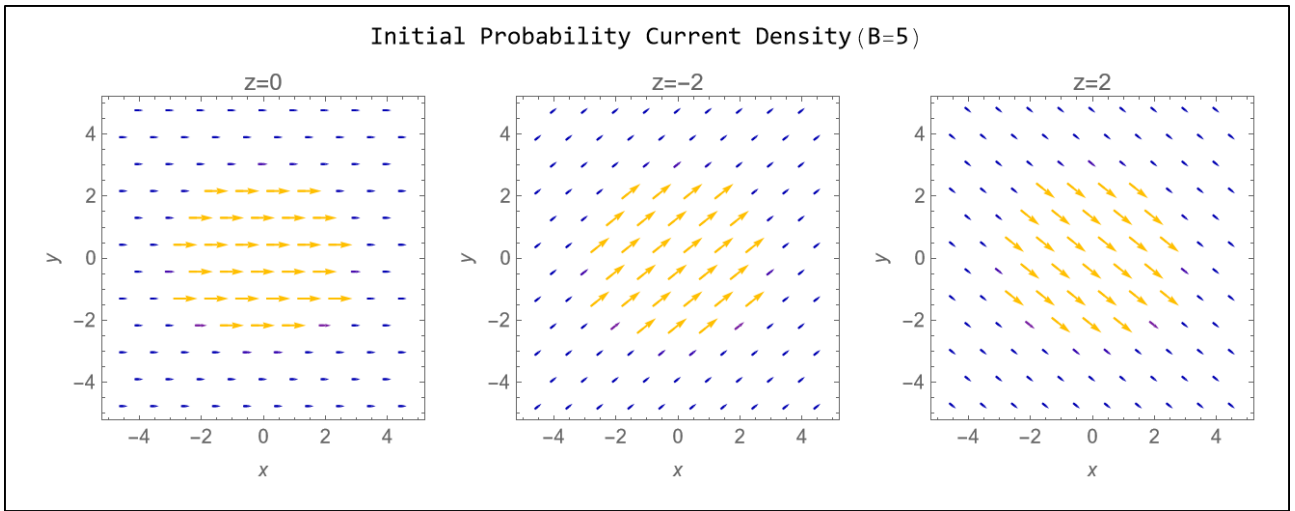


Figure 2.2: Initial probability current density \mathcal{J}^{Ψ_0} for different value of z , $\theta = \frac{\pi}{2}$ and $\phi = 0$. The magnitude of the probability current density is represented by the length and color of the arrows.

For $z = 0$, the spin term contributes only to the third component of the quantum flux \mathcal{J}^{Ψ_t} , which cannot be depicted in Figure 2.2. Thus, only the convective flux is effectively visualized. However, when z changes, the flux direction varies. In Figure 2.2, the probability flux is oriented upwards for $z = -2$ and downwards for $z = 2$. In reality, the probability current streamlines form a spiral structure when the third component is visualized together in a three-dimensional plotting.

The probability current density \mathcal{J}^{Ψ_t} evolves over time, with the magnetic field being switched off at some moment. For comparison, the magnetic field will first be constant indefinitely. Next, the same initial probability flux will evolve, but the magnetic field will be turned off at $t = 0.3$. This allows the influence of the magnetic field on the probability flux to be studied in greater detail.

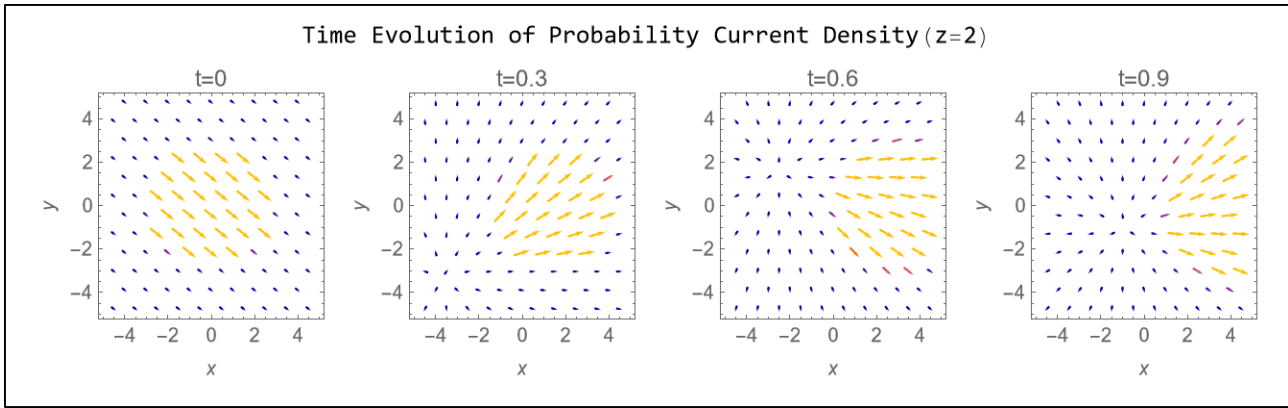


Figure 2.3: Time evolution of the probability current density \mathcal{J}^{Ψ_t} for $z = 2$ and $\theta = \frac{\pi}{2}$ and $\phi = 0$, with a constant magnetic field that remains active indefinitely.

Figure 2.3 illustrates the probability current density for $z = 2$, not for $z = 0$ because the spin probability current density for $z = 0$ contributes only to the third component of the probability flux, which cannot be visualized in xy -plane. Over time, the probability current density flows predominantly in x -direction due to the convective flux. Simultaneously, the arrows oscillate slightly upwards and downwards periodically due to the spin flux. This oscillation persists with constant frequency as long as the magnetic field remains active, although its amplitude decreases over time, resulting in a damped oscillation. This behavior will be quantitatively analyzed in detail in Subsection 2.4.4.

Next, the magnetic field is turned off at $t = 0.3$, while the initial probability current density is prepared identically to the previous case.

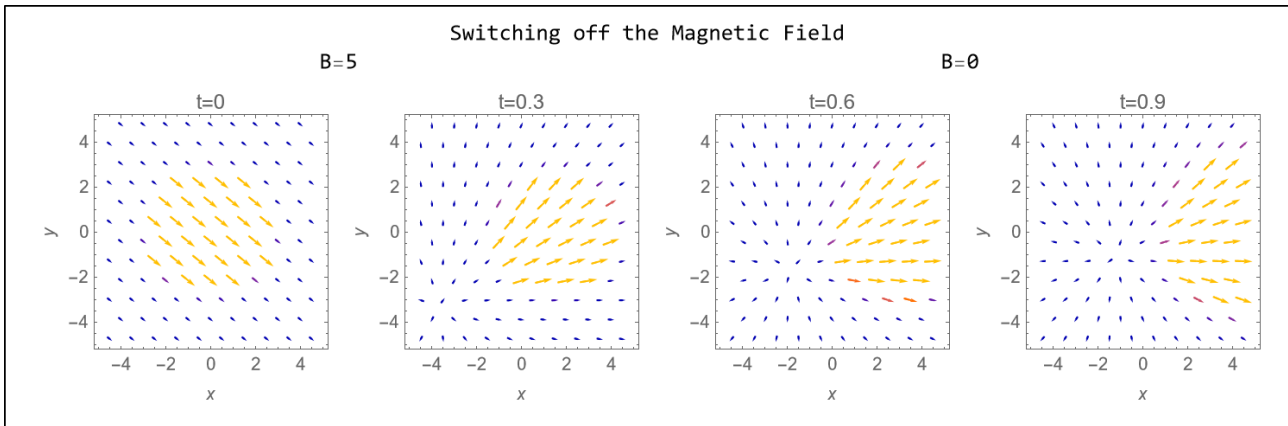


Figure 2.4: Time evolution of the probability current density \mathcal{J}^{Ψ_t} for $z = 2$, $\theta = \frac{\pi}{2}$ and $\phi = 0$, with the constant magnetic field switched off at $t = 0.3$.

In this scenario, the oscillation ceases at $t = 0.3$, as confirmed by comparing Figure 2.3 and 2.4. At $t = 0.3$, the arrows in both figures point upwards. However, $t = 0.6$, the arrows in Figure 2.3 point downwards, whereas they point upwards in Figure 2.4. This discrepancy arises because the magnetic field was switched off at $t = 0.3$, halting the oscillatory motion.

Interestingly, at $t = 0.9$, the probability current density appears identical in both cases. This is due to the damping effect described by the prefactor $|\gamma_t|^5$ in equation 2.53, which is independent of the magnetic field. Hence, the damping continues to suppress the spin flux even after the

magnetic field is turned off. This indicates that the probability current density \mathcal{J}^{Ψ_t} converges to the convective probability current density \mathcal{J}_{conv}^Ψ , which may lead to suppression of the backflow effect.

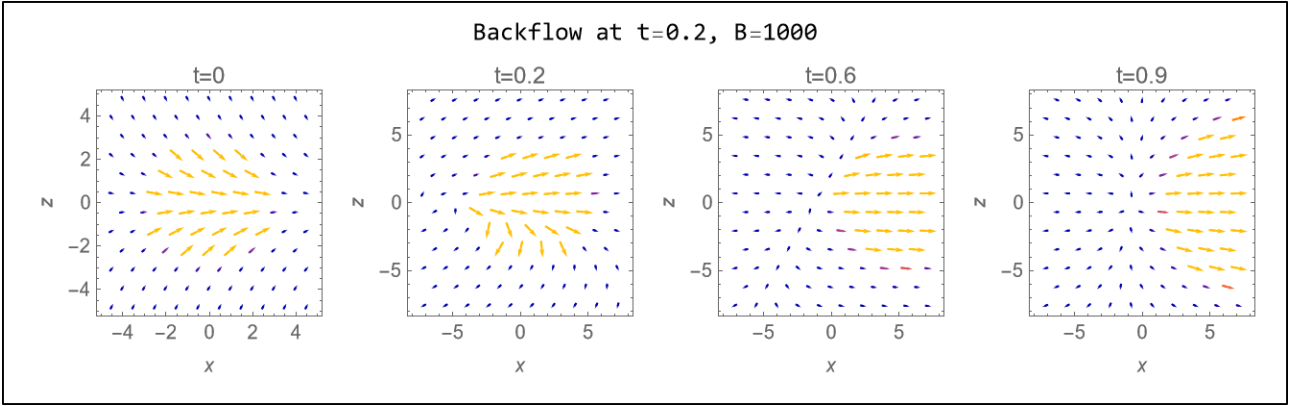


Figure 2.5: Time evolution of \mathcal{J}^Ψ for $y = 0$, $\theta = \frac{\pi}{2}$ and $\phi = 0$, with a strong constant magnetic field that remains active indefinitely.

Figure 2.5 shows that the backflow effect is found on the surface around $x = -2$ at $t = 0.2$ during the evolution of \mathcal{J}^{Ψ_t} in the strong constant magnetic field. If the damping did not exist, this backflow effect should occur periodically because of the constant frequency of oscillatory motion. However, the backflow effect seems not to occur for later times, as confirmed at $t = 0.6$ and $t = 0.9$. Still, we cannot determine that the backflow effect will not occur after some moment in time. Therefore, the suppression of the backflow effect will be studied in the following subsection in detail.

2.4.4 Relative Magnitudes of Convective and Spin Fluxes

The goal of this subsection is to quantitatively demonstrate how the magnitude of the spin probability current density $\mathcal{J}_{spin}^{\Psi_t}$ decreases faster than the magnitude of the convective probability current density $\mathcal{J}_{conv}^{\Psi_t}$.

To begin, the probability current density will be evaluated at the center of the Gaussian wave packet, where it has the most significant value. The probability of finding a neutral particle is highest around the center. Assuming the wave packet starts propagating from the origin with a wave vector $\vec{k}_0 = (k_{0x}, 0, 0)^\top$, the evaluation will be performed at $x = k_{0x}t$. Additionally, the spin state is assumed to be aligned with the x -direction, which corresponds to $\theta = \frac{\pi}{2}$, $\phi = 0$.

The ratio of the magnitude of the convective flux to the magnitude of the spin flux is given as:

$$\Phi^{\Psi_t} := \frac{\|\mathcal{J}_{conv}^{\Psi_t}\|}{\|\mathcal{J}_{spin}^{\Psi_t}\|} = \frac{\|\text{Im} [2\gamma_t \vec{r}_t - i\vec{k}_0]\|}{\|(\gamma_t^* + \gamma_t)\vec{r}_t \times \chi_t^* \vec{\sigma} \chi_t\|}. \quad (2.55)$$

The numerator is calculated as follows:

$$\begin{aligned} \|\text{Im} [2\gamma_t \vec{r}_t - i\vec{k}_0]\| &= \left\| \frac{-4t}{1+4t^2} \vec{r}_t - \vec{k}_0 \right\| \\ &= \left\| \frac{4t}{1+4t^2} (0, y, z)^\top + (k_{0x}, 0, 0)^\top \right\| \\ &= \sqrt{k_{0x}^2 + \left(\frac{4yt}{1+4t^2} \right)^2 + \left(\frac{4zt}{1+4t^2} \right)^2} \end{aligned} \quad (2.56)$$

The denominator is computed as:

$$\begin{aligned}
\|(\gamma_t^* + \gamma_t)\vec{r}_t \times \chi_t^* \vec{\sigma} \chi_t\| &= \frac{2}{1 + 4t^2} \|\vec{r}_t \times \chi_t^* \vec{\sigma} \chi_t\| \\
&= \frac{2}{1 + 4t^2} \left\| \begin{pmatrix} z \sin(2B_z t) \\ z \cos(2B_z t) \\ -y \cos(2B_z t) \end{pmatrix} \right\| \\
&= \frac{2}{1 + 4t^2} \sqrt{z^2 + y^2 \cos^2(2B_z t)} \tag{2.57}
\end{aligned}$$

The second line of the equation (2.57) is obtained by applying the given conditions, $\theta = \frac{\pi}{2}$, $\phi = 0$, into the following equation:

$$\vec{r}_t \times \chi_t^* \vec{\sigma} \chi_t = \begin{pmatrix} \tilde{y} \cos(\theta) + \tilde{z} \sin(\theta) \sin(2B_z t - \phi) \\ \tilde{z} \sin(\theta) \cos(2B_z t - \phi) - \tilde{x} \cos(\theta) \\ -\tilde{x} \sin(\theta) \sin(2B_z t - \phi) - \tilde{y} \sin(\theta) \cos(2B_z t - \phi) \end{pmatrix}$$

Substituting these results into the ratio yields:

$$\frac{\|\mathcal{J}_{conv}^{\Psi_t}\|}{\|\mathcal{J}_{spin}^{\Psi_t}\|} = \frac{\sqrt{k_{0x}^2(1 + 4t^2)^2 + (4ty)^2 + (4tz)^2}}{2\sqrt{z^2 + y^2 \cos^2(2B_z t)}} \tag{2.58}$$

$$\begin{aligned}
&= \frac{t^2}{2} \sqrt{\frac{k_{0x}^2(4 + \frac{1}{t^2})^2 + (\frac{4y}{t})^2 + (\frac{4z}{t})^2}{z^2 + y^2 \cos^2(2B_z t)}} \\
&\geq \frac{t^2}{2} \sqrt{\frac{k_{0x}^2(4 + \frac{1}{t^2})^2 + (\frac{4y}{t})^2 + (\frac{4z}{t})^2}{z^2 + y^2}} \tag{2.59}
\end{aligned}$$

At later times ($t \rightarrow \infty$), the square root term in the numerator can be approximated by:

$$\lim_{t \rightarrow \infty} \sqrt{\frac{k_{0x}^2(4 + \frac{1}{t^2})^2 + (\frac{4y}{t})^2 + (\frac{4z}{t})^2}{z^2 + y^2}} = \frac{4k_{0x}}{\sqrt{z^2 + y^2}} \tag{2.60}$$

Thus, the ratio Φ^{Ψ_t} at later times is simplified to:

$$\Phi^{\Psi_t} = \frac{\|\mathcal{J}_{conv}^{\Psi_t}\|}{\|\mathcal{J}_{spin}^{\Psi_t}\|} \approx \frac{2t^2 k_{0x}}{\sqrt{z^2 + y^2 \cos^2(2B_z t)}} \geq \frac{2t^2 k_{0x}}{\sqrt{z^2 + y^2}} \quad (y, z) \in \mathbb{R}^2 \setminus \{(0, 0)\} \tag{2.61}$$

Note that the lower bound of the ratio is given by:

$$\Phi_{lower}^{\Psi_t} := \frac{2t^2 k_{0x}}{\sqrt{z^2 + y^2}} \quad (y, z) \in \mathbb{R}^2 \setminus \{(0, 0)\} \tag{2.62}$$

This implies that the ratio grows quadratically with time t for any fixed $y, z \neq 0$. In other words, the spin flux decreases quadratically faster than the convective flux.

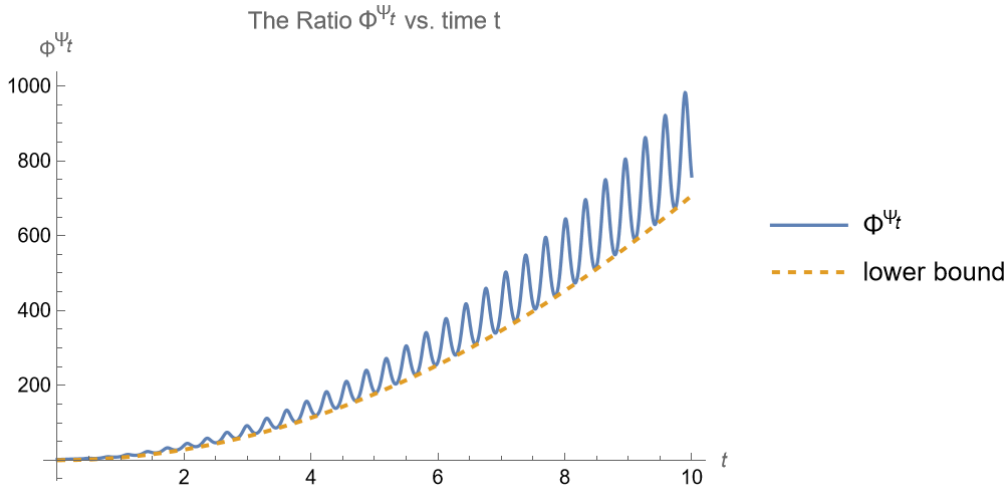


Figure 2.6: The ratio of the magnitude of the convective flux to the spin flux ($y = 1, z = 1$) under a permanent constant magnetic field.

As argued previously, the ratio Φ^{Ψ_t} in Figure 2.6 is bounded below. The ratio Φ^{Ψ_t} oscillates because of the cosine function in the denominator. Nevertheless, it is bounded below by $\Phi_{lower}^{\Psi_t}$, which increases quadratically. Therefore, the ratio Φ^{Ψ_t} grows at least quadratically.

Additionally, it is interesting to examine how the ratio Φ^{Ψ_t} behaves near the center in y - and z - directions. To analyze this, the ratio is evaluated at multiple units of width away from the center. One unit of width, σ_t , is given by:

$$\sigma_t = \frac{1}{\sqrt{2(\gamma_t^* + \gamma_t)}} = \frac{\sqrt{1 + 4t^2}}{2} \quad (2.63)$$

By substituting $y = n\sigma, z = n\sigma$ into equation (2.59), the ratio becomes:

$$\Phi^{\Psi_t} = \frac{\sqrt{k_{0x}^2(1 + 4t^2)^2 + 2(4tn\sigma)^2}}{2n\sigma_t\sqrt{1 + \cos^2(2B_z t)}} \quad (2.64)$$

$$= \sqrt{\frac{\left(\frac{k_{0x}}{n}\right)^2(4t^2 + 1) + 8t^2}{1 + \cos^2(2B_z t)}} \quad (2.65)$$

For large t , the term $\frac{4t^2}{\sqrt{1+4t^2}}$ approximates to $2t$. Therefore, at later times, the ratio Φ^{Ψ_t} approximates to:

$$\Phi^{\Psi_t} \approx \frac{t\sqrt{4\left(\frac{k_{0x}}{n}\right)^2 + 8}}{\sqrt{1 + \cos^2(2B_z t)}} \geq t\sqrt{2\left(\frac{k_{0x}}{n}\right)^2 + 4} \quad (2.66)$$

This indicates that the ratio is bounded below, and this lower bound grows linearly with time. Consequently, the ratio Φ^{Ψ_t} also increases linearly with time, even far away from the center.

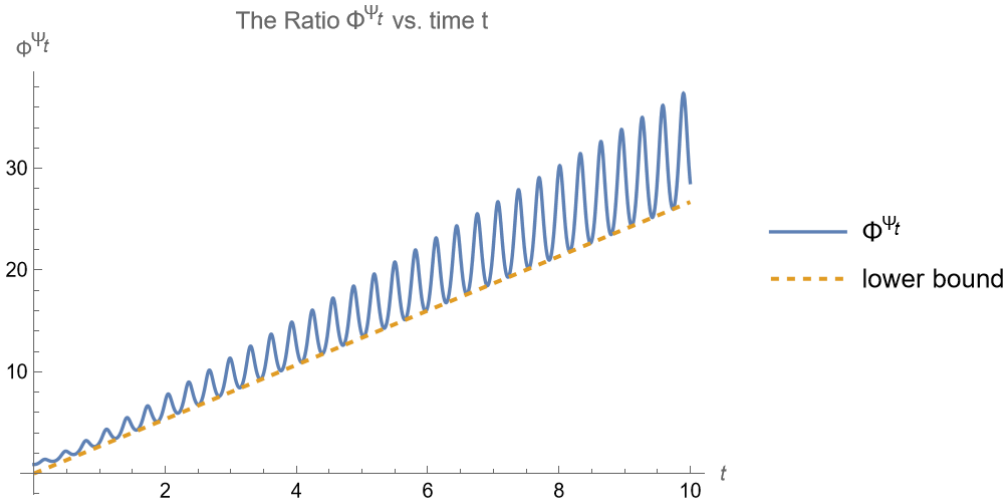


Figure 2.7: The ratio of the magnitude of the convective flux to the magnitude of the spin flux at $4\sqrt{2}\sigma$ away from the center, i.e., at $y = 4\sigma, z = 4\sigma$.

It is also noteworthy that the growth of Φ^{Ψ_t} is extremely rapid. For instance, in real time units (see subsection 2.4.1), $t = 10$ in non-dimensionalized time corresponds to $8 \cdot 10^{-7}$ s approximately, yet the ratio already reaches nearly 25. This rapid growth implies that detecting the spin probability current density $\mathcal{J}_{spin}^{\Psi_t}$ in experiments would be exceedingly difficult.

The outcome of this analysis is that the backflow effect is strongly suppressed in the far field. Suppose a backflow detector, modeled as a flat surface, is placed perpendicular to the wave vector \vec{k}_0 in the far field. In such a scenario, the spin flux $\mathcal{J}_{spin}^{\Psi_t}$ diminishes so rapidly that the detector would measure only the convective flux $\mathcal{J}_{conv}^{\Psi_t}$. As a result, backflow would be practically undetectable in this setting.

In this chapter, the dynamics of a neutral particle under the influence of a sharply localized magnetic barrier will be addressed. As in Chapter 2, the Hamiltonian and the Pauli equation will be defined. Subsequently, the time-dependent wave function for the Pauli equation will be derived using the propagator for this problem, which is derived via the Laplace transform in Appendix B.1. Finally, the dynamics of the neutral particle will be discussed.

3.1 Hamiltonian and Pauli Equation

The magnetic field is varying along the x -axis, with its direction along the z -axis. By placing the magnetic barrier at $x = 0$, we represented it using the Dirac-delta distribution $\delta(x)$ with a strength λ . Here, λ determines the intensity of the magnetic barrier. However, it differs from the field intensity B because λ has the dimension of energy multiplied by length. This distinction arises from the Dirac-delta distribution, which has the inverse dimension of its argument.

As outlined in Subsection 2.2.1, the Hamiltonian \hat{H} is given by:

$$\hat{H} = -\frac{\hbar^2}{2m}\nabla^2 + \lambda\sigma_z\delta(x). \quad (3.1)$$

The parameter λ is analogous to μB_z of Subsection 2.2.1. Using this Hamiltonian, the Pauli equation is expressed, in accordance with equation 2.19, as:

$$\hat{H}\Psi_t(\vec{r}) = \left[-\frac{\hbar^2}{2m}\nabla^2 + \lambda\sigma_z\delta(x)\right]\Psi_t(\vec{r}) = i\hbar\frac{\partial}{\partial t}\Psi_t(\vec{r}). \quad (3.2)$$

The initial wave function is assumed to be a Gaussian wave packet, as in Chapter 2:

$$\Psi_0(\vec{r}) = \left(\frac{2a}{\pi}\right)^{\frac{3}{4}} \exp\left[-a(\vec{r} - \vec{r}_c)^2 + ik_0 \cdot \vec{r}\right] \chi_0, \quad (3.3)$$

where χ_0 is the initial spin wave function represented as a Bloch vector. Initially, the particle is located far away to the left of the barrier. In this region, the initial wave function approximately satisfies the free Pauli equation (3.2).

3.2 Time-Dependent Solution to the Pauli Equation

To begin, we express the wave function Ψ_t as follows:

$$\Psi_t(\vec{r}) = \begin{bmatrix} \Psi_t^{up}(\vec{r}) \\ \Psi_t^{down}(\vec{r}) \end{bmatrix} \quad (3.4)$$

Then this equation is inserted into equation (3.2), resulting in:

$$i\hbar \frac{\partial}{\partial t} \Psi_t^{up}(\vec{r}) = \left[-\frac{\hbar^2}{2m} \nabla^2 + \lambda \delta(x) \right] \Psi_t^{up}(\vec{r}) \quad (3.5)$$

$$i\hbar \frac{\partial}{\partial t} \Psi_t^{down}(\vec{r}) = \left[-\frac{\hbar^2}{2m} \nabla^2 - \lambda \delta(x) \right] \Psi_t^{down}(\vec{r}) \quad (3.6)$$

The solution can be expressed as follows:

$$\Psi_t^{up/down}(\vec{r}) = \int_{\mathbb{R}^3} K_{\Delta}(\vec{r}, t, \vec{r}', 0) \Psi_0^{up/down}(\vec{r}') d^3 r' \quad (3.7)$$

where K_{Δ} is a suitable propagator, determined below. This suggests that Ψ_t^{up} is derived at first, then Ψ_t^{down} can be obtained by changing the sign of λ . Thereafter, the time-dependent wave function for the Pauli equation (3.2) can be obtained by substituting λ with $\lambda \sigma_z$.

As before, we start with separating Gaussian wave function as follows for simplicity:

$$\Psi_0^{up}(\vec{r}) = \xi_0(x) \eta_0(y) \zeta_0(z) \chi_0^{up} \quad (3.8)$$

ξ_0 , η_0 , and ζ_0 are the same as in equation (2.12), and $\chi_0^{up} = \cos\left(\frac{\theta}{2}\right)$ is the upper component of the Bloch vector. Correspondingly, the propagator is also applied separately for the x -, y -, and z -coordinates. Since the magnetic barrier depends only on x , the propagators for η_0 , ζ_0 are free-particle propagator K_0 . However, the propagator for ξ_0 is specific to the delta potential (see Appendix B.1 for its derivation):

$$K_{\delta}(x, t, x', 0) = -\frac{m\lambda}{2\hbar^2} \exp\left[\frac{m\lambda}{\hbar^2}(|x| + |x'|) + \frac{im\lambda^2}{2\hbar^3}t\right] \operatorname{erfc}\left[\sqrt{\frac{m}{2i\hbar t}}\left(|x| + |x'| + \frac{i\lambda t}{\hbar}\right)\right] \\ + \sqrt{\frac{m}{2\pi i\hbar t}} \exp\left[\frac{im(x-x')^2}{2\hbar t}\right] \quad (3.9)$$

Using this, the propagator $K_{\Delta}(\vec{r}, t, \vec{r}', 0)$ can also be separated as follows:

$$K_{\Delta}(\vec{r}, t, \vec{r}', 0) = K_{\delta}(x, t, x', 0) K_0(y, t, y', 0) K_0(z, t, z', 0) \quad (3.10)$$

Then, equation (3.7) can be written as:

$$\Psi_t(\vec{r}) = \chi_0^{up} \int_{-\infty}^{\infty} K_{\delta}(x, t, x', 0) \xi_0(x') dx' \int_{-\infty}^{\infty} K_0(y, t, y', 0) \eta_0(y') dy' \int_{-\infty}^{\infty} K_0(z, t, z', 0) \zeta_0(z') dz' \quad (3.11)$$

The last two integral, i.e., the time-dependent wave functions η_t and ζ_t were already derived in Chapter 2:

$$\eta_t(y) = \left(\frac{2a}{\pi}\right)^{\frac{1}{4}} \sqrt{\gamma_t} \exp\left[-a\gamma_t \tilde{y}_t^2 + i\left(k_{0y}y - \frac{\hbar k_{0y}^2}{2m}t\right)\right] \quad (3.12)$$

$$\zeta_t(z) = \left(\frac{2a}{\pi}\right)^{\frac{1}{4}} \sqrt{\gamma_t} \exp\left[-a\gamma_t \tilde{z}_t^2 + i\left(k_{0z}z - \frac{\hbar k_{0,z}^2}{2m}t\right)\right] \quad (3.13)$$

It remained only the wave function $\xi_t(x)$ to be derived:

$$\xi_t(x) = \int dx' K_\delta(x, t, x', 0) \xi_0(x') \quad (3.14)$$

The integration is complicated by the presence of the term $|x'|$ in the propagator $K_\delta(x, t, x', 0)$. To address this, the integration must be split into two regions: $x' < 0$ and $x' \geq 0$.

This problem can be simplified if $|x'|$ is transformed into x' or $-x'$. To achieve this, an assumption is required that the initial wave function $\xi_0(x')$ is located far to the left of the barrier, such that the initial wave function $\xi_0(x') \approx 0$ for $x' \geq 0$ [AD04]. Consequently, the integral for $x' \geq 0$ vanishes, and the integration for $x' < 0$ can be extended over $x' \in \mathbb{R}$. Under this assumption, $|x'|$ is replaced with $-x'$ and the propagator $K(x, t, x', 0)$ becomes

$$\begin{aligned} K_\delta(x, t, x', 0) = & -\frac{m\lambda}{2\hbar^2} \exp\left[\frac{m\lambda}{\hbar^2}(|x| - x') + \frac{im\lambda^2}{2\hbar^3}t\right] \operatorname{erfc}\left[\sqrt{\frac{m}{2i\hbar t}}\left(|x| - x' + \frac{i\lambda t}{\hbar}\right)\right] \\ & + \sqrt{\frac{m}{2\pi i\hbar t}} \exp\left[\frac{im(x - x')^2}{2\hbar t}\right]. \end{aligned} \quad (3.15)$$

Now, the integration can proceed without splitting the integration range:

$$\begin{aligned} \xi_t(x) &= \int_{-\infty}^{\infty} dx' K(x, t, x', 0) \xi_0(x) \chi_0^{up} \\ &= \int_{-\infty}^{\infty} dx' \sqrt{\frac{m}{2\pi i\hbar t}} \exp\left[\frac{im(x - x')^2}{2\hbar t}\right] \xi_0(x) \\ &\quad - \int_{-\infty}^{\infty} dx' \frac{m\lambda}{2\hbar^2} \exp\left[\frac{m\lambda}{\hbar^2}(|x| - x') + \frac{im\lambda^2}{2\hbar^3}t\right] \operatorname{erfc}\left[\sqrt{\frac{m}{2i\hbar t}}\left(|x| - x' + \frac{i\lambda t}{\hbar}\right)\right] \xi_0(x) \end{aligned} \quad (3.16)$$

The first term on the right-hand side corresponds to a free propagating particle and its solution was obtained in Chapter 2. The second term can be evaluated using the integral formula (see Appendix C.3)

$$\int_{-\infty}^{\infty} \exp[-fx^2 + gx] \operatorname{erfc}[px + q] dx = \sqrt{\frac{\pi}{f}} \exp\left[\frac{g^2}{4f}\right] \operatorname{erfc}\left[q\sqrt{\frac{f}{f+p^2}} + \frac{pg}{2\sqrt{f(f+p^2)}}\right]. \quad (3.17)$$

By comparing equation (3.16) with equation (3.17), the coefficients $f, g, p,$ and q can be identified as:

$$f = a, \quad g = 2ax_c - \frac{m\lambda}{\hbar^2} + ik_{0x}, \quad p = -\sqrt{\frac{m}{2i\hbar t}}, \quad q = \sqrt{\frac{m}{2i\hbar t}}\left(|x| + \frac{i\lambda t}{\hbar}\right). \quad (3.18)$$

Substituting these into equation (3.17) yields the time-dependent wave function $\xi_t(x)\chi_t$:

$$\begin{aligned} \xi_t(x) &= \left(\frac{2a}{\pi}\right)^{\frac{1}{4}} \sqrt{\gamma_t} \exp\left[-a\gamma_t \tilde{x}_t^2 + i\left(k_{0x}x - \frac{\hbar k_{0x}^2}{2m}t\right)\right] \\ &\quad - \frac{m\lambda}{2\hbar^2} \left(\frac{2\pi}{a}\right)^{\frac{1}{4}} \exp\left[\frac{m\lambda}{\hbar^2}(|x| - x_c) + \frac{m^2\lambda^2}{4a\gamma_t\hbar^4} + ik_{0x}\left(-\frac{m\lambda}{2a\hbar^2} + x_c\right) - \frac{k_{0x}^2}{4a}\right] \\ &\quad \cdot \operatorname{erfc}\left[\sqrt{a\gamma_t}(|x| - x_c) + \frac{\lambda m}{2\sqrt{a\gamma_t}\hbar^2} - \frac{ik_{0x}\sqrt{\gamma_t}}{2\sqrt{a}}\right] \end{aligned} \quad (3.19)$$

Note that ξ_t includes λ , while η_t, ζ_t does not. It will be hard to distinguish ξ_t for Ψ_t^{up} and Ψ_t^{down} , since they differ by the sign of λ . Therefore, we now mark ξ_t with *up/down*.

By combining ξ_t^{up} with η_t, ζ_t and χ_t^{up} , the time-dependent wave function $\Psi_t^{up}(\vec{r})$ is reconstructed:

$$\begin{aligned}
\Psi_t^{up}(\vec{r}) &= \xi_t^{up}(x)\eta_t(y)\zeta_t(z)\chi_t^{up} \\
&= \left(\frac{2a}{\pi}\right)^{\frac{3}{4}} \sqrt{\gamma_t} \exp\left[-a\gamma_t(\tilde{x}_t^2 + \tilde{y}_t^2) + i\left(k_{0x}x + k_{0y}y - \frac{\hbar(k_{0x}^2 + k_{0y}^2)}{2m}t\right)\right] \\
&\quad \cdot \left(\sqrt{\gamma_t} \exp\left[-a\gamma_t\tilde{x}_t^2 + i\left(k_{0x}x - \frac{\hbar k_{0x}^2}{2m}t\right)\right]\right) \\
&\quad - \frac{m\lambda}{2\hbar^2} \sqrt{\frac{\pi}{a}} \exp\left[\frac{m\lambda}{\hbar^2}(|x| - x_c) + \frac{m^2\lambda^2}{4a\gamma_t\hbar^4} + ik_{0x}\left(-\frac{m\lambda}{2a\hbar^2} + x_c\right) - \frac{k_{0x}^2}{4a}\right] \\
&\quad \cdot \operatorname{erfc}\left[\sqrt{a\gamma_t}(|x| - x_c) + \frac{\lambda m}{2\sqrt{a\gamma_t}\hbar^2} - \frac{ik_{0x}\sqrt{\gamma_t}}{2\sqrt{a}}\right] \chi_0^{up}
\end{aligned} \tag{3.20}$$

As described above, the spin-down component $\Psi_t^{down}(\vec{r})$ of the wave function can be obtained by changing the sign of λ :

$$\begin{aligned}
\Psi_t^{down}(\vec{r}) &= \xi_t^{down}(x)\eta_t(y)\zeta_t(z)\chi_t^{down} \\
&= \left(\frac{2a}{\pi}\right)^{\frac{3}{4}} \sqrt{\gamma_t} \exp\left[-a\gamma_t(\tilde{x}_t^2 + \tilde{y}_t^2) + i\left(k_{0x}x + k_{0y}y - \frac{\hbar(k_{0x}^2 + k_{0y}^2)}{2m}t\right)\right] \\
&\quad \cdot \left(\sqrt{\gamma_t} \exp\left[-a\gamma_t\tilde{x}_t^2 + i\left(k_{0x}x - \frac{\hbar k_{0x}^2}{2m}t\right)\right]\right) \\
&\quad + \frac{m\lambda}{2\hbar^2} \sqrt{\frac{\pi}{a}} \exp\left[\frac{-m\lambda}{\hbar^2}(|x| - x_c) + \frac{m^2\lambda^2}{4a\gamma_t\hbar^4} + ik_{0x}\left(\frac{m\lambda}{2a\hbar^2} + x_c\right) - \frac{k_{0x}^2}{4a}\right] \\
&\quad \cdot \operatorname{erfc}\left[\sqrt{a\gamma_t}(|x| - x_c) - \frac{\lambda m}{2\sqrt{a\gamma_t}\hbar^2} - \frac{ik_{0x}\sqrt{\gamma_t}}{2\sqrt{a}}\right] \chi_0^{down}.
\end{aligned} \tag{3.21}$$

Similar to χ_0^{up} , the initial spin wave function for spin-down component corresponds to the second component of the Bloch vector

$$\chi_0^{down} = \sin\left(\frac{\theta}{2}\right) \exp[i\phi]. \tag{3.22}$$

The complementary error function is an entire function. Hence, the spin-up and spin-down wave functions can be combined into a single equation using the Pauli matrix σ_z :

$$\begin{aligned}
\Psi_t(\vec{r}) &= \xi_t(x)\eta_t(y)\zeta_t(z)\chi_t \\
&= \left(\frac{2a}{\pi}\right)^{\frac{3}{4}} \sqrt{\gamma_t} \exp\left[-a\gamma_t(\tilde{x}_t^2 + \tilde{y}_t^2) + i\left(k_{0x}x + k_{0y}y - \frac{\hbar^2(k_{0x}^2 + k_{0y}^2)}{2m\hbar}t\right)\right] \\
&\quad \cdot \left(\sqrt{\gamma_t} \exp\left[-a\gamma_t\tilde{x}_t^2 + i\left(k_{0x}x - \frac{\hbar^2 k_{0x}^2}{2m\hbar}t\right)\right]\right) \\
&\quad - \frac{m\lambda\sigma_z}{2\hbar^2} \sqrt{\frac{\pi}{a}} \exp\left[\frac{m\lambda\sigma_z}{\hbar^2}(|x| - x_c) + \frac{m^2\lambda^2}{4a\gamma_t\hbar^4} + ik_{0x}\left(-\frac{m\lambda\sigma_z}{2a\hbar^2} + x_c\right) - \frac{k_{0x}^2}{4a}\right] \\
&\quad \cdot \operatorname{erfc}\left[\sqrt{a\gamma_t}(|x| - x_c) + \frac{\lambda\sigma_z m}{2\sqrt{a\gamma_t}\hbar^2} - \frac{ik_{0x}\sqrt{\gamma_t}}{2\sqrt{a}}\right] \chi_0
\end{aligned} \tag{3.23}$$

Note that χ_t cannot be space-spin factorized, because there is one term that involve σ_z and x .

Now we need to show that this is a solution to the Pauli equation (3.2) in the sense that it is a weak solution because of the discontinuity of the Hamiltonian (see equation (3.1)). This is shown in Appendix B.2.

3.3 Probability Density ρ^ψ and Probability Current Density \mathcal{J}^ψ

The goal of this chapter is to identify the presence of backflow and determine if they are stable enough for detection. Note that placing a detector near the barrier is not desirable, as it would disturb the incident wave function. In other words, backflow must be observed far from the barrier and after a considerable duration to ensure a meaningful detection setup. To achieve this goal, the probability density ρ^{Ψ_t} and the probability current density \mathcal{J}^{Ψ_t} need to be calculated and plotted in the far field. However, the time-dependent wave function is complex. Therefore, the non-dimensionalization is applied before proceeding with the calculations.

3.3.1 Non-Dimensionalization Convention

As mentioned in Chapter 2, the non-dimensionalization is necessary to simplify the calculations. Additionally, it helps prevent overflow issues during the computer-based computation of the probability density and probability flux.

The variables are substituted as follows, with the overline notation dropped for simplicity in all related equations:

$$\sqrt{a}\vec{r} = \vec{r}, \quad \frac{\vec{k}}{\sqrt{a}} = \vec{k}, \quad \frac{m\lambda}{2\hbar^2\sqrt{a}} = \bar{\lambda}, \quad \frac{\hbar a t}{m} = \bar{t}, \quad \frac{\Psi_t(\vec{r})}{a^{\frac{3}{4}}} = \bar{\Psi}_t(\vec{r}) \quad (3.24)$$

After applying these substitutions, the wave functions take the following forms:

$$\begin{aligned} \xi_t(x) = & \left(\frac{2}{\pi}\right)^{\frac{1}{4}} \sqrt{\gamma_t} \exp\left[-\gamma_t \tilde{x}_t^2 + i\left(k_{0x}x - \frac{k_{0x}^2 t}{2}\right)\right] \\ & - (2\pi)^{\frac{1}{4}} \lambda \sigma_z \exp\left[2\lambda \sigma_z (|x| - x_c) + \frac{\lambda^2}{\gamma_t} - ik_{0x}(\lambda \sigma_z - x_c) - \frac{k_{0x}^2}{4}\right] \\ & \times \operatorname{erfc}\left[\sqrt{\gamma_t}(|x| - x_c) + \frac{\lambda \sigma_z}{\sqrt{\gamma_t}} - \frac{ik_{0x}\sqrt{\gamma_t}}{2}\right] \end{aligned} \quad (3.25)$$

$$\eta_t(y) = \left(\frac{2}{\pi}\right)^{\frac{1}{4}} \sqrt{\gamma_t} \exp\left[-\gamma_t \tilde{y}_t^2 + i\left(k_{0y}y - \frac{k_{0y}^2 t}{2}\right)\right] \quad (3.26)$$

$$\zeta_t(z) = \left(\frac{2}{\pi}\right)^{\frac{1}{4}} \sqrt{\gamma_t} \exp\left[-\gamma_t \tilde{z}_t^2 + i\left(k_{0z}z - \frac{k_{0z}^2 t}{2}\right)\right] \quad (3.27)$$

$$(3.28)$$

where

$$\gamma_t = \frac{1}{1 + 2it}, \quad \tilde{\vec{r}} = \vec{r} - \vec{r}_c - \vec{k}_0 t = \begin{pmatrix} x - x_c - k_{0x}t \\ y - y_c - k_{0y}t \\ z - z_c - k_{0z}t \end{pmatrix} = \begin{pmatrix} \tilde{x} \\ \tilde{y} \\ \tilde{z} \end{pmatrix} \quad (3.29)$$

As in chapter 2, it is helpful to illustrate the correspondence between the non-dimensionalized and physical real units. For the same setup with $a = 2 \cdot 10^{14} \text{m}^{-2}$, the unit conversions are as follows:

- $x = 1$ corresponds to $7.0710678119 \cdot 10^{-8} \text{m}$
- $k = 1$ corresponds to $1.414213562 \cdot 10^7 \text{m}^{-1}$
- $t = 1$ corresponds to $7.941273265 \cdot 10^{-8} \text{s}$
- $\lambda = 1$ corresponds to $1.878022471 \cdot 10^{-34} \text{J} \cdot \text{m}$

3.3.2 Probability Density

The probability current density is given by:

$$\begin{aligned} \rho^{\Psi_t}(\vec{r}) &= \Psi_t^*(\vec{r})\Psi_t(\vec{r}) \\ &= \underbrace{[\Psi_t^{up}(\vec{r})]^*\Psi_t^{up}(\vec{r})}_{\rho_{up}^{\Psi_t}} + \underbrace{[\Psi_t^{down}(\vec{r})]^*\Psi_t^{down}(\vec{r})}_{\rho_{down}^{\Psi_t}} \end{aligned} \quad (3.30)$$

It is sufficient to calculate only the spin-up component of the probability density ρ^{Ψ_t} . The spin-down component can be obtained by changing the sign of λ and replacing χ_0^{up} with χ_0^{down} . For the spin-up component, the probability density is expressed as:

$$\begin{aligned} \rho_{up}^{\Psi_t}(\vec{r}) &= \left(\frac{2}{\pi}\right) \gamma_t^* \gamma_t \exp [-(\gamma_t^* + \gamma_t)(\tilde{y}_t^2 + \tilde{z}_t^2)] \cdot \left\{ \sqrt{\frac{2}{\pi}} \sqrt{\gamma_t^* \gamma_t} \exp [-(\gamma_t^* + \gamma_t)\tilde{x}_t^2] \right. \\ &\quad + \sqrt{2\pi} \lambda^2 \exp \left[4\lambda(|x| - x_c) + 2\lambda^2 - \frac{k_{0x}^2}{2} \right] \left\| \text{erfc} \left[\sqrt{\gamma_t}(|x| - x_c - \frac{ik_{0x}}{2}) + \frac{\lambda}{\sqrt{\gamma_t}} \right] \right\|^2 \\ &\quad - 2 \text{Re} \left[\sqrt{2\gamma_t} \lambda \exp \left[-\gamma_t \tilde{x}_t^2 + 2\lambda(|x| - x_c) - \frac{k_{0x}^2}{4} + \frac{\lambda^2}{\gamma_t^*} + ik_{0x} \left(x - x_c + \lambda - \frac{k_{0x}t}{2} \right) \right] \right. \\ &\quad \left. \cdot \text{erfc} \left[\sqrt{\gamma_t^*} \left(|x| - x_c + \frac{ik_{0x}}{2} \right) + \frac{\lambda}{\sqrt{\gamma_t^*}} \right] \right\} \cos^2 \left(\frac{\theta}{2} \right) \end{aligned} \quad (3.31)$$

Similarly, the spin-down component is given by:

$$\begin{aligned} \rho_{down}^{\Psi_t}(\vec{r}) &= \left(\frac{2}{\pi}\right) \gamma_t^* \gamma_t \exp [-(\gamma_t^* + \gamma_t)(\tilde{y}_t^2 + \tilde{z}_t^2)] \cdot \left\{ \sqrt{\frac{2}{\pi}} \sqrt{\gamma_t^* \gamma_t} \exp [-(\gamma_t^* + \gamma_t)\tilde{x}_t^2] \right. \\ &\quad + \sqrt{2\pi} \lambda^2 \exp \left[-4\lambda(|x| - x_c) + 2\lambda^2 - \frac{k_{0x}^2}{2} \right] \left\| \text{erfc} \left[\sqrt{\gamma_t}(|x| - x_c - \frac{ik_{0x}}{2}) - \frac{\lambda}{\sqrt{\gamma_t}} \right] \right\|^2 \\ &\quad + 2 \text{Re} \left[\sqrt{2\gamma_t} \lambda \exp \left[-\gamma_t \tilde{x}_t^2 - 2\lambda(|x| - x_c) - \frac{k_{0x}^2}{4} + \frac{\lambda^2}{\gamma_t^*} + ik_{0x} \left(x - x_c - \lambda - \frac{k_{0x}t}{2} \right) \right] \right. \\ &\quad \left. \cdot \text{erfc} \left[\sqrt{\gamma_t^*} \left(|x| - x_c + \frac{ik_{0x}}{2} \right) - \frac{\lambda}{\sqrt{\gamma_t^*}} \right] \right\} \sin^2 \left(\frac{\theta}{2} \right) \end{aligned} \quad (3.32)$$

Now, the probability density can be analyzed. Initially, the probability density is centered at $\vec{x}_c = (-10, 0, 0)^\top$, with parameters $\lambda = 5$ and $\vec{k}_0 = (10, 0, 0)^\top$.

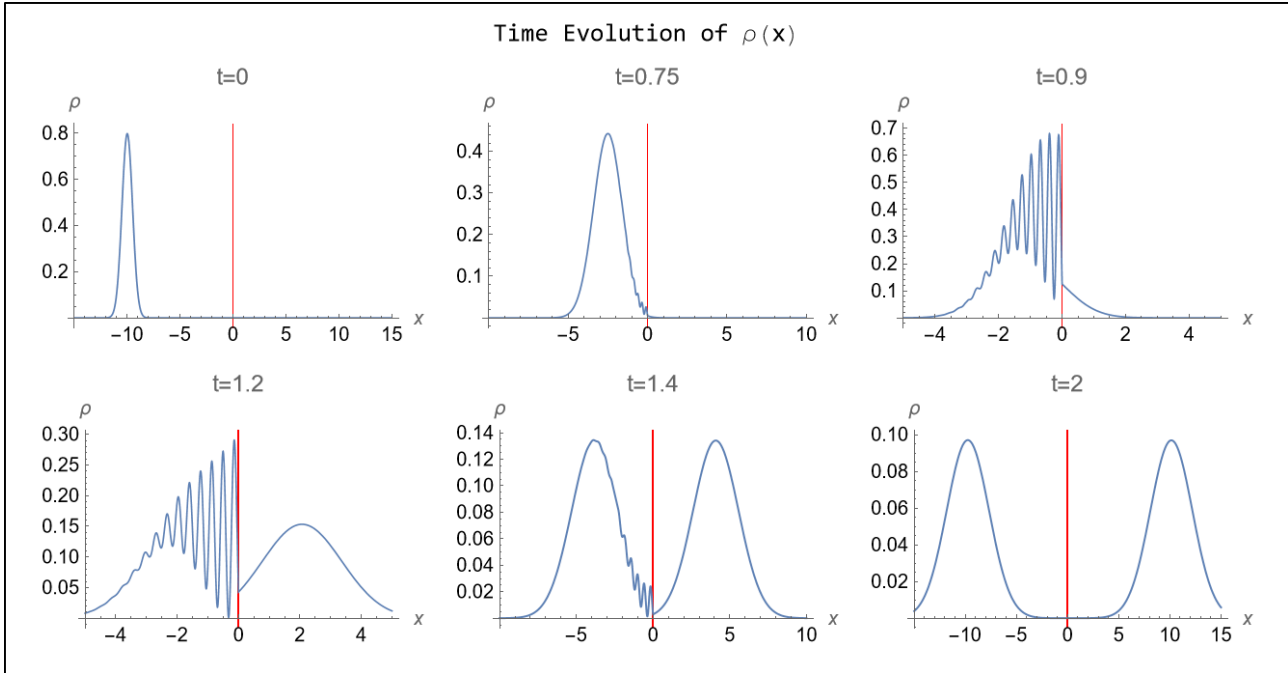


Figure 3.1: Time evolution of the probability density. The vertical red line at the origin represents the magnetic barrier.

Figure 3.1 shows the dynamics of the probability density. Initially, the wave function propagates as a free particle. Upon reaching the magnetic barrier at $t = 0.75$, the wave function begins to interact with the magnetic barrier, creating an interference pattern, which results from the interference between the incident and reflected wave packets. By $t = 1.4$, the reflected and transmitted wave packet become distinguishable. At $t = 2$, the interference pattern disappears.

Note that the transmitted and reflected probability density have equal magnitudes. This balance can be modified by varying the parameters such as \vec{k}_0 . Changing \vec{k}_0 affects the relative magnitudes of reflection and transmission, which will be examined further in the following figure.

Figure 3.2 demonstrates how the magnitudes of the reflected and transmitted probability densities change with varying k_{0x} . It is also evident that wave functions with different wave vectors reach the magnetic barrier at different times. This can be observed by initializing the wave function at $\vec{r}_c = (-200, 0, 0)^\top$, as the wave vector determines the propagation speed of the wave function. A larger wave vector corresponds to faster propagation. For instance, the second row of the figure shows that the collision time reduces from $t = 24$ to $t = 14.5$ as k_{0x} increases from 7 to 13.

In the last row of Figure 3.2, it can be seen that the magnitude of transmission increases as k_{0x} increases. This can be interpreted: A wave vector with higher energy is more likely to pass through the magnetic barrier, if it propagates faster. Conversely, the magnitude of reflection decreases with increasing k_{0x} . This behavior is due to the unitarity of the time evolution operator, which ensures the conservation of the total probability, which is one.

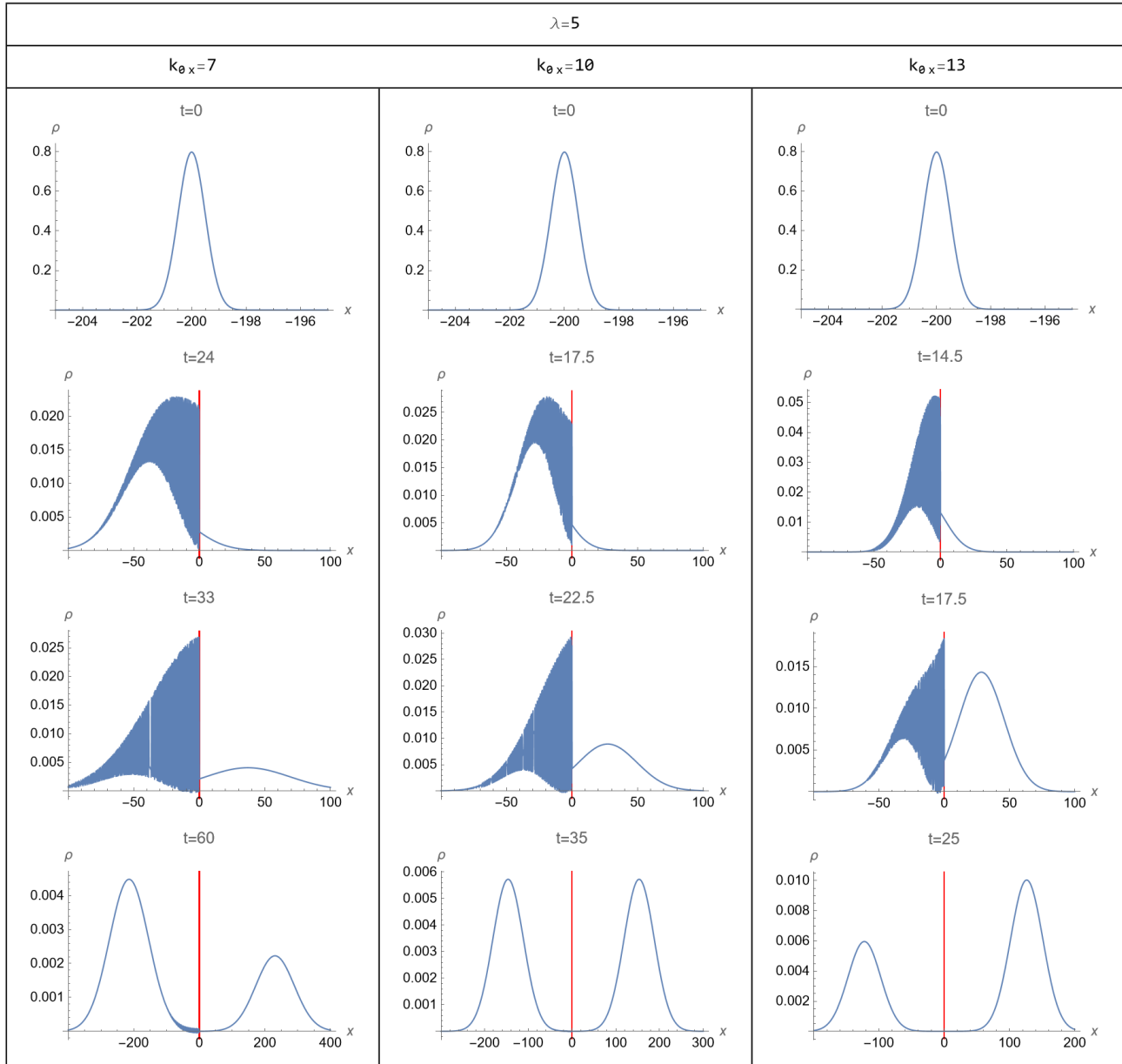
Time Evolution of $\rho(x)$ with various Wave Vector k_x 

Figure 3.2: Probability density for various value of k_{0x} . For each value, the time evolution of the probability density is illustrated vertically. The red line at the origin represents the magnetic barrier.

Additionally it is widely known that the relative magnitudes of the reflected and transmitted probability densities remain the same if the ratio $\frac{\lambda}{k_{0x}}$ is constant. It implies that it is valuable to explore the relationship between reflection, transmission and the parameter λ in detail.

To investigate this relationship, the probability density is integrated over $x < 0$ and $x \geq 0$ for various value of λ , with k_{0x} fixed at 10. The integral for $x < 0$ corresponds to the area under the reflected probability density, and vice versa. These integrals yields the reflection coefficient and transmission coefficient, respectively. The calculated values are then compared to the well-known formulas [AD04]:

$$R(\lambda, k_{0x}) = \frac{\lambda^2}{\lambda^2 + k_{0x}^2/4}, \quad T(\lambda, k_{0x}) = \frac{k_{0x}^2/4}{\lambda^2 + k_{0x}^2/4} \quad (3.33)$$

Here, $R(\lambda, k_{0x})$ represents the reflection coefficient, and $T(\lambda, k_{0x})$ represents transmission coefficient.

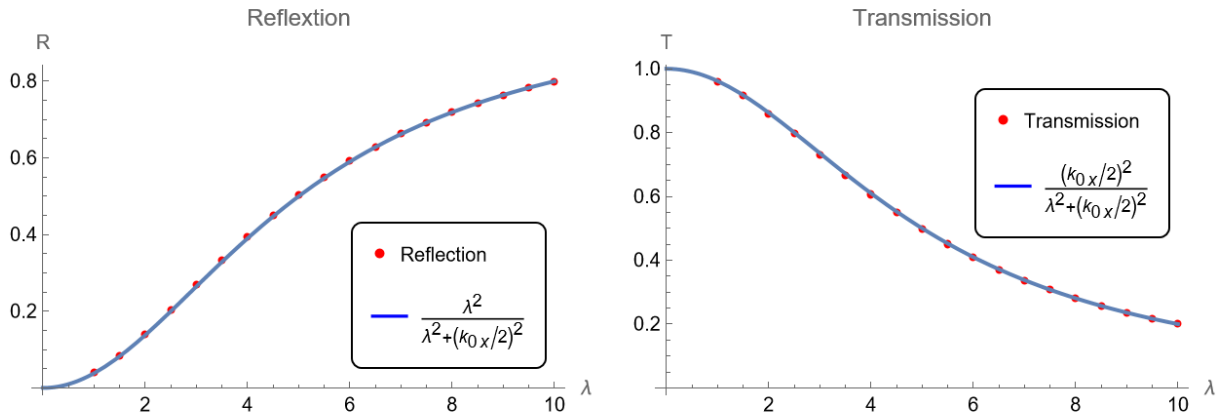


Figure 3.3: Numerical results for the reflection and transmission coefficients for the obtained Gaussian wave packet. Red dots are the calculated values, while the blue line is equation (3.33).

The results of numerical integration agree with equation (3.33). The reflection coefficient increases as the strength of magnetic barrier grows. Similarly, the transmission coefficients decreases. This can be explained intuitively: a stronger barrier is more likely to reflect the wave function than to allow it to be transmitted.

This relationship between the reflection and transmission coefficients can be illustrated more clearly by comparing them directly.

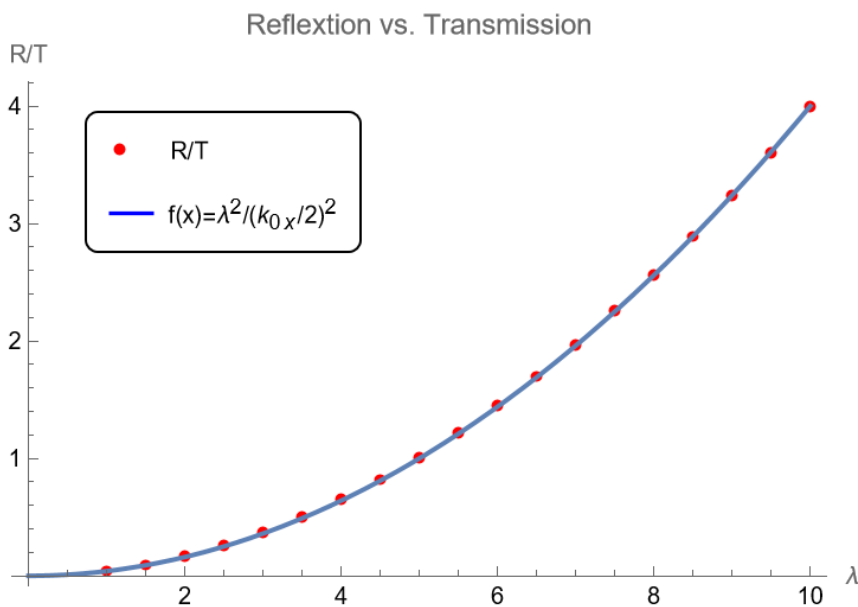


Figure 3.4: Reflection vs. Transmission. Red dots represent the numerically calculated values, while the blue line is equation (3.33).

Figure 3.4 shows how the reflection coefficient increases relative to the transmission coefficient. It is apparent that the ratio grows quadratically.

3.3.3 Probability Current Density

In this subsection, the occurrence of the backflow effect will be discussed. To this end, the probability current density \mathcal{J}^{Ψ_t} must first be calculated. As shown in equation 1.3, the probability current density consists of the convective component $\mathcal{J}_{conv}^{\Psi_t}$ and the spin component $\mathcal{J}_{spin}^{\Psi_t}$. Both components involve spatial derivatives of the wave function. The derivatives for the Gaussian wave packet of a free particle were derived in Chapter 2 (see equation (2.41)):

$$\frac{\partial}{\partial y} \eta_t(y) = \eta_t(y) (-2\gamma_t \tilde{y}_t + ik_{0y}) \quad (3.34)$$

$$\frac{\partial}{\partial z} \zeta_t(z) = \zeta_t(z) (-2\gamma_t \tilde{z}_t + ik_{0z}) \quad (3.35)$$

The derivative of $\xi_t(x)$, however, must still be computed given that ξ_t is no longer a Gaussian wave function. Since $\xi_t(x)$ can be represented as $(\xi_t^{up}(x), \xi_t^{down}(x))^T$, its derivative with regards to x is $(\partial_x \xi_t^{up}(x), \partial_x \xi_t^{down}(x))^T$. Similar to the previous subsection, the upper component is calculated first, and the lower component is obtained by replacing λ with $-\lambda$. The derivative of $\xi_t(x)$ can then be expressed as a single equation with the Pauli matrix σ_z .

The derivative of $\xi_t(x)$ with respect to x is (the derivative of complementary error function can be found in Appendix C.1):

$$\begin{aligned} \frac{\partial}{\partial x} \xi_t(x) &= (-2\gamma_t \tilde{x}_t + ik_{0x}) \left(\frac{2}{\pi}\right)^{\frac{1}{4}} \sqrt{\gamma_t} \exp \left[-\gamma_t \tilde{x}_t^2 + i \left(k_{0x} x - \frac{k_{0x}^2 t}{2} \right) \right] \\ &+ 2\lambda \sigma_z \operatorname{sgn}[x] \left(\frac{2}{\pi}\right)^{\frac{1}{4}} \sqrt{\gamma_t} \exp \left[-\gamma_t (|x| - x_c - k_{0x} t)^2 + i \left(k_{0x} |x| - \frac{k_{0x}^2 t}{2} \right) \right] \\ &- (2\pi)^{\frac{1}{4}} 2\lambda^2 \operatorname{sgn}[x] \exp \left[2\lambda \sigma_z (|x| - x_c) + \frac{\lambda^2}{\gamma_t} - ik_{0x} (\lambda \sigma_z - x_c) - \frac{k_{0x}^2}{4} \right] \\ &\cdot \operatorname{erfc} \left[\sqrt{\gamma_t} (|x| - x_c) + \frac{\lambda \sigma_z}{\sqrt{\gamma_t}} - \frac{ik_{0x} \sqrt{\gamma_t}}{2} \right]. \end{aligned} \quad (3.36)$$

Now, the convective flux and the spin flux can be calculated as follows: The spatial arguments of the wave function are omitted for clarity. The convective flux is given by

$$\begin{aligned} \mathcal{J}_{conv}^{\Psi_t} &= \operatorname{Im} \Psi_t^* \nabla \Psi_t \\ &= \operatorname{Im} \left[(\Psi_t^{up}, \Psi_t^{down}) \cdot (\nabla \Psi_t^{up}, \nabla \Psi_t^{down})^T \right] \\ &= \operatorname{Im} \left[(\Psi_t^{up})^* \nabla \Psi_t^{up} + (\Psi_t^{down})^* \nabla \Psi_t^{down} \right] \\ &= \operatorname{Im} \left(\begin{array}{c} \|\eta_t \zeta_t\|^2 \left[(\xi_t^{up})^* \partial_x \xi_t^{up} + (\xi_t^{down})^* \partial_x \xi_t^{down} \right] \\ \rho^{\Psi_t} (-2\gamma_t \tilde{y}_t + ik_{0y}) \\ \rho^{\Psi_t} (-2\gamma_t \tilde{z}_t + ik_{0z}) \end{array} \right), \end{aligned} \quad (3.37)$$

The spin flux is given by:

$$\begin{aligned} \mathcal{J}_{spin}^{\Psi_t} &= \frac{1}{2} \nabla \times (\Psi_t^* \vec{\sigma} \Psi_t) = \frac{1}{2} \begin{pmatrix} \partial_x \\ \partial_y \\ \partial_z \end{pmatrix} \times \begin{pmatrix} \Psi_t^* \sigma_x \Psi_t \\ \Psi_t^* \sigma_y \Psi_t \\ \Psi_t^* \sigma_z \Psi_t \end{pmatrix} \\ &= \frac{1}{2} \begin{pmatrix} \partial_x \\ \partial_y \\ \partial_z \end{pmatrix} \times \begin{pmatrix} 2 \operatorname{Re} \left[(\Psi_t^{down})^* \Psi_t^{up} \right] \\ -2 \operatorname{Im} \left[(\Psi_t^{down})^* \Psi_t^{up} \right] \\ (\Psi_t^{up})^* \Psi_t^{up} - (\Psi_t^{down})^* \Psi_t^{down} \end{pmatrix} \end{aligned} \quad (3.38)$$

$$\begin{aligned}
 &= \frac{1}{2} \|\eta_t \zeta_t\|^2 \left[\begin{aligned} &\left(\begin{aligned} &-2(\gamma_t^* + \gamma_t) \tilde{y}_t \left[\|\xi_t^{up}\|^2 \cos^2\left(\frac{\theta}{2}\right) - \|\xi_t^{down}\|^2 \sin^2\left(\frac{\theta}{2}\right) \right] \\ &-2(\gamma_t^* + \gamma_t) \tilde{z}_t \sin(\theta) \operatorname{Re} \left[(\xi_t^{down})^* \xi_t^{up} \exp(-i\phi) \right] \\ &-\sin(\theta) \exp(-i\phi) \left(\operatorname{Im} \left[\xi_t^{up} (\partial_x \xi_t^{down})^* + \xi_t^{down} (\partial_x \xi_t^{up})^* \right] \right) \end{aligned} \right) \\ &+ \left(\begin{aligned} &-2(\gamma_t^* + \gamma_t) \tilde{z}_t \sin(\theta) \operatorname{Im} \left[(\xi_t^{down})^* \xi_t^{up} \exp(-i\phi) \right] \\ &2 \operatorname{Re} \left[\partial_x (\xi_t^{up})^* \xi_t^{up} \cos^2\left(\frac{\theta}{2}\right) - \partial_x (\xi_t^{down})^* \xi_t^{down} \sin^2\left(\frac{\theta}{2}\right) \right] \\ &-2(\gamma_t^* + \gamma_t) \tilde{y}_t \sin(\theta) \operatorname{Re} \left[(\xi_t^{down})^* \xi_t^{up} \exp(-i\phi) \right] \end{aligned} \right) \end{aligned} \right] \quad (3.39)
 \end{aligned}$$

The spin flux could not be simplified further because the wave function is not space-spin factorized as in Chapter 2 (see equation (2.41)). Still, this spin flux can be simplified with the following assumption: The initial spin wave function is oriented in the z -direction ($\theta = 0, \phi = 0$). Then, the spin flux is given by:

$$\mathcal{J}_{spin}^{\Psi_t} = \|\eta_t \zeta_t\|^2 \begin{pmatrix} -\frac{2}{1+4t^2} \tilde{y}_t \|\xi_t^{up}\|^2 \\ \operatorname{Re} [\partial_x (\xi_t^{up})^* \xi_t^{up}] \\ 0 \end{pmatrix} \quad (3.40)$$

This choice also simplifies the analysis of backflow because of the reasons: First, the sign of the first and second component of \mathcal{J}^{Ψ_t} does not change by varying z . Second, x, y cannot change the sign of the third component of \mathcal{J}^{Ψ_t} . How these lead to the simplification of the analysis will be clear in Subsection 3.3.4. Now, the probability current density can be analyzed, with $\vec{r}_c = (-10, 0, 0)^\top$, $\vec{k}_0 = (10, 0, 0)^\top$ and $\lambda = 5$.

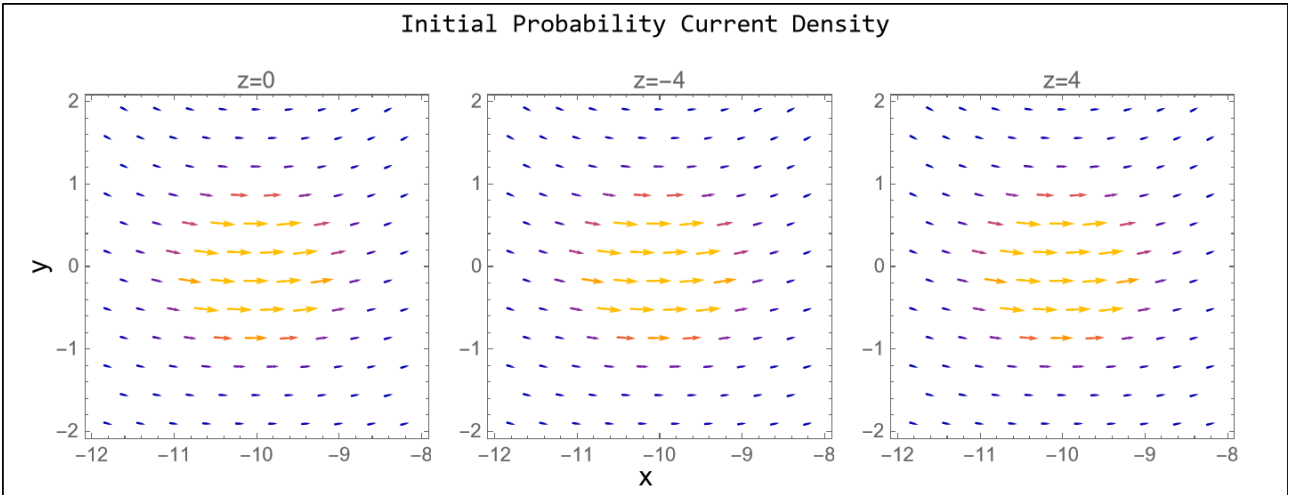


Figure 3.5: $x - y$ components of the initial probability current density for different values of z .

Figure 3.5 illustrates that the spin flux does not vanish at $z = 0$ due to the orientation of the initial spin wave function, which is different from the case examined in Subsection 2.4.3. Also, the flux looks independent of z because the first and second components of \mathcal{J}^{Ψ_t} is the symmetric in z except for $\|\zeta(z)\|^2$ and ρ^{Ψ_t} that determine only the magnitude of the arrows (see equation (3.39) and (3.37)). Additionally, the third component of the spin flux disappears, leaving only convective flux.

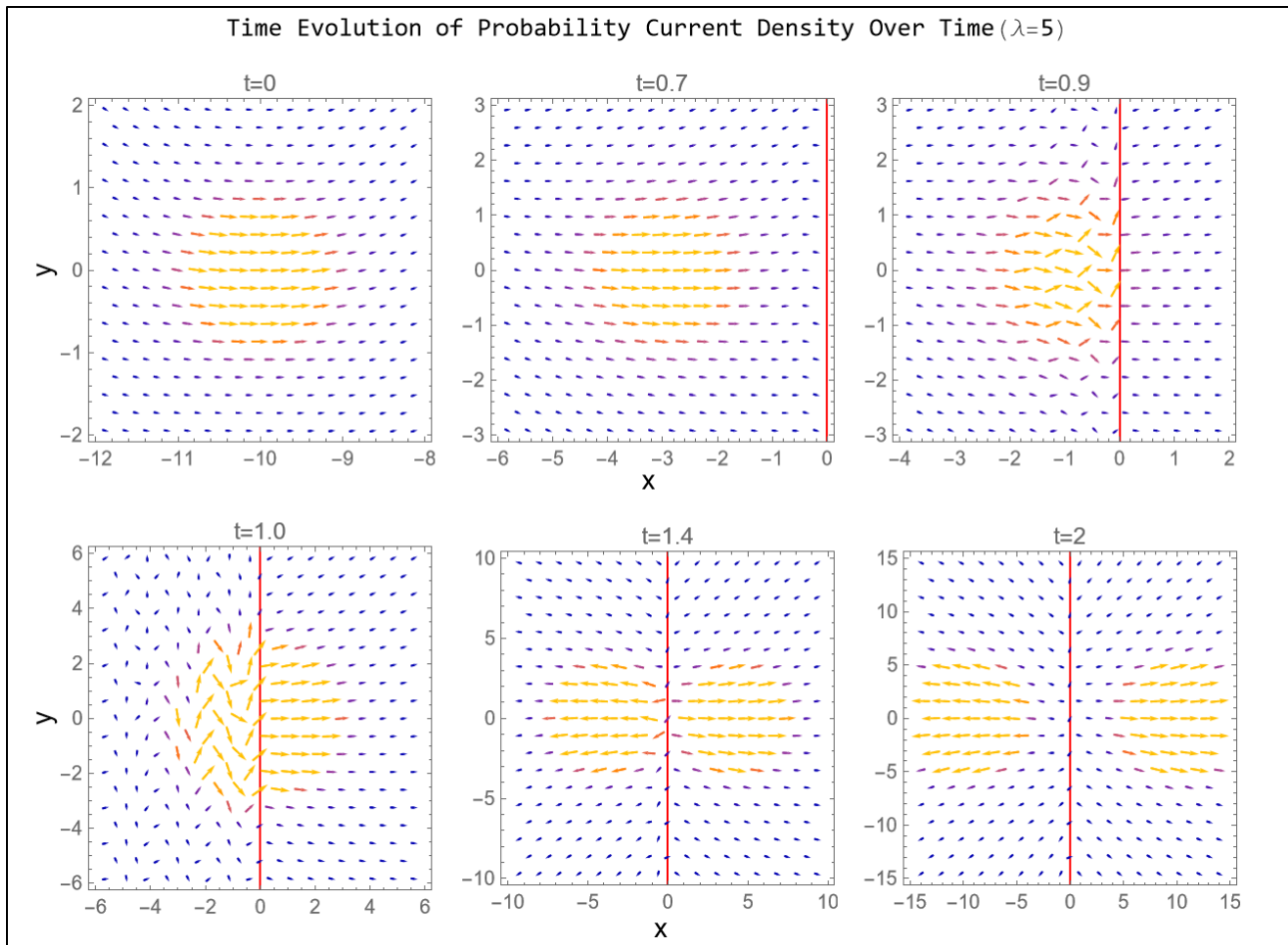


Figure 3.6: Time evolution of $x - y$ component of the probability current density for $z = 0$. The red line represents the magnetic barrier.

The initial probability current density begins to evolve as time progresses. Figure 3.6 illustrates that, at first, it propagates like a free particle. At $t = 0.9$, the probability flux starts to rotate counterclockwise at the magnetic barrier. However, at $t = 1.0$, the rotation direction of the probability flux in front of the magnetic barrier is mixed due to the strong interference of the reflected and incident fluxes. As time advances further, part of the probability density is reflected at the magnetic barrier, while partly transmitted through it.

Figure 3.7 shows that the probability flux rotates clockwise at the magnetic barrier. Although the probability flux exhibits mixed rotational motion in front of the magnetic field in both cases, it highlights that the direction of rotation at the magnetic barrier depends on the sign of λ . This can be verified by comparing the flux direction in both figures at $t = 1.0$ at the magnetic field.

Recall that λ incorporates both the magnetic dipole moment of the neutral particle and the intensity of the magnetic field. When the direction of the magnetic barrier is fixed to the positive z -direction, the magnetic dipole moment of the particle determines whether the probability current density points upward or downward at the magnetic barrier. For example, the probability current density for a neutron will rotate clockwise at the magnetic barrier because λ is negative due to its negative magnetic dipole moment [BD65, p.241].

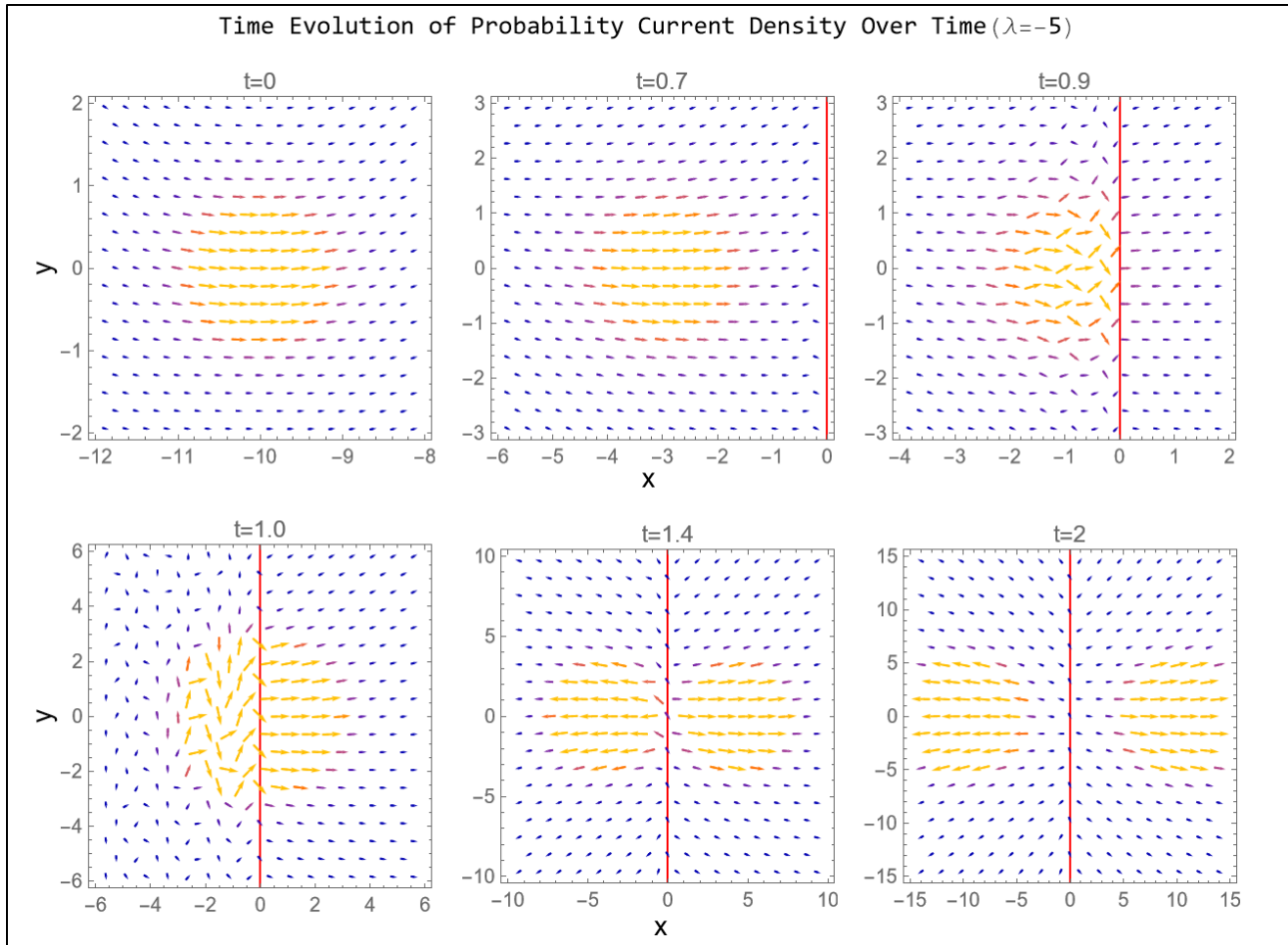


Figure 3.7: Time evolution of $x - y$ component of the probability current density at $z = 0$ for $\lambda = -5$. The red line represents the magnetic barrier.

For either sign of λ , the probability current density resumes propagating like a free particle after the collision.

3.3.4 Backflow and Stability

In this subsection, the existence of backflow will be examined, followed by a discussion on its stability.

To identify backflow, it is necessary to specify on which surface backflow occurs. However, there are uncountably many possible surfaces to choose from. Thus, some well-motivated restrictions must be imposed. Equation (3.37) and (3.39), along with the condition $\theta = \phi = 0$, suggest that surfaces should be chosen perpendicular to the x - or y -axis, as the third component of probability current density consists solely of free-propagating convective flux. This implies that backflow does not occur on surfaces perpendicular to z -axis. This will be further clarified later.

Additionally, we cannot predetermine where backflow is supposed to appear. Placing a surface at random positions and checking for the backflow effect would be inefficient. Instead, it is more effective to investigate the components of the probability current density individually over a broad range of x, y, z, t .

Before proceeding with that investigation, it is useful to specify how backflow should be identi-

fied. Consider a surface perpendicular to the x -axis at $x = \bar{x}$. This surface is denoted as $S_x(\bar{x})$. The generalized definition for an arbitrary surface perpendicular to p -axis is given by:

$$\begin{aligned} S_p : \mathbb{R} &\rightarrow \{\text{flat surface } S \subset \mathbb{R}^3\} \\ a &\mapsto S_p(a) = \{(x, y, z) \in \mathbb{R}^3 | p = a, p = x, y, z\} \end{aligned} \quad (3.41)$$

Then, $S_p(a)$ represents a flat surface perpendicular to p -axis at $p = a$. On S_x , the sign of the first component of the probability flux determines the occurrence of the backflow effect. The second and third components only contribute to directions parallel to the surface.

The backflow effect on $S_x(\bar{x})$ is confirmed if the sign of the first component of the probability flux changes on the surface. Similarly, backflow on S_y is determined by the sign of the second component of the probability current density. However, on S_z , the third component of \mathcal{J}^{Ψ_t} , composed only of the convective flux, ensures that backflow cannot occur because variation of x, y cannot change the sign of the third component of \mathcal{J}^{Ψ_t} (see equation (3.37) and (3.40)). Thus, surfaces S_z are excluded from further consideration.

To locate backflow, the first and second components are analyzed over a large domain with fixed z -value. However, plotting these components for the three parameters (x, y, t) simultaneously is impractical. To address this, at least one parameter must be kept fixed for ease of visualization. Additionally, each component is normalized by its norm respectively, as its magnitude is too small to discern changes in the sign clearly:

$$[\mathcal{J}^{\Psi_t}]_{norm}^i = \begin{cases} 1 & \text{for } [\mathcal{J}^{\Psi_t}]^i < 0 \\ 0 & \text{for } [\mathcal{J}^{\Psi_t}]^i = 0 \\ -1 & \text{for } [\mathcal{J}^{\Psi_t}]^i > 0 \end{cases} \quad (3.42)$$

$[\mathcal{J}^{\Psi_t}]^i$ denotes i -th component of \mathcal{J}^{Ψ_t} .

Then, the procedure of finding backflow is summarized as follows: First, we check by plotting if the sign of normalized first and second component of \mathcal{J}^{Ψ_t} changes over its domain (x, y, t) . The change of sign is a candidate of backflow. Second, we specify the position of the candidate given that it is found. Third, we put a flat surface at this specified position. This flat surface is S_x for the first component, and S_y for the second component. If the flux changes its sign on this surface, this candidate is identified as backflow.

To begin, we investigate $[\mathcal{J}^{\Psi_t}]_{norm}^1$ with $z = 0$ at first.

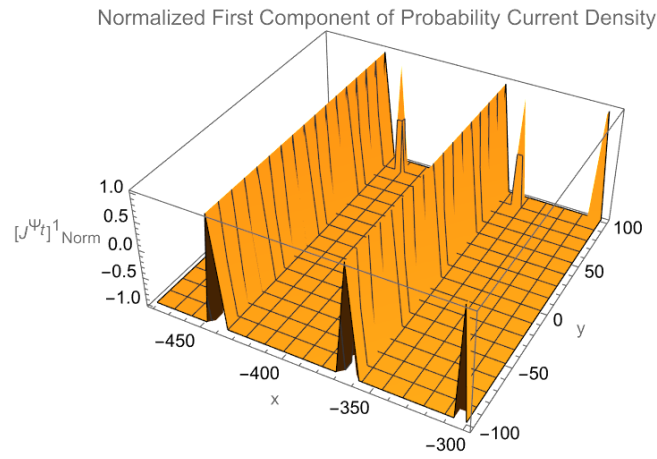


Figure 3.8: Normalized first component of the probability current density for $t = 20.047$ at $z = 0$.

Figure 3.8 depicts several peaks within $-450 < x < -300$ and $-100 < y < 100$, identified by manipulating t .

These peaks are potential candidates for the backflow effect. However, a peak cannot represent a backflow if it is aligned parallel to the y -axis, as this implies no change in the sign of the first component across the surface. To analyze the structure in more detail, the region around $x = -440$ is magnified.

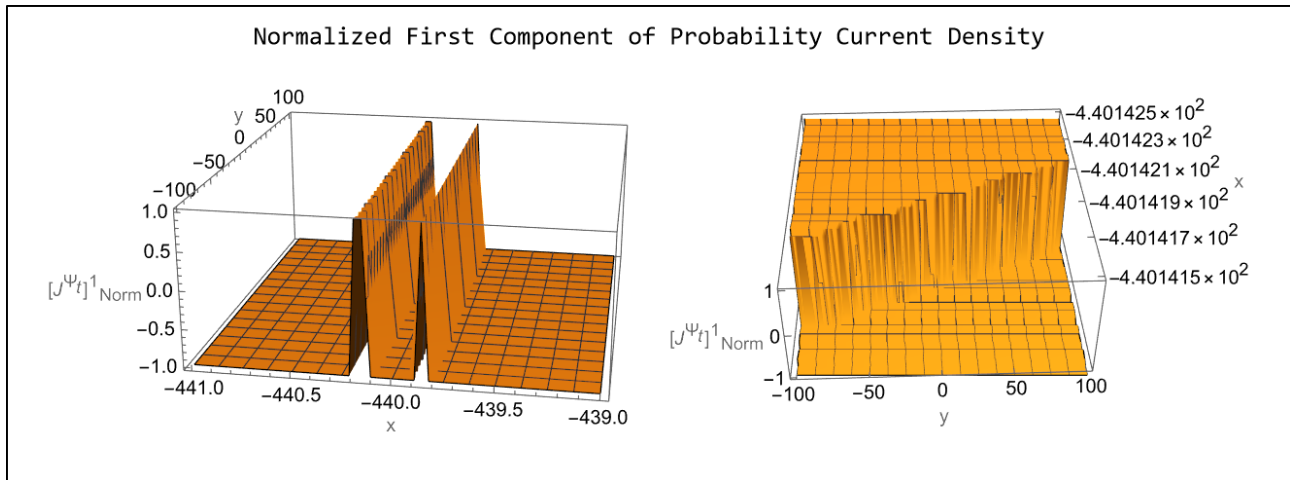


Figure 3.9: Normalized first component of the probability current density zoomed around $x = -440$ for $t = 20.047$ and $z = 0$.

On the left side of Figure 3.9, an additional peak is revealed, indicating that the previously observed peaks are actually narrower than depicted in Figure 3.8. This happened because of the resolution of the plotting software. Further magnification on the right side reveals structural details.

Normalization of the first component reveals a "cliff" where sign changes. An interesting observation is that this cliff does not extend parallel to the y -axis. This confirms that the peak represents backflow, since the normalized first component decreases from 1 to -1 along the y -axis on surfaces that intersect the cliff.

A more detailed investigation can be conducted by evaluating the first component of the probability current density on surfaces placed at intervals of 0.0001 along the x -axis, from $x = -440.1425$ to $x = -440.1415$. The backflow effect was ultimately found on a surface around $x = -440.1418$.

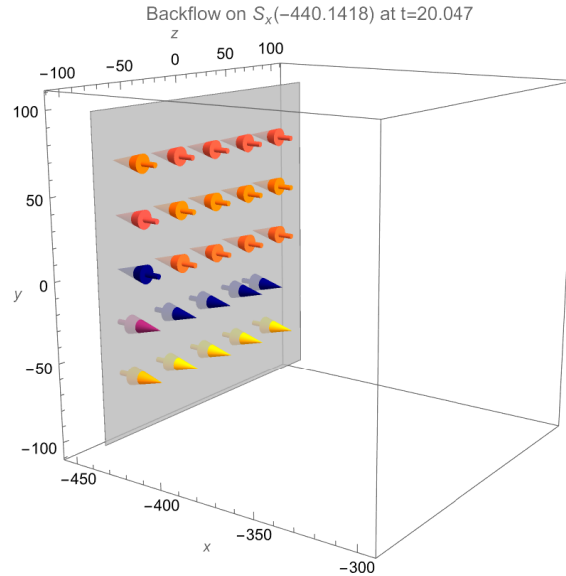


Figure 3.10: The normalized first component of the probability current density at $x = -440.1418$ for $t = 20.047$.

The probability current density is now evaluated on $S_x(-440.1418)$. Figure 3.10 illustrates the first component of the probability current density, showing that it changes sign on portions of $S_x(-440.1418)$. This confirms the presence of backflow on this surface. Notably, the surface is positioned farther from the magnetic barrier than the center of the initial Gaussian wave packet. Although, this does not correspond to far-field conditions, it suggests that backflow can occur not only near the magnetic barrier, but also farther away.

By applying the same analysis to the other candidates, it is confirmed that all identified peaks qualify as a backflow due to their similar structure. However, the stability of backflow over time must also be examined.

The left side of Figure 3.11 shows that backflow emerges around $t = 20$, at which the center of the Gaussian wave packet reaches the magnetic barrier. At this point, interference between the reflected and incident wave functions is, in a sense, maximal, producing backflow at multiple locations. This behavior is confirmed by the figure on the right panel.

Post collision, however, backflow situations no longer appear at $z = 0$. They emerge briefly around $t = 20$ and disappear instantaneously. Furthermore, when considering the corresponding real-scale value of x (see Subsection 3.3.1), the width of the backflow bundle is found to be less than 700nm. This narrow width makes detection impractical. Consequently, attempting to detect the backflow effect on $S_x(\bar{x})$ for some $\bar{x} \in \mathbb{R}$ may hardly be feasible.

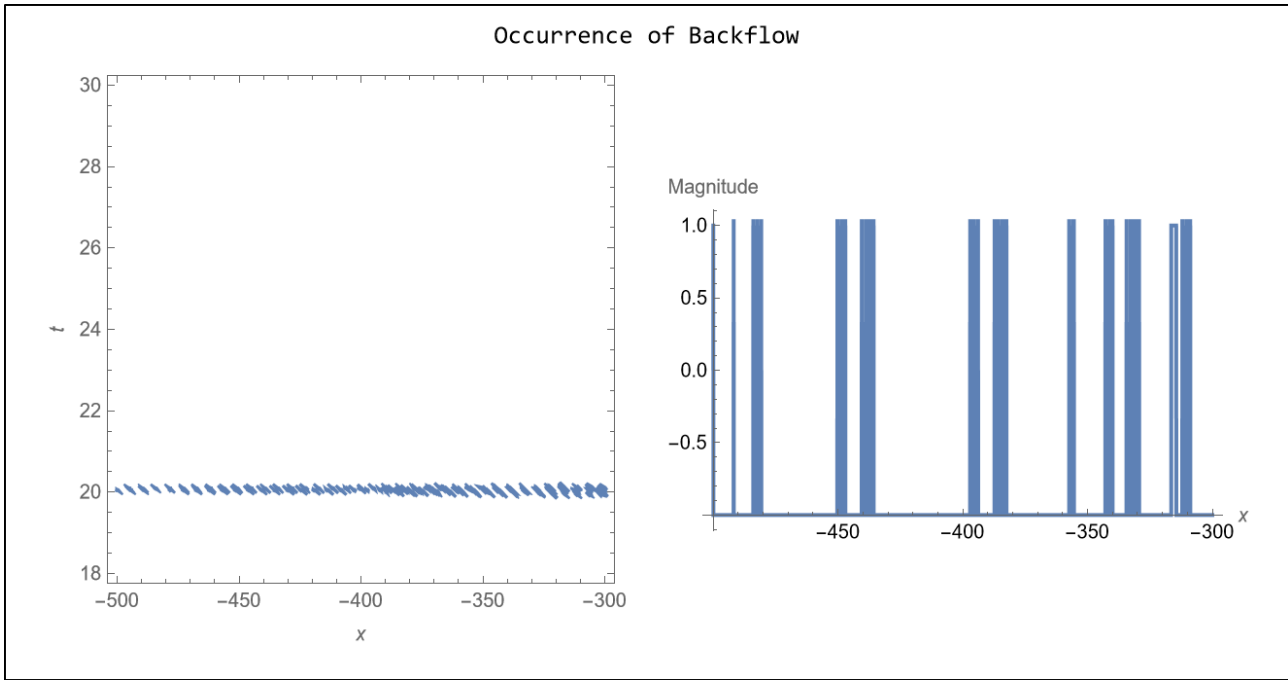


Figure 3.11: Occurrence of the backflow effect with respect to x and t (left) and the position of backflow situations at $t = 20.047$ (right).

Next, backflow will be investigated on $S_y(\bar{y})$ for some $\bar{y} \in \mathbb{R}$. Similar to the surfaces S_x , the backflow effect is identified through analogous procedures. By varying t , it is observed that peaks appear and disappear persistently. However, all observed peaks are automatically qualified as a backflow, as they extend in the y -direction. For example, a peak is specified at $y = \bar{y}$ around $x = \bar{x}$. To see if this peak represents a backflow, we vary x at $y = \bar{y}$, because we are investigating the normalized second component of \mathcal{J}^{Ψ_t} . On the variation of x , we can always find backflow around $x = \bar{x}$. If peaks had extended in x -direction, we would have necessarily investigated if the cliff of the peaks extends parallel to x -axis, as in the case of the normalized first component of \mathcal{J}^{Ψ_t} .

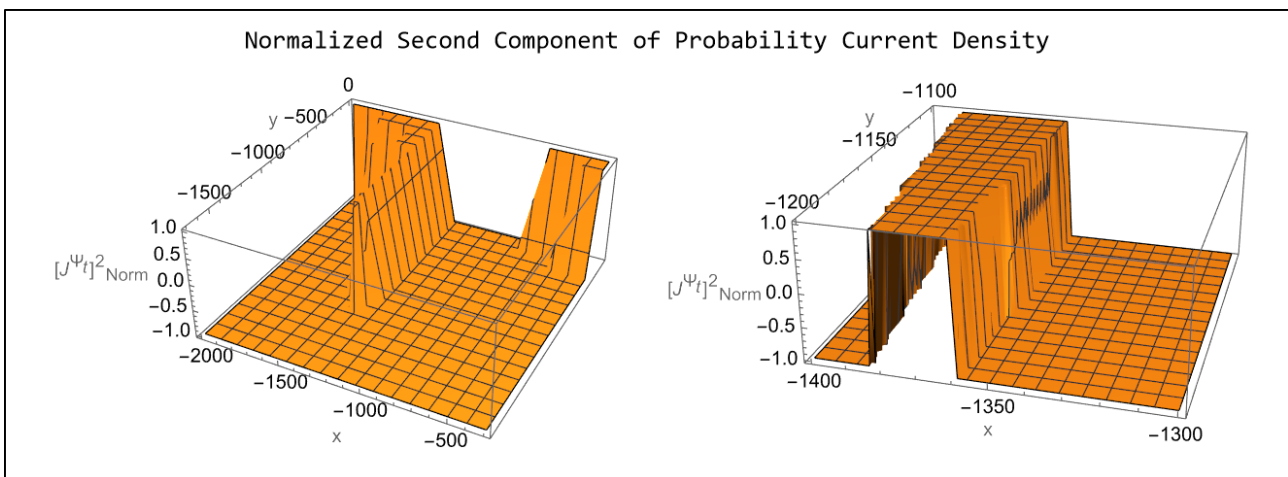


Figure 3.12: Normalized second component of the probability current density at $t = 85100$ and $z = 0$. A peak is identified over a large area (left), which is zoomed around $x = -1350$ (right).

In Figure 3.12, a peak is detected at $t = 85100$. The magnified view on the right panel reveals

that the peak has a real-scale width of approximately $1.8\mu\text{m}$.

Backflow can be identified for any $y \in [-1200, 0]$. However, values around $y = 0$ are not practical for detection. A detector placed in this region would likely disturb the wave function before it reaches the magnetic barrier. This interaction alters the wave function evolution, making it no longer well-described by the solution obtained in this chapter.

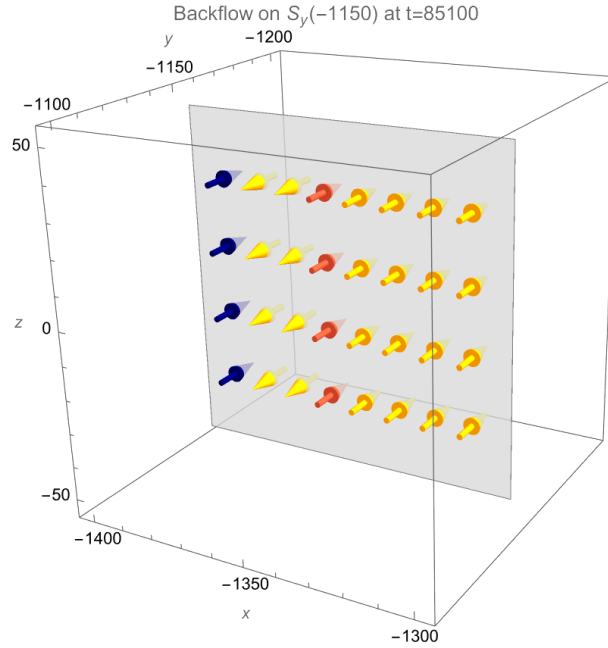


Figure 3.13: Normalized second component of the probability current density on $S_y(-1150)$ at $t = 85100$.

Figure 3.13 confirms the presence of backflow on $S_y(-1150)$ at $t = 85100$. Consistent with Figure 3.12, the backflow is evident from the change in the direction of the normalized second components of the probability current density as a function of x .

In comparison with the backflow effect on S_x , that on S_y is observed for $t \gg 20$, indicating that they are relatively more stable over time. Still, it is not sufficient for practical detection because backflow appears and disappears. Moreover, their positions are extremely unstable. Backflow moves in the x -direction as time progresses.

To analyze this behavior and stability of backflow in more detail, the second component of the probability current density must also be examined over an interval of time. This can be performed by visualizing regions where the normalized second component is positive, with t .

Figure 3.14 demonstrates that backflow persists over a long timespan. In the left panel, it can be seen that backflow regions move in the negative x -direction. The spikes observed show why backflow appears and disappears. This indicates that the backflow identified in Figure 3.12 is one of these spikes. On the right panel, the spikes are shown to originate near $y = 0$.

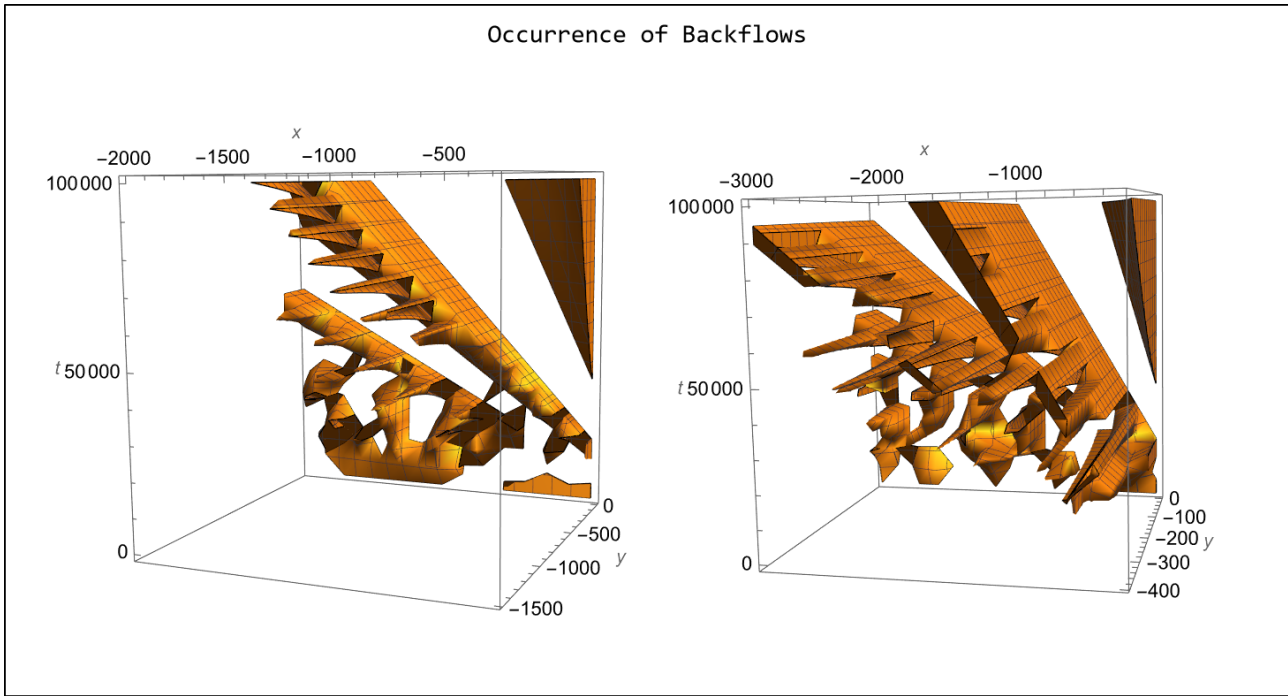


Figure 3.14: Domains of positive values of second component of the probability current density. The occurrence of backflow on S_y over t is confirmed. The right panel provides a zoomed view for $-400 < y < 0$.

Additionally, it is important to note that the center of the wave function is located at $x = k_{0x} \cdot t$. It means that the backflow effect generated is at the tail of the wave function. This poses a significant challenge for detecting the backflow effect, as particles are rarely found in the tails of the wave packet.

Further analysis reveals that almost the entire region with positive y -values is occupied by the area of positive second component values. This suggests that the backflow effect occurs more frequently for negative y -values because, on S_y that intersect this area, the sign of the second component changes more frequently

Although backflow consistently appears, their domains are unstable and shift with time. When a surface S_y is placed, the backflow effect is observed to move in the negative x -direction.

In conclusion, the delta magnetic potential enhances backflow compared to the scenario in Chapter 2. However, this backflow remains relatively unstable both with regards to position and time.

4.1 Results of the Analysis

In the introduction, it was stated that backflow is identified as occurring, but is unstable in both time and position. In Chapter 2, the effect of a simple time varying magnetic field on the dynamics of a neutral spin- $\frac{1}{2}$ particle was examined where the field is abruptly removed at a predetermined time. The result showed that backflow is suppressed because the spin flux decays much faster than the convective flux. Consequently, backflows cannot practically be detected in this scenario.

In chapter 3, a delta-magnetic barrier was introduced to amplify backflow through the interference of the incident and reflected components of the wave function. As a result, backflow is induced on surfaces perpendicular to the x -axis at the moment of impact of the wave packet. Furthermore, backflow could be identified on surfaces perpendicular to the y -axis, even after the time of impact. However, it was found that the backflow is unstable both in time and position, presenting a significant experimental challenge for detecting it.

In conclusion, the detection of backflow will be extremely difficult in the analyzed experimental setups due to their instability.

4.2 Outlook

The spin-flux was observed to decay in open space in Chapter 2, spreading out across the domain. This behavior is a characteristic of the Gaussian wave packet. This observation suggests that the wavefunction must be confined within some barriers to prevent the spin flux from dispersing throughout space. In such a configuration, the spin flux may be expected to be more strong, potentially making backflow stand out more. [DD19]

A.1 Propagator for Free Particle

To find the time-dependent wavefunction for a free particle with a Gaussian wave packet, the propagator for a free particle must first be determined. As shown in Subsection 1.4.3, the propagator can be derived by applying the Laplace transform to the Schrödinger equation:

$$i\hbar s\phi_s(x) - i\hbar\psi_0(x) = -\frac{\hbar^2}{2m}\partial_x^2\phi_s(x)$$

The homogeneous solutions $u_s^1(x), u_s^2(x)$ to this differential equation are straightforward:

$$\begin{cases} u_s^1(x) = \exp\left[i\sqrt{\frac{2ims}{\hbar}}x\right] \\ u_s^2(x) = \exp\left[-i\sqrt{\frac{2ims}{\hbar}}x\right] \end{cases} \quad (\text{A.1})$$

Substituting $u_s^1(x)$ and $u_s^2(x)$ into equations (1.19) and (1.20) gives the particular solution:

$$\begin{aligned} \phi_s^p(x) = & \sqrt{\frac{m}{2i\hbar s}} \left[\exp\left(i\sqrt{\frac{2ims}{\hbar}}x\right) \int_{-\infty}^x \exp\left(-i\sqrt{\frac{2ims}{\hbar}}x'\right) \psi_0(x') dx' \right. \\ & \left. - \exp\left(-i\sqrt{\frac{2ims}{\hbar}}x\right) \int_{-\infty}^x \exp\left(i\sqrt{\frac{2ims}{\hbar}}x'\right) \psi_0(x') dx' \right], \end{aligned} \quad (\text{A.2})$$

where the Wronskian of $u_s^1(x)$ and $u_s^2(x)$ is given by:

$$W[u_s^1(x'), u_s^2(x')] = -2i\sqrt{\frac{2ims}{\hbar}} \quad (\text{A.3})$$

To determine the coefficient α_s and β_s of the complementary solution, boundary conditions are applied. For a free particle, the wavefunction must converge to zero as $x \rightarrow \pm\infty$, since it represents a Gaussian wave packet. Consequently, the Laplace-transformed wavefunction $\phi_s(x)$ also converges to zero as $x \rightarrow \pm\infty$. This implies that the general solution, comprising the particular and complementary solutions, vanishes as x diverges in either direction.

In the first condition ($x \rightarrow -\infty$), the general solution equals the complementary solution, as the particular solution vanishes, leading to:

$$\begin{aligned} \lim_{x \rightarrow -\infty} \phi_s^c(x) = & \alpha_s \lim_{x \rightarrow -\infty} \exp\left[i\sqrt{\frac{2ims}{\hbar}}x\right] + \beta_s \lim_{x \rightarrow -\infty} \exp\left[-i\sqrt{\frac{2ims}{\hbar}}x\right] \\ & \stackrel{!}{=} 0 \end{aligned} \quad (\text{A.4})$$

The first term in this equation diverges:

$$\lim_{x \rightarrow -\infty} \exp \left[i \sqrt{\frac{2ims}{\hbar}} x \right] = \lim_{x \rightarrow -\infty} \exp \left[(i-1) \sqrt{\frac{ms}{\hbar}} x \right] = \infty \quad (\text{A.5})$$

Therefore, it must be that $\alpha_s = 0$.

In the case of second condition ($x \rightarrow \infty$), the particular solution does not vanish. However, using $\alpha_s = 0$, the coefficient β_s can be determined as follows:

$$\lim_{x \rightarrow \infty} \beta_s = \lim_{x \rightarrow \infty} \exp \left[i \sqrt{\frac{2ims}{\hbar}} x \right] \phi_s(x) - \lim_{x \rightarrow \infty} \exp \left[i \sqrt{\frac{2ims}{\hbar}} x \right] \phi_s^p(x) \quad (\text{A.6})$$

$$= - \lim_{x \rightarrow \infty} \exp \left[i \sqrt{\frac{2ims}{\hbar}} x \right] \phi_s^p(x) \quad (\text{A.7})$$

$$= - \lim_{x \rightarrow \infty} \sqrt{\frac{m}{2i\hbar s}} \left[\exp \left(2i \sqrt{\frac{2ims}{\hbar}} x \right) \int_{-\infty}^x \exp \left(-i \sqrt{\frac{2ims}{\hbar}} x' \right) \psi_0(x') dx' \right. \\ \left. - \int_{-\infty}^x \exp \left(i \sqrt{\frac{2ims}{\hbar}} x' \right) \psi_0(x') dx' \right] \quad (\text{A.8})$$

$$= \sqrt{\frac{m}{2i\hbar s}} \int_{-\infty}^{\infty} \exp \left(i \sqrt{\frac{2ims}{\hbar}} x' \right) \psi_0(x') dx' \quad (\text{A.9})$$

$$= \beta_s \quad (\text{A.10})$$

The first term on the right-hand side in equation (A.6) vanishes because both the exponential function and the general solution $\phi_s(x)$ converge to zero. The first term in equation (A.8) also converges to zero due to the vanishing exponential function.

By substituting α_s and β_s , the general solution $\phi_s(x)$ becomes: $\phi_s(x)$ is:

$$\phi_s(x) = \sqrt{\frac{m}{2i\hbar s}} \left[\exp \left(i \sqrt{\frac{2ims}{\hbar}} x \right) \int_{-\infty}^x \exp \left(-i \sqrt{\frac{2ims}{\hbar}} x' \right) \psi_0(x') dx' \right. \\ \left. - \exp \left(-i \sqrt{\frac{2ims}{\hbar}} x \right) \int_{-\infty}^x \exp \left(i \sqrt{\frac{2ims}{\hbar}} x' \right) \psi_0(x') dx' \right] \\ + \sqrt{\frac{m}{2i\hbar s}} \exp \left(-i \sqrt{\frac{2ims}{\hbar}} x \right) \int_{-\infty}^{\infty} \exp \left(i \sqrt{\frac{2ims}{\hbar}} x' \right) \psi_0(x') dx' \quad (\text{A.11})$$

$$= \sqrt{\frac{m}{2i\hbar s}} \left[\int_{-\infty}^x \exp \left(i \sqrt{\frac{2ims}{\hbar}} (x - x') \right) \psi_0(x') dx' \right. \\ \left. - \int_{-\infty}^x \exp \left(i \sqrt{\frac{2ims}{\hbar}} (x' - x) \right) \psi_0(x') dx' + \int_{-\infty}^{\infty} \exp \left(i \sqrt{\frac{2ims}{\hbar}} (x' - x) \right) \psi_0(x') dx' \right] \quad (\text{A.12})$$

$$= \sqrt{\frac{m}{2i\hbar s}} \left[\int_{-\infty}^x \exp\left(i\sqrt{\frac{2ims}{\hbar}}(x-x')\right) \psi_0(x') dx' + \int_x^{\infty} \exp\left(i\sqrt{\frac{2ims}{\hbar}}(x'-x)\right) \psi_0(x') dx' \right] \quad (\text{A.13})$$

$$= \sqrt{\frac{m}{2i\hbar s}} \left[\int_{-\infty}^x \exp\left(i\sqrt{\frac{2ims}{\hbar}}\|x-x'\|\right) \psi_0(x') dx' + \int_x^{\infty} \exp\left(i\sqrt{\frac{2ims}{\hbar}}\|x-x'\|\right) \psi_0(x') dx' \right] \quad (\text{A.14})$$

$$= \sqrt{\frac{m}{2i\hbar s}} \int_{-\infty}^{\infty} \exp\left(i\sqrt{\frac{2ims}{\hbar}}\|x-x'\|\right) \psi_0(x') dx' \quad (\text{A.15})$$

In equation (A.13), $x-x'$ and $x'-x$ in the argument of exponential function are both positive over the respective ranges of integration, which allows to substitute them with $\|x-x'\|$.

Additionally, it was revealed that, in equation (A.12), the last term corresponds to a second homogeneous solution multiplied by some constant value, which indicates that the particular solution $\phi_s^p(x)$ includes a homogeneous solution. This included homogeneous solution, however, compensates $\beta_s u_s^2(x)$, making the complementary solution vanishes.

Equation (A.15) is the Laplace-transformed wavefunction, therefore, the inverse Laplace transform must be applied to obtain the time-dependet wavefunction $\psi_t(x)$. To achieve this, the following formula is used [Pro+54]:

$$\mathcal{L}^{-1} \left[\frac{1}{\sqrt{s}} \exp\left(i\sqrt{2ias}\right) \right] = \frac{\exp\left(\frac{ia}{2t}\right)}{\sqrt{\pi t}}, \quad a > 0 \quad (\text{A.16})$$

The inverse Laplace transform of $\phi_s(x)$ is then:

$$\psi_t(x) = \mathcal{L}^{-1}[\phi_s(x)] \quad (\text{A.17})$$

$$= \mathcal{L}^{-1} \left[\sqrt{\frac{m}{2i\hbar s}} \int_{-\infty}^{\infty} \exp\left(i\sqrt{\frac{2ims}{\hbar}}\|x-x'\|\right) \psi_0(x') dx' \right] \quad (\text{A.18})$$

$$= \sqrt{\frac{m}{2\pi i\hbar t}} \int_{-\infty}^{\infty} \exp\left[\frac{im(x-x')^2}{2\hbar t}\right] \psi_0(x') dx' \quad (\text{A.19})$$

Comparing with equation (1.16), the one-dimensional propagator for a free particle $K_0(x, t, x', 0)$ is obtained as:

$$K_0(x, t, x', 0) = \sqrt{\frac{m}{2\pi i\hbar t}} \exp\left[\frac{im(x-x')^2}{2\hbar t}\right] \quad (\text{A.20})$$

For a three-dimensional case, this propagator can applied to the initial wavefunction by treating the $x, y,$ and z coordinates separately, provided that the wavefunction $\psi_0(\vec{r})$ is separable in the $x, y,$ and z components.

A.2 Time-Dependent Wavefunction for a Free Particle

The time-dependent wavefunction can be obtained by integrating the initial wavefunction $\xi_0(x')$ over x' , together with the propagator $K_0(x, t, x', 0)$. The calculation proceeds as follows:

$$\begin{aligned}\xi_t(x) &= \int_{-\infty}^{\infty} K_0(x, t, x', 0) \xi_0(x') dx' \\ &= \left(\frac{2a}{\pi}\right)^{\frac{1}{4}} \sqrt{\frac{m}{2\pi i \hbar t}} \int_{-\infty}^{\infty} \exp\left[\frac{im(x-x')^2}{2\hbar t} - a(x'-x_c)^2 + ik_{0x}x'\right] dx'\end{aligned}\quad (\text{A.21})$$

To evaluate this integral, the argument of the exponential function must be expressed as a perfect square term. This can be done by completing the square.

$$\begin{aligned}&\left(\frac{2a}{\pi}\right)^{\frac{1}{4}} \sqrt{\frac{m}{2\pi i \hbar t}} \int_{-\infty}^{\infty} \exp\left[\frac{im(x-x')^2}{2\hbar t} - a(x'-x_c)^2 + ik_{0x}x'\right] dx' \\ &= \left(\frac{2a}{\pi}\right)^{\frac{1}{4}} \sqrt{\frac{m}{2\pi i \hbar t}} \int_{-\infty}^{\infty} \exp\left[-\left(a - \frac{im}{2\hbar t}\right)x'^2 + \left(ik_{0x} - \frac{imx}{\hbar t} + 2ax_c\right)x'\right] \\ &\quad \cdot \exp\left[-ax_c^2 + \frac{imx^2}{2\hbar t}\right] dx' \\ &= \left(\frac{2a}{\pi}\right)^{\frac{1}{4}} \sqrt{\frac{m}{2\pi i \hbar t}} \int_{-\infty}^{\infty} \exp\left[-\left(a - \frac{im}{2\hbar t}\right)\left(x' - \frac{ik_{0x} - \frac{imx}{\hbar t} + 2ax_c}{2\left(a - \frac{im}{2\hbar t}\right)}\right)^2\right] \\ &\quad \cdot \exp\left[\frac{\left(ik_{0x} - \frac{imx}{\hbar t} + 2ax_c\right)^2}{4\left(a - \frac{im}{2\hbar t}\right)} - ax_c^2 + \frac{imx^2}{2\hbar t}\right] dx'\end{aligned}\quad (\text{A.22})$$

This integral is calculated using the Gaussian integral formula:

$$= \left(\frac{2a}{\pi}\right)^{\frac{1}{4}} \sqrt{\frac{m}{2\pi i \hbar t}} \sqrt{\frac{\pi}{a - \frac{im}{2\hbar t}}} \exp\left[-ax_c^2 + \frac{imx^2}{2\hbar t}\right] \exp\left[\frac{\left(ik_{0x} - \frac{imx}{\hbar t} + 2ax_c\right)^2}{4\left(a - \frac{im}{2\hbar t}\right)}\right]\quad (\text{A.23})$$

This equation can be simplified further as follows:

$$\begin{aligned}&\left(\frac{2a}{\pi}\right)^{\frac{1}{4}} \sqrt{\frac{m}{2\pi i \hbar t}} \sqrt{\frac{\pi}{a - \frac{im}{2\hbar t}}} \exp\left[-ax_c^2 + \frac{imx^2}{2\hbar t}\right] \exp\left[\frac{\left(ik_{0x} - \frac{imx}{\hbar t} + 2ax_c\right)^2}{4\left(a - \frac{im}{2\hbar t}\right)}\right] \\ &= \left(\frac{2a}{\pi}\right)^{\frac{1}{4}} \sqrt{\frac{m}{m + 2i\hbar at}} \exp\left[\frac{m}{m + 2i\hbar at} \left(-a(x-x_c)^2 + ik_{0x}x - i\frac{\hbar^2 k_{0x}^2 t}{2m\hbar}\right)\right] \\ &\quad \cdot \exp\left[\frac{m}{m + 2i\hbar at} \frac{-\hbar at k_{0x} x_c}{m}\right] \\ &= \left(\frac{2a}{\pi}\right)^{\frac{1}{4}} \sqrt{\frac{m}{m + 2i\hbar at}} \exp\left[\frac{-ma(x-x_c)^2}{m + 2i\hbar at} + \left(1 - \frac{2i\hbar at}{m + 2i\hbar at}\right) \left(ik_{0x}x - i\frac{\hbar^2 k_{0x}^2 t}{2m\hbar}\right)\right] \\ &\quad \cdot \exp\left[\frac{m}{m + 2i\hbar at} \frac{-\hbar at k_{0x} x_c}{m}\right] \\ &= \left(\frac{2a}{\pi}\right)^{\frac{1}{4}} \sqrt{\frac{m}{m + 2i\hbar at}} \exp\left[\frac{-ma}{m + 2i\hbar at} \left(x - x_c - \frac{\hbar k_{0x} t}{m}\right)^2 + i\left(k_{0x}x - \frac{\hbar^2 k_{0x}^2 t}{2m\hbar}\right)\right]\end{aligned}\quad (\text{A.24})$$

Hence, the time-dependent wavefunction for a free particle is

$$\xi_t(x) = \left(\frac{2a}{\pi}\right)^{\frac{1}{4}} \sqrt{\frac{m}{m + 2i\hbar at}} \exp\left[\frac{-ma}{m + 2i\hbar at} \left(x - x_c - \frac{\hbar k_{0x} t}{m}\right)^2 + i\left(k_{0x} x - \frac{\hbar^2 k_{0x}^2 t}{2m\hbar}\right)\right] \quad (\text{A.25})$$

This expression shows how an initial Gaussian wave packet centered at x_c evolves over time with a wave vector k_{0x} .

A.3 Wavefunction as a Solution to the Schrödinger Equation

The time-dependent wavefunction for a free particle was found in Subsection 2.1.3:

$$\psi_t(\vec{r}) = \left(\frac{2a}{\pi}\right)^{\frac{3}{4}} \gamma_t^{\frac{3}{2}} \exp\left[-a\gamma_t \left(\vec{r} - \vec{r}_c - \frac{\hbar\vec{k}_0 t}{m}\right)^2 + i\left(\vec{k}_0 \cdot \vec{r} - \frac{\hbar^2 k_0^2 t}{2m\hbar}\right)\right] \quad (\text{A.26})$$

To show that this wavefunction $\psi_t(\vec{r})$ is a solution to the Schrödinger equation for a free particle, the wavefunction $\psi_t(\vec{r})$ is inserted into the Schrödinger equation. If the time- and spatial derivatives are the same, this wavefunction is a solution to the Schrödinger equation. Assume that

$$\psi_t(\vec{r}) = \left(\frac{2a}{\pi}\right)^{\frac{3}{4}} \gamma_t^{\frac{3}{2}} \exp\left[-a\gamma_t \vec{r}_t^2 + i\left(\vec{k}_0 \cdot \vec{r} - \frac{\hbar^2 k_0^2 t}{2m\hbar}\right)\right] \quad (\text{A.27})$$

$$\text{where } \vec{r}_t = \vec{r} - \vec{r}_c - \frac{\hbar\vec{k}_0 t}{m}.$$

The left-hand side of the Schrödinger equation is evaluated at first. The coefficient $\left(\frac{2a}{\pi}\right)^{\frac{3}{4}}$ will be ignored because it is a constant coefficient for both sides:

$$\begin{aligned} & i\hbar \frac{\partial \psi_t(\vec{r})}{\partial t} \\ &= \frac{\partial \gamma_t^{\frac{3}{2}}}{\partial t} \cdot \exp\left[-a\gamma_t \vec{r}_t^2 + i\left(\vec{k}_0 \cdot \vec{r} - \frac{\hbar^2 k_0^2 t}{2m\hbar}\right)\right] + \gamma_t^{\frac{3}{2}} \frac{\partial}{\partial t} \exp\left[-a\gamma_t \vec{r}_t^2 + i\left(\vec{k}_0 \cdot \vec{r} - \frac{\hbar^2 k_0^2 t}{2m\hbar}\right)\right] \\ &= \gamma_t^{\frac{3}{2}} \exp\left[-a\gamma_t \vec{r}_t^2 + i\left(\vec{k}_0 \cdot \vec{r} - \frac{\hbar^2 k_0^2 t}{2m\hbar}\right)\right] \cdot \left(\frac{3\gamma_t \hbar^2 a}{m} - \frac{2\hbar^2 a^2 \gamma_t^2 \vec{r}_t^2}{m} + \frac{2i\hbar^2 a \gamma_t \vec{r}_t \cdot \vec{k}_0}{m} + \frac{\hbar^2 k_0^2}{2m}\right) \end{aligned} \quad (\text{A.28})$$

The right-hand side of the Schrödinger-equation is

$$\begin{aligned} & -\frac{\hbar^2}{2m} \nabla^2 \psi_t(\vec{r}) \\ &= \gamma_t^{\frac{3}{2}} \exp\left[-a\gamma_t \vec{r}_t^2 + i\left(\vec{k}_0 \cdot \vec{r} - \frac{\hbar^2 k_0^2 t}{2m\hbar}\right)\right] \cdot \left(\frac{3\gamma_t \hbar^2 a}{m} - \frac{2\hbar^2 a^2 \gamma_t^2 \vec{r}_t^2}{m} + \frac{2i\hbar^2 a \gamma_t \vec{r}_t \cdot \vec{k}_0}{m} + \frac{\hbar^2 k_0^2}{2m}\right) \end{aligned} \quad (\text{A.29})$$

Equations (A.28) and (A.29) are the same. As a result, the given time-dependent wavefunction $\psi_t(\vec{r})$ is a time-dependent solution to the Schrödinger equation for a free particle.

B.1 Propagator for a Delta-Potential

In this section, the one-dimensional propagator $K_{\delta}^{\sigma_z}(x, t, x', 0)$ for delta potential is derived. In Chapter 3, the Hamiltonian is given as:

$$\hat{H} = -\frac{\hbar^2}{2m}\nabla^2 + \lambda\sigma_z\delta(x) \quad (\text{B.1})$$

To simplify the derivation of the propagator, the Pauli matrix σ_z is omitted because the Pauli equation can be decoupled into spin-up part and spin-down components:

$$\Psi_t(x) = \begin{pmatrix} \Psi_t^{up}(x) \\ \Psi_t^{down}(x) \end{pmatrix} \quad (\text{B.2})$$

These components satisfy the following equations:

$$\begin{cases} i\hbar\frac{\partial}{\partial t}\Psi_t^{up}(x) = -\frac{\hbar^2}{2m}\nabla^2\Psi_t^{up}(x) + \lambda\delta(x)\Psi_t^{up}(x) \\ i\hbar\frac{\partial}{\partial t}\Psi_t^{down}(x) = -\frac{\hbar^2}{2m}\nabla^2\Psi_t^{down}(x) - \lambda\delta(x)\Psi_t^{down}(x) \end{cases} \quad (\text{B.3})$$

Then, the propagator $K_{\delta}(x, t, x', 0)$ for the spin-up component is derived, as the propagator for the spin-down component can be obtained by simply changing the sign of λ . This will be applied in the Section 3.2. As a last step, λ is replaced by $\lambda\sigma_z$ to recover the propagator $K_{\delta}^{\sigma_z}(x, t, x', 0)$, which is a 2×2 matrix.

To derive the propagator $K_{\delta}(x, t, x', 0)$ for a delta-potential, the Laplace-transformed Schrödinger equation is solved at first [Cam09]. Subsequently, The kernal of the integral operator is obtained by applying the inverse Laplace transform, which provides the propagator for a delta-potential.

B.1.1 Solution to the Laplace-transformed Schrödinger Equation

The Laplace-transformed Schrödinger equation is (see 1.17):

$$i\hbar s\phi_s(x) - i\hbar\psi_0(x) = -\frac{\hbar^2}{2m}\partial_x^2\phi_s(x) + \lambda\delta(x)\phi_s(x) \quad (\text{B.4})$$

Since this equation includes the Dirac delta distribution $\delta(x)$, the solution for this differential equation is not smooth at $x = 0$. Therefore, this equation must be solved separately for $x < 0$ and $x > 0$.

The homogeneous differential equation, which omits the non-homogeneous term, is:

$$i\hbar s\phi_s(x) = -\frac{\hbar^2}{2m}\partial_x^2\phi_s(x) + \lambda\delta(x)\phi_s(x) \quad (\text{B.5})$$

For $x \neq 0$, this homogeneous differential equation is equivalent to that of a free particle. The homogeneous solution is:

$$\phi_s^h(x) = \begin{cases} \alpha_s \exp \left[i\sqrt{\frac{2ims}{\hbar}}x \right] + \beta_s \exp \left[-i\sqrt{\frac{2ims}{\hbar}}x \right], & x < 0 \\ \mu_s \exp \left[i\sqrt{\frac{2ims}{\hbar}}x \right] + \nu_s \exp \left[-i\sqrt{\frac{2ims}{\hbar}}x \right], & x > 0 \end{cases} \quad (\text{B.6})$$

The particular solution $\phi_s^p(x)$ for non-homogeneous differential equation for $x > 0$ and $x < 0$ is (see equation (A.2)):

$$\phi_s^p(x) = \sqrt{\frac{m}{2i\hbar s}} \left[\int_{-\infty}^x \exp \left(i\sqrt{\frac{2ims}{\hbar}}(x-x') \right) \psi_0(x') dx' - \int_{-\infty}^x \exp \left(i\sqrt{\frac{2ims}{\hbar}}(x'-x) \right) \psi_0(x') dx' \right], \quad x \neq 0 \quad (\text{B.7})$$

This particular solution includes homogeneous solution implicitly (see Appendix A.1). This can be shown by rewriting the second term:

$$\begin{aligned} & \int_{-\infty}^x \exp \left[i\sqrt{\frac{2ims}{\hbar}}(x'-x) \right] \psi_0(x') dx' \\ &= \int_{-\infty}^{\infty} \exp \left[i\sqrt{\frac{2ims}{\hbar}}(x'-x) \right] \psi_0(x') dx' - \int_x^{\infty} \exp \left[i\sqrt{\frac{2ims}{\hbar}}(x'-x) \right] \psi_0(x') dx' \end{aligned} \quad (\text{B.8})$$

The first term represents an exponential function of x multiplied by a coefficient. This first term is excluded from the particular solution and included into the homogeneous solution.

Additionally, $x - x'$ in the first term and $x' - x$ in the second term of equation (B.7) are always positive in the respective ranges of integration. Therefore, they can be substituted with $|x - x'|$. Then, the homogeneous solution $\phi_s^h(x)$ and particular solution $\phi_s(x)$ are

$$\phi_s^h(x) = \begin{cases} \alpha_s \exp \left[i\sqrt{\frac{2ims}{\hbar}}x \right] + \tilde{\beta}_s \exp \left[-i\sqrt{\frac{2ims}{\hbar}}x \right], & x < 0 \\ \mu_s \exp \left[i\sqrt{\frac{2ims}{\hbar}}x \right] + \tilde{\nu}_s \exp \left[-i\sqrt{\frac{2ims}{\hbar}}x \right], & x > 0 \end{cases} \quad (\text{B.9})$$

$$\phi_s^p(x) = \sqrt{\frac{m}{2i\hbar s}} \int_{-\infty}^{\infty} \exp \left[i\sqrt{\frac{2ims}{\hbar}}|x-x'| \right] \psi_0(x') dx', \quad x \neq 0 \quad (\text{B.10})$$

where

$$\begin{aligned} \tilde{\beta}_s &= \beta_s - \int_{-\infty}^{\infty} \exp \left[i\sqrt{\frac{2ims}{\hbar}}x' \right] \psi_0(x') dx' \\ \tilde{\nu}_s &= \nu_s - \int_{-\infty}^{\infty} \exp \left[i\sqrt{\frac{2ims}{\hbar}}x' \right] \psi_0(x') dx' \end{aligned} \quad (\text{B.11})$$

The coefficients $\alpha_s, \beta_s, \mu_s,$ and ν_s are now determined by satisfying three boundary conditions. First, the solution $\phi_s(x) = \phi_s^h(x) + \phi_s^p(x)$ must converge to zero as $x \rightarrow \pm\infty$:

$$\lim_{x \rightarrow \infty} \phi_s(x) = 0, \quad \lim_{x \rightarrow -\infty} \phi_s(x) = 0 \quad (\text{B.12})$$

From these two conditions, it follows that:

$$\begin{aligned}\alpha_s &= 0 \\ \tilde{\nu}_s &= 0\end{aligned}\tag{B.13}$$

Additionally, the homogeneous solution can be combined into a single equation by replacing $-x$ and x with $|x|$, and by renaming the coefficient $\tilde{\beta}_s$ as μ_s . The general solution $\phi_s(x)$ is then given by:

$$\phi_s(x) = \mu_s \exp \left[i \sqrt{\frac{2ims}{\hbar}} |x| \right] + \sqrt{\frac{m}{2i\hbar s}} \int_{-\infty}^{\infty} \exp \left[i \sqrt{\frac{2ims}{\hbar}} |x - x'| \right] \psi_0(x') dx', \quad x \neq 0 \tag{B.14}$$

At this point, only the coefficient μ_s remains to be determined. This is achieved by applying a third condition, which is derived by integrating the Schrödinger equation over the interval $[-\epsilon, \epsilon]$ with respect to x , and taking the limit as $\epsilon \rightarrow 0$:

$$\lim_{\epsilon \rightarrow 0} \int_{-\epsilon}^{\epsilon} i\hbar s \phi_s(x) dx = \lim_{\epsilon \rightarrow 0} \int_{-\epsilon}^{\epsilon} \left[-\frac{\hbar^2}{2m} \partial_x^2 \phi_s(x) + \lambda \delta(x) \phi_s(x) \right] dx \tag{B.15}$$

The left-hand side of this equation vanishes because the integration domain has zero measure. The second term of the right-hand side can be computed using the property of the Dirac delta distribution:

$$\int_a^b f(x) \delta(x - c) dx = f(c) \quad \text{for } a < c < b \tag{B.16}$$

The third boundary condition, obtained from equation (B.15), is:

$$\lim_{\epsilon \rightarrow 0} [\partial_x \phi_s(\epsilon) - \partial_x \phi_s(-\epsilon)] = \frac{2m\lambda}{\hbar^2} \phi_s(0) \tag{B.17}$$

By applying this condition to equation (B.14), the coefficient μ_s is determined:

$$\mu_s = \sqrt{\frac{m}{2i\hbar s}} \frac{\lambda}{i\hbar} \phi_s(0) \tag{B.18}$$

However, the value of $\phi_s(0)$ in this expression is the Laplace-transformed wavefunction at $x = 0$, which can be calculated by evaluating equation (B.14) at $x = 0$:

$$\phi_s(0) = \frac{\sqrt{\frac{m}{2i\hbar s}}}{1 - \sqrt{\frac{m}{2i\hbar s}} \frac{\lambda}{i\hbar}} \int_{-\infty}^{\infty} \exp \left[i \sqrt{\frac{2ims}{\hbar}} |x'| \right] \psi_0(x') dx' \tag{B.19}$$

Substituting this result into the time-dependent solution (B.14), the final expression for $\phi_s(x)$ is:

$$\begin{aligned}\phi_s(x) &= -\frac{\lambda}{2\hbar^2} \frac{1}{\sqrt{s}} \frac{m}{\sqrt{s} + \sqrt{\frac{im}{2\hbar}} \frac{\lambda}{\hbar}} \int_{-\infty}^{\infty} \exp \left[i \sqrt{\frac{2ims}{\hbar}} (|x| + |x'|) \right] \psi_0(x') dx' \\ &\quad + \sqrt{\frac{m}{2i\hbar s}} \int_{-\infty}^{\infty} \exp \left[i \sqrt{\frac{2ims}{\hbar}} |x - x'| \right] \psi_0(x') dx'\end{aligned}\tag{B.20}$$

B.1.2 Inverse Laplace Transform of the Solution

To obtain the propagator $K(x, t, x', 0)$ for a delta potential, the inverse Laplace transform must be applied to the following equation:

$$\begin{aligned} \psi_t(x) = \mathcal{L}^{-1} \left\{ -\frac{\lambda}{2\hbar^2} \frac{1}{\sqrt{s}} \frac{m}{\sqrt{s} + \sqrt{\frac{im\lambda}{2\hbar}}} \int_{-\infty}^{\infty} \exp \left[i\sqrt{\frac{2ims}{\hbar}} (|x| + |x'|) \right] \psi_0(x') dx' \right. \\ \left. + \sqrt{\frac{m}{2i\hbar s}} \int_{-\infty}^{\infty} \exp \left[i\sqrt{\frac{2ims}{\hbar}} |x - x'| \right] \psi_0(x') dx' \right\} \end{aligned} \quad (\text{B.21})$$

$$= \mathcal{L}^{-1} \left\{ \int_{-\infty}^{\infty} \mathcal{L}[K(x, t, x', 0)] \psi_0(x') dx' \right\} \quad (\text{B.22})$$

By comparing these two equations, the Laplace transform of the propagator is given by:

$$\begin{aligned} \mathcal{L}[K(x, t, x', 0)] = -\frac{\lambda}{2\hbar^2} \frac{1}{\sqrt{s}} \frac{m}{\sqrt{s} + \sqrt{\frac{im\lambda}{2\hbar}}} \exp \left[i\sqrt{\frac{2ims}{\hbar}} (|x| + |x'|) \right] \\ + \sqrt{\frac{m}{2i\hbar s}} \exp \left[i\sqrt{\frac{2ims}{\hbar}} |x - x'| \right] \end{aligned} \quad (\text{B.23})$$

Using equation (A.16) and the following inverse Laplace transform (see C.1)

$$\mathcal{L}^{-1} \left[\frac{\exp(-a\sqrt{s})}{\sqrt{s}(\sqrt{s} + b)} \right] = \exp(ab + b^2t) \operatorname{erfc} \left(b\sqrt{t} + \frac{a}{2\sqrt{t}} \right), \quad (\text{B.24})$$

the propagator $K_\delta(x, t, x', 0)$ can be obtained as follows:

$$\begin{aligned} K_\delta(x, t, x', 0) = -\frac{m\lambda}{2\hbar^2} \exp \left[\frac{m\lambda}{\hbar^2} (|x| + |x'|) + \frac{im\lambda^2}{2\hbar^3} t \right] \operatorname{erfc} \left[\sqrt{\frac{m}{2i\hbar t}} \left(|x| + |x'| + \frac{i\lambda t}{\hbar} \right) \right] \\ + \sqrt{\frac{m}{2\pi i\hbar t}} \exp \left[\frac{im(x - x')^2}{2\hbar t} \right] \end{aligned} \quad (\text{B.25})$$

Note that the second term of the propagator $K_\delta(x, t, x', 0)$ corresponds to the propagator K_0 for a free particle (see equation (A.20)). Since, σ_z is diagonal, we can recover the propagator $K_\delta^{\sigma_z}(x, t, x', 0)$ by replacing λ with $\lambda\sigma_z$:

$$\begin{aligned} K_\delta^{\sigma_z}(x, t, x', 0) = -\frac{m\lambda\sigma_z}{2\hbar^2} \exp \left[\frac{m\lambda\sigma_z}{\hbar^2} (|x| + |x'|) + \frac{im\lambda^2}{2\hbar^3} t \right] \operatorname{erfc} \left[\sqrt{\frac{m}{2i\hbar t}} \left(|x| + |x'| + \frac{i\lambda\sigma_z t}{\hbar} \right) \right] \\ + \sqrt{\frac{m}{2\pi i\hbar t}} \exp \left[\frac{im(x - x')^2}{2\hbar t} \right] \end{aligned} \quad (\text{B.26})$$

B.2 Wave function as a Weak Solution

The Pauli equation for a delta-magnetic potential is discontinuous at $x = 0$ due to the delta distribution $\delta(x)$. Thus, it must be proved that Ψ_t , which is given by

$$\begin{aligned}
\Psi_t(\vec{r}) &= \xi_t(x)\eta_t(y)\zeta_t(z)\chi_t \\
&= \left(\frac{2a}{\pi}\right)^{\frac{3}{4}} \sqrt{\gamma_t} \exp\left[-a\gamma_t(\tilde{x}_t^2 + \tilde{y}_t^2) + i\left(k_{0x}x + k_{0y}y - \frac{\hbar^2(k_{0x}^2 + k_{0y}^2)}{2m\hbar}t\right)\right] \\
&\quad \cdot \left(\sqrt{\gamma_t} \exp\left[-a\gamma_t\tilde{x}_t^2 + i\left(k_{0x}x - \frac{\hbar^2k_{0x}^2}{2m\hbar}t\right)\right]\right) \\
&\quad - \frac{m\lambda\sigma_z}{2\hbar^2} \sqrt{\frac{\pi}{a}} \exp\left[\frac{m\lambda\sigma_z}{\hbar^2}(|x| - x_c) + \frac{m^2\lambda^2}{4a\gamma_t\hbar^4} + ik_{0x}\left(-\frac{m\lambda\sigma_z}{2a\hbar^2} + x_c\right) - \frac{k_{0x}^2}{4a}\right] \\
&\quad \cdot \operatorname{erfc}\left[\sqrt{a\gamma_t}(|x| - x_c) + \frac{\lambda\sigma_z m}{2\sqrt{a\gamma_t}\hbar^2} - \frac{ik_{0x}\sqrt{\gamma_t}}{2\sqrt{a}}\right] \chi_0,
\end{aligned} \tag{B.27}$$

is a weak solution. To verify this, a smooth, compactly supported test function $\phi(x)$ is employed, which must satisfy (see theorem 1.4.6):

$$\int_{-\infty}^{\infty} \hat{H}_\xi \xi_t(x) \phi(x) dx = \int_{-\infty}^{\infty} \left(-\frac{\hbar^2}{2m} \xi_t(x) \frac{\partial^2 \phi(x)}{\partial x^2} + \lambda\sigma_z \delta(x) \xi_t(x) \phi(x)\right) dx \tag{B.28}$$

As shown in Chapter 2, the right-hand side of this equation is integrated by parts after introducing $\epsilon > 0$ and taking the limits $\epsilon \rightarrow 0$, resulting in:

$$\begin{aligned}
\int_{-\infty}^{\infty} \hat{H}_\xi \Psi_t(\vec{r}) \phi(t) dt &= \lim_{\epsilon \rightarrow 0} \int_{-\infty}^{-\epsilon} \left(-\frac{\hbar^2}{2m} \phi(x) \frac{\partial^2 \xi_t(x)}{\partial x^2} + \lambda\sigma_z \delta(x) \xi_t(x) \phi(x)\right) dx \\
&\quad + \lim_{\epsilon \rightarrow 0} \int_{\epsilon}^{\infty} \left(-\frac{\hbar^2}{2m} \phi(x) \frac{\partial^2 \xi_t(x)}{\partial x^2} + \lambda\sigma_z \delta(x) \xi_t(x) \phi(x)\right) dx
\end{aligned} \tag{B.29}$$

The boundary term from the partial integration vanish because the test function $\phi(t)$ is compactly supported.

By comparing with the time derivative $i\hbar \frac{\partial}{\partial t} \xi_t(x)$:

$$\begin{aligned}
\int_{-\infty}^{\infty} \hat{H}_\xi \Psi_t(\vec{r}) \phi(t) dt &= \lim_{\epsilon \rightarrow 0} \int_{-\infty}^{-\epsilon} \phi(x) \left(i\hbar \frac{\partial \xi_t(x)}{\partial t} - \lambda\sigma_z \delta(x) \bar{\xi}_t(x) + \lambda\sigma_z \delta(x) \xi_t(x)\right) dx \\
&\quad + \lim_{\epsilon \rightarrow 0} \int_{\epsilon}^{\infty} \phi(x) \left(i\hbar \frac{\partial \xi_t(x)}{\partial t} - \lambda\sigma_z \delta(x) \bar{\xi}_t(x) + \lambda\sigma_z \delta(x) \xi_t(x)\right) dx
\end{aligned} \tag{B.30}$$

where

$$\begin{aligned}
\bar{\xi}_t(x) &= \left(\frac{2a}{\pi}\right)^{\frac{1}{4}} \sqrt{\gamma_t} \exp\left[-a\gamma_t\left(|x| - x_c - \frac{\hbar k_{0x} t}{m}\right)^2 + i\left(k_{0x}|x| - \frac{\hbar^2 k_{0x}^2}{2m\hbar}t\right)\right] \\
&\quad - \frac{m\lambda\sigma_z}{2\hbar^2} \left(\frac{2\pi}{a}\right)^{\frac{1}{4}} \exp\left[\frac{m\lambda\sigma_z}{\hbar^2}(|x| - x_c) + \frac{m^2\lambda^2}{4a\gamma_t\hbar^4} + ik_{0x}\left(-\frac{m\lambda\sigma_z}{2a\hbar^2} + x_c\right) - \frac{k_{0x}^2}{4a}\right] \\
&\quad \cdot \operatorname{erfc}\left[\sqrt{a\gamma_t}(|x| - x_c) + \frac{\lambda\sigma_z m}{2\sqrt{a\gamma_t}\hbar^2} - \frac{ik_{0x}\sqrt{\gamma_t}}{2\sqrt{a}}\right].
\end{aligned} \tag{B.31}$$

In the terms involving the delta distribution, $|x|$ can be replaced with x , because $|x| = x$ for $x = 0$, and this terms are zero for $x \neq 0$ due to the delta distribution. From this, it follows that

$$\delta(x)\overline{\xi_t}(x) = \delta(x)\xi_t(x) \quad (\text{B.32})$$

Thus, only time derivative remains on the right-hand side of equation (B.30):

$$\int_{-\infty}^{\infty} \hat{H}_\xi \Psi_t(\vec{r}) \phi(t) dt = i\hbar \lim_{\epsilon \rightarrow 0} \int_{-\infty}^{-\epsilon} \phi(x) \frac{\partial \xi_t(x)}{\partial t} dx + i\hbar \lim_{\epsilon \rightarrow 0} \int_{\epsilon}^{\infty} \phi(x) \frac{\partial \xi_t(x)}{\partial t} dx \quad (\text{B.33})$$

Since the left and right limits of the time derivative of $\xi_t(x)$ and $\partial_t \xi_t(0)$ are equal, the limit can be removed:

$$i\hbar \lim_{\epsilon \rightarrow 0} \int_{-\infty}^{-\epsilon} \phi(x) \frac{\partial \xi_t(x)}{\partial t} dx + i\hbar \lim_{\epsilon \rightarrow 0} \int_{\epsilon}^{\infty} \phi(x) \frac{\partial \xi_t(x)}{\partial t} dx = i\hbar \int_{-\infty}^{\infty} \phi(x) \frac{\partial \xi_t(x)}{\partial t} dx \quad (\text{B.34})$$

With the definition of the Schrödinger equation, the time derivative of $\xi_t(x)$ can be substituted with \hat{H}_ξ , resulting in:

$$i\hbar \int_{-\infty}^{\infty} \phi(x) \frac{\partial \xi_t(x)}{\partial t} dx = \int_{-\infty}^{\infty} \phi(x) \hat{H}_\xi \xi_t(x) dx \quad (\text{B.35})$$

Consequently, equation (B.27) is a weak solution to the Schrödinger equation for a delta-magnetic potential.

APPENDIX C

DERIVATION OF FORMULA

C.1 Laplace Transformation with Complementary Error Function

In deriving the propagator for a delta-potential, the following inverse Laplace transform was used [Zil18, p.769]:

$$\mathcal{L}^{-1} \left[\frac{\exp(-a\sqrt{s})}{\sqrt{s}(\sqrt{s}+b)} \right] = \exp(ab + b^2t) \operatorname{erfc} \left(b\sqrt{t} + \frac{a}{2\sqrt{t}} \right), \quad a > 0 \quad (\text{C.1})$$

To demonstrate this formula, it is sufficient to compute the Laplace transform of the right-hand side and compare it to the left-hand side. The Laplace transform of the right-hand side is

$$\int_0^{\infty} \exp(ab + b^2t) \operatorname{erfc} \left(b\sqrt{t} + \frac{a}{2\sqrt{t}} \right) \exp[-st] dt \quad (\text{C.2})$$

Since the first term in the argument of the exponential function, $ab + b^2t$, is independent of t , it can be ignored. Let the time-dependent portion of the expression be defined as a function of s and a :

$$I(s, a) = \int_0^{\infty} \exp[(b^2 - s)t] \operatorname{erfc} \left(b\sqrt{t} + \frac{a}{2\sqrt{t}} \right) dt \quad (\text{C.3})$$

This function can be partially differentiated with respect to a :

$$\frac{\partial I(s, a)}{\partial a} = -\frac{\exp[-ab]}{\sqrt{\pi}} \int_0^{\infty} \frac{\exp[-st - \frac{a^2}{4t}]}{\sqrt{t}} dt \quad (\text{C.4})$$

where the derivative of the complementary error function is used:

$$\begin{aligned} \frac{d}{dz} \operatorname{erfc}[z] &= \frac{d}{dz} \left(1 - \frac{2}{\sqrt{\pi}} \int_0^z \exp[-x^2] dx \right) \\ &= -\left(\frac{2}{\sqrt{\pi}} \right) \exp[-z^2]. \end{aligned} \quad (\text{C.5})$$

Since the integration range is positive real numbers, the substitution $t = x^2$ can be applied:

$$\begin{aligned} \frac{\partial I(s, a)}{\partial a} &= -\frac{2}{\sqrt{\pi}} \exp[-ab] \int_0^{\infty} \exp \left[-sx^2 - \frac{a^2}{4x^2} \right] dx \\ &= -\frac{2}{\sqrt{\pi}} \exp[-ab - \sqrt{sa}] \int_0^{\infty} \exp \left[-\left(\sqrt{sx} - \frac{a}{2x} \right)^2 \right] dx \end{aligned} \quad (\text{C.6})$$

Using the Cauchy-Schlömilch transformation [Amd+10]:

$$\int_0^{\infty} \exp \left[- \left(mx - \frac{n}{x} \right)^2 \right] dx = \frac{1}{m} \int_0^{\infty} \exp[-x^2] dx \quad \text{for } m > 0 \wedge n > 0, \quad (\text{C.7})$$

the integral can be calculated:

$$\begin{aligned} \frac{\partial I(s, a)}{\partial a} &= -\frac{2}{\sqrt{\pi}} \exp[-ab - \sqrt{sa}] \frac{1}{\sqrt{s}} \int_0^{\infty} \exp[-x^2] dx \\ &= -\frac{\exp[-(b + \sqrt{s})a]}{\sqrt{s}} \end{aligned} \quad (\text{C.8})$$

Integrating this equation with respect to a gives:

$$I(s, a) = \frac{\exp[-(b + \sqrt{s})a]}{\sqrt{s}(b + \sqrt{s})} + C \quad (\text{C.9})$$

The integration constant C can be chosen to be zero. As a result, the Laplace transformation of equation C.1 becomes:

$$\begin{aligned} \mathcal{L} \left[\exp(ab + b^2t) \operatorname{erfc} \left(b\sqrt{t} + \frac{a}{2\sqrt{t}} \right) \right] &= \exp[ab] I(s, a) \\ &= \frac{\exp(-a\sqrt{s})}{\sqrt{s}(\sqrt{s} + b)} \end{aligned} \quad (\text{C.10})$$

However, this Laplace transform is not complete because, in Chapter 3, the coefficient that corresponds to a is a complex number. To validate this Laplace transform for the complex domain, the given Cauchy-Schlömilch transformation, which assumes a is a real number (see equation (C.7)), must be extended to the complex domain. It will be shown in Appendix C.2 that the condition can be generalized to

$$0 < m \in \mathbb{R} \quad \text{and} \quad \operatorname{Re}[n] \geq |\operatorname{Im}[n]| \quad \text{for } n \in \mathbb{C}. \quad (\text{C.11})$$

With this extended Cauchy-Schlömilch transformation, the inverse Laplace transformation in equation (C.1) is validated, and it can be utilized in the derivation of the propagator in Appendix B.1.

C.2 Extension of Cauchy-Schlömilch Transformation

To extend the Cauchy-Schlömilch transformation to complex domain, equation (C.7) is derived using contour integration. The integral to be evaluated is:

$$I = \int_0^{\infty} \exp \left[- \left(mx - \frac{n}{x} \right)^2 \right] dx, \quad 0 < m \in \mathbb{R}, \quad n \in \mathbb{C} \quad (\text{C.12})$$

Using the substitution $x = \frac{n}{mt}$ [bla19], the integral is transformed into

$$I = \lim_{\lambda \rightarrow \infty} \int_0^{\lambda(a+ib)} \frac{n}{mt^2} \exp \left[- \left(mt - \frac{n}{t} \right)^2 \right] dt. \quad (\text{C.13})$$

To explicitly show the integration range, n is expressed as $a+ib$, where $a = \operatorname{Re}[n]$ and $b = \operatorname{Im}[n]$. The goal is to verify the following equality using contour integration:

$$\lim_{\lambda \rightarrow \infty} \int_0^{\lambda(a+ib)} \frac{n}{mt^2} \exp \left[- \left(mt - \frac{n}{t} \right)^2 \right] dt = \int_0^{\infty} \frac{n}{mt^2} \exp \left[- \left(mt - \frac{n}{t} \right)^2 \right] dt. \quad (\text{C.14})$$

For this equality to hold, $\operatorname{Re}[n] = a$ must be a positive real number. Next, a path $\Gamma = \gamma_1 + \gamma_2 + \gamma_3$ is defined as follows:

$$\begin{aligned} \gamma_1 &: \{z = x \mid x \in (0, R] \subset \mathbb{R}\} \\ \gamma_2 &: \left\{ z = R \exp[i\phi] \mid \phi \in [0, \alpha], \alpha = \tan^{-1} \left(\frac{\operatorname{Im}[n]}{\operatorname{Re}[n]} \right) \right\} \\ \gamma_3 &: \{z = x \exp[i\alpha] \mid x \in [R, 0]\} \end{aligned} \quad (\text{C.15})$$

The singularity at $z = 0 + 0i$ is excluded from the path. This does not affect the integral since the measure of a single point is zero. Furthermore, the zero in the integration range is implicitly defined as a limit.

Since the closed path Γ does not enclose any poles, the contour integration along Γ evaluates to zero. This implies that the integrals along γ_1 and γ_3 are equivalent if the integral along γ_2 vanishes as $R \rightarrow \infty$. The limit of the integral along γ_2 as $R \rightarrow \infty$ is given by:

$$\begin{aligned} & \lim_{R \rightarrow \infty} \int_0^{\alpha} \frac{n \exp[-2i\phi]}{mR^2} \exp \left[- \left(mRe^{i\phi} - \frac{ne^{-i\phi}}{R} \right)^2 \right] dt \\ &= \lim_{R \rightarrow \infty} \int_0^{\alpha} \frac{n \exp[-2i\phi]}{mR^2} \exp \left[-m^2 R^2 e^{2i\phi} - \frac{n^2 e^{-2i\phi}}{R^2} + mn \right] dt \\ &\leq \lim_{R \rightarrow \infty} \left\| \int_0^{\alpha} \frac{n \exp[-2i\phi]}{mR^2} \exp \left[-m^2 R^2 e^{2i\phi} - \frac{n^2 e^{-2i\phi}}{R^2} + mn \right] dt \right\| \\ &\leq \lim_{R \rightarrow \infty} \int_0^{\alpha} \left\| \frac{n \exp[-2i\phi]}{mR^2} \exp \left[-m^2 R^2 e^{2i\phi} - \frac{n^2 e^{-2i\phi}}{R^2} + mn \right] \right\| dt \\ &= \lim_{R \rightarrow \infty} \int_0^{\alpha} \frac{\|n\|}{mR^2} \left\| \exp \left[-m^2 R^2 e^{2i\phi} - \frac{n^2 e^{-2i\phi}}{R^2} + mn \right] \right\| dt \end{aligned} \quad (\text{C.16})$$

Expanding the exponential term using $e^{ix} = \cos x + i \sin x$ and noting $\|e^{ix}\| = 1$, this reduces to

$$\lim_{R \rightarrow \infty} \int_0^{\alpha} \frac{a^2 + b^2}{mR^2} \exp \left[-m^2 R^2 \cos(2\phi) - \frac{(a^2 - b^2) \cos(2\phi) + 2ab \sin(2\phi)}{R^2} + ma \right] dt \quad (\text{C.17})$$

In this expression, the second term in the argument of the exponential function vanishes as $R \rightarrow \infty$, and the third term is constant. Thus, the convergence of the integral depends on $\cos(2\phi)$ in the first term. If $\cos(2\phi)$ is positive, i.e., $\phi \in [-\pi/4, \pi/4]$, the limit of the integral is zero. In this interval of ϕ , the following inequality for n holds:

$$\operatorname{Re}[n] \geq |\operatorname{Im}[n]| > 0 \quad (\text{C.18})$$

Therefore, the condition for equation (C.14) can be expressed as follows:

$$\lim_{\lambda \rightarrow \infty} \int_0^{\lambda(\operatorname{Re}[n] + i\operatorname{Im}[n])} \frac{n}{mt^2} \exp \left[- \left(mt - \frac{n}{t} \right)^2 \right] dt = \int_0^{\infty} \frac{n}{mt^2} \exp \left[- \left(mt - \frac{n}{t} \right)^2 \right] dt \quad (\text{C.19})$$

$$\text{for } \operatorname{Re}[n] \geq |\operatorname{Im}[n]| > 0$$

Next, the substituted form of equation (C.13) is added to its original form:

$$\begin{aligned} 2I &= \int_0^{\infty} \exp \left[- \left(mx - \frac{n}{x} \right)^2 \right] dx + \int_0^{\infty} \frac{n}{mt^2} \exp \left[- \left(mt - \frac{n}{t} \right)^2 \right] dt \\ &= \frac{1}{m} \int_0^{\infty} \left(m + \frac{n}{x^2} \right) \exp \left[- \left(mx - \frac{n}{x} \right)^2 \right] dx \\ &= \frac{1}{m} \lim_{\lambda \rightarrow \infty} \int_{-\lambda(a+ib)}^{\infty} \exp \left[-y^2 \right] dy \end{aligned} \quad (\text{C.20})$$

In the last step, the following substitution was applied:

$$mx - \frac{n}{x} = y, \quad dy = \left(m + \frac{n}{x^2} \right) dx. \quad (\text{C.21})$$

Finally, the following equality must be demonstrated using contour integration:

$$\lim_{\lambda \rightarrow \infty} \int_{-\lambda(a+ib)}^{\infty} \exp \left[-y^2 \right] dy = \int_{-\infty}^{\infty} \exp \left[-y^2 \right] dy \quad (\text{C.22})$$

A closed path $\Gamma = \gamma_1 + \gamma_2 + \gamma_3$ is defined as:

$$\begin{aligned} \gamma_1 &: \{z = xR \mid x \in [-a, a] \subset \mathbb{R}\} \\ \gamma_2 &: \{z = -R(a + ix) \mid x \in [0, b]\} \\ \gamma_3 &: \left\{ z = aR(x - 1) + ibR \frac{(x - 2)}{2} \mid x \in [0, 2] \right\} \end{aligned} \quad (\text{C.23})$$

Since the integrand $\exp[-z^2]$ is analytic in \mathbb{C} , the contour integral along Γ evaluates to zero. Consequently, the behavior of the integral along γ_2 as $R \rightarrow \infty$ must be analyzed. This limit is given by:

$$\begin{aligned} \lim_{R \rightarrow \infty} \int_{\gamma_2} \exp \left[-z^2 \right] dz &= \lim_{R \rightarrow \infty} \int_0^b -iR \exp \left[-R^2(a + ix)^2 \right] dx \\ &\leq \lim_{R \rightarrow \infty} \int_0^b R \exp \left[-R^2(a^2 - x^2) \right] dx \end{aligned} \quad (\text{C.24})$$

The second line is obtained by taking the norm of the right-hand side of the first line.

Note that the integral in the second line converges to zero as $R \rightarrow \infty$ even in the worst case

($b = a$). The integral vanishes everywhere except at $x = a$, but the measure of a single point is zero. Thus, the limit of the integral along γ_2 is

$$\lim_{R \rightarrow \infty} \int_{\gamma_2} \exp[-z^2] dz = 0 \quad (\text{C.25})$$

Substituting this result into equation (C.20) gives:

$$\begin{aligned} 2I &= \frac{1}{m} \int_{-\infty}^{\infty} \exp[-y^2] dy \\ &= \frac{2}{m} \int_0^{\infty} \exp[-y^2] dy \end{aligned} \quad (\text{C.26})$$

Therefore, the following identity is proven:

$$I = \int_0^{\infty} \exp\left[-\left(mx - \frac{n}{x}\right)^2\right] dx = \frac{1}{m} \int_0^{\infty} \exp[-x^2] dx \quad (\text{C.27})$$

$$\text{for } \operatorname{Re}[n] \geq |\operatorname{Im}[n]| > 0$$

C.3 Infinite Integral with Complementary Error Function

In Chapter 3, the following integral must be evaluated to determine the time-dependent wavefunction:

$$I = \int_{-\infty}^{\infty} \exp[-ax^2 + bx] \operatorname{erfc}[mx + n] dx \quad (\text{C.28})$$

However, direct evaluation of this integral is challenging because the complementary error function is not an elementary function. To facilitate the calculation, the integral I is redefined as a function of n , i.e., $I = I(n)$. Differentiating $I(n)$ with respect to n and completing the square yields:

$$\begin{aligned} \frac{\partial I(n)}{\partial n} &= -\left(\frac{2}{\sqrt{\pi}}\right) \exp\left[-n^2 + \frac{(b - 2mn)^2}{4(a + m^2)}\right] \underbrace{\int_{-\infty}^{\infty} \exp\left[-(a + m^2) \left(x - \frac{b - 2mn}{2(a + m^2)}\right)^2\right]}_{=\sqrt{\frac{\pi}{a+m^2}}} \\ &= -\left(\frac{2}{\sqrt{a + m^2}}\right) \exp\left[-n^2 + \frac{(b - 2mn)^2}{4(a + m^2)}\right] \end{aligned} \quad (\text{C.29})$$

$$(\text{C.30})$$

Here, the derivative of the complementary error function is used:

$$\begin{aligned} \frac{d}{dz} \operatorname{erfc}[z] &= \frac{d}{dz} \left(1 - \frac{2}{\sqrt{\pi}} \int_0^z \exp[-x^2] dx\right) \\ &= -\left(\frac{2}{\sqrt{\pi}}\right) \exp[-z^2]. \end{aligned} \quad (\text{C.31})$$

To proceed, the argument of the exponential function is rewritten by completing the square once more:

$$\frac{\partial I(n)}{\partial n} = -\frac{2}{\sqrt{a+m^2}} \exp\left[\frac{b^2}{4a}\right] \exp\left[-\left(\sqrt{\frac{a}{a+m^2}}n + \frac{mb}{2\sqrt{a(a+m^2)}}\right)^2\right] \quad (\text{C.32})$$

The last exponential term matches the form of the derivative of the complementary error function. Integrating this expression gives:

$$\begin{aligned} I(n) &= -\frac{2}{\sqrt{a+m^2}} \exp\left[\frac{b^2}{4a}\right] \int_z^\infty \exp\left[-\left(\sqrt{\frac{a}{a+m^2}}n + \frac{mb}{2\sqrt{a(a+m^2)}}\right)^2\right] dn \\ &= \sqrt{\frac{\pi}{a}} \exp\left[\frac{b^2}{4a}\right] \underbrace{\left(-\frac{2}{\sqrt{\pi}}\right) \sqrt{\frac{a}{a+m^2}} \int_z^\infty \exp\left[-\left(\sqrt{\frac{a}{a+m^2}}n + \frac{mb}{2\sqrt{a(a+m^2)}}\right)^2\right] dn}_{=\text{erfc}\left[\sqrt{\frac{a}{a+m^2}}n + \frac{mb}{2\sqrt{a(a+m^2)}}\right]} \quad (\text{C.33}) \end{aligned}$$

Recognizing the integral as a complementary error function yields:

$$I = I(n) = \sqrt{\frac{\pi}{a}} \exp\left[\frac{b^2}{4a}\right] \text{erfc}\left[\sqrt{\frac{a}{a+m^2}}n + \frac{mb}{2\sqrt{a(a+m^2)}}\right]. \quad (\text{C.34})$$

Thus, the integral I is successfully evaluated.

BIBLIOGRAPHY

- [Jin+17] Fangzhou Jin et al. “Experimental test of Born’s rule by inspecting third-order quantum interference on a single spin in solids”. In: *Phys. Rev. A* 95 (1 Jan. 2017), p. 012107. DOI: [10.1103/PhysRevA.95.012107](https://doi.org/10.1103/PhysRevA.95.012107). URL: <https://link.aps.org/doi/10.1103/PhysRevA.95.012107>.
- [Söl+11] Immo Söllner et al. “Testing Born’s Rule in Quantum Mechanics for Three Mutually Exclusive Events”. In: *Foundations of Physics* 42.6 (Sept. 2011), pp. 742–751. ISSN: 1572-9516. DOI: [10.1007/s10701-011-9597-5](https://doi.org/10.1007/s10701-011-9597-5). URL: <http://dx.doi.org/10.1007/s10701-011-9597-5>.
- [Gou21] Arseni Goussev. “Quantum backflow in a ring”. In: *Phys. Rev. A* 103 (2 Feb. 2021), p. 022217. DOI: [10.1103/PhysRevA.103.022217](https://doi.org/10.1103/PhysRevA.103.022217). URL: <https://link.aps.org/doi/10.1103/PhysRevA.103.022217>.
- [Von14] Nicola Vona. *On Time in Quantum Mechanics*. 2014. arXiv: [1403.2496 \[math-ph\]](https://arxiv.org/abs/1403.2496). URL: <https://arxiv.org/abs/1403.2496>.
- [Gre00] Walter Greiner. *Relativistic Quantum Mechanics. Wave Equations*. Jan. 2000. ISBN: 978-3-540-67457-3. DOI: [10.1007/978-3-662-04275-5](https://doi.org/10.1007/978-3-662-04275-5).
- [Wil20] James M Wilkes. “The Pauli and Lévy-Leblond equations, and the spin current density”. In: *European Journal of Physics* 41.3 (Mar. 2020), p. 035402. DOI: [10.1088/1361-6404/ab7495](https://doi.org/10.1088/1361-6404/ab7495). URL: <https://dx.doi.org/10.1088/1361-6404/ab7495>.
- [RS75] Michael C. Reed and Barry Simon. *Methods of Modern Mathematical Physics. 2. Fourier Analysis, Self-adjointness*. 1975. URL: <https://api.semanticscholar.org/CorpusID:222378746>.
- [Sch99] Joel Schiff. *The Laplace Transform: Theory and Applications*. Jan. 1999. ISBN: 978-1-4757-7262-3. DOI: [10.1007/978-0-387-22757-3](https://doi.org/10.1007/978-0-387-22757-3).
- [Hof07] K. Hoffman. *Banach Spaces of Analytic Functions*. Dover Books on Mathematics. Dover Publications, 2007. ISBN: 9780486458748. URL: <https://books.google.de/books?id=-vWJAAQBAJ>.
- [SN20] J. J. Sakurai and Jim Napolitano. *Modern Quantum Mechanics*. 3rd ed. Cambridge University Press, 2020.
- [Ros07] S.L. Ross. *Differential Equations, 3rd Ed*. Wiley India Pvt. Limited, 2007. ISBN: 9788126515370. URL: <https://books.google.de/books?id=TkQEROzMqQMC>.
- [Eva98] L.C. Evans. *Partial Differential Equations*. Graduate studies in mathematics. American Mathematical Society, 1998. ISBN: 9780821807729. URL: https://books.google.de/books?id=5Pv4LVB_m8AC.
- [GS18] David J. Griffiths and Darrell F. Schroeter. *Introduction to Quantum Mechanics*. 3rd ed. Cambridge University Press, 2018.

- [AS23] Peter Christian Aichelburg and Christian Spreitzer. *Spin interaction of non-relativistic neutrons with an ultrashort laser pulse*. 2023. arXiv: [2312.01079](https://arxiv.org/abs/2312.01079) [quant-ph]. URL: <https://arxiv.org/abs/2312.01079>.
- [MM20] S.V. Mousavi and S. Miret-Artés. “Quantum backflow for dissipative two-identical-particle systems”. In: *Results in Physics* 19 (2020), p. 103426. ISSN: 2211-3797. DOI: <https://doi.org/10.1016/j.rinp.2020.103426>. URL: <https://www.sciencedirect.com/science/article/pii/S2211379720318908>.
- [AD04] M A Andreatta and V V Dodonov. “Tunnelling of narrow Gaussian packets through delta potentials”. In: *Journal of Physics A: Mathematical and General* 37.6 (Jan. 2004), p. 2423. DOI: [10.1088/0305-4470/37/6/031](https://doi.org/10.1088/0305-4470/37/6/031). URL: <https://dx.doi.org/10.1088/0305-4470/37/6/031>.
- [BD65] James D. Bjorken and Sidney D. Drell. *Relativistic Quantum Mechanics*. International Series In Pure and Applied Physics. New York: McGraw-Hill, 1965. ISBN: 978-0-07-005493-6.
- [DD19] Siddhant Das and Detlef Dürr. “Arrival Time Distributions of Spin-1/2 Particles”. In: *Scientific Reports* 9 (Feb. 2019). DOI: [10.1038/s41598-018-38261-4](https://doi.org/10.1038/s41598-018-38261-4).
- [Pro+54] Bateman Manuscript Project et al. *Tables of Integral Transforms: Based, in Part, on Notes Left by Harry Bateman*. Tables of Integral Transforms: Based, in Part, on Notes Left by Harry Bateman V. 1. McGraw-Hill, 1954. URL: <https://books.google.de/books?id=HfZQAAAAMAAJ>.
- [Cam09] Joel Campbell. “Some exact results for the Schrödinger wave equation with a time-dependent potential”. In: *Journal of Physics A: Mathematical and Theoretical* 42 (Aug. 2009), p. 365212. DOI: [10.1088/1751-8113/42/36/365212](https://doi.org/10.1088/1751-8113/42/36/365212).
- [Zil18] D.G. Zill. *Advanced Engineering Mathematics*. Jones & Bartlett Learning, 2018. ISBN: 9781284105902. URL: <https://books.google.de/books?id=tFARDQAAQBAJ>.
- [Amd+10] T. Amdeberhan et al. *The Cauchy-Schlömilch transformation*. 2010. arXiv: [1004.2445](https://arxiv.org/abs/1004.2445) [math.CA]. URL: <https://arxiv.org/abs/1004.2445>.
- [bla19] blackpenredpen. *You need to try this integral[Video file]*. Nov. 2019. URL: <https://youtu.be/SEApEblBR28?si=5uFeyLV2LNE636ss&t=26>.

DECLARATION OF AUTHORSHIP

I hereby declare that this thesis is my own work and that no sources were used other than those cited.

Munich, January 29th, 2025

Name